

Surface Atmosphere Integrated Field Laboratory (SAIL) Science Plan

D Feldman	A Aiken
W Boos	R Carroll
V Chandrasekar	W Collins
S Collis	J Deems
P DeMott	J Fan
A Flores	D Gochis
J Harrington	M Kumijian
LR Leung	T O'Brien
M Raleigh	A Rhoades
S McKenzie Skiles	J Smith
R Sullivan	P Ullrich
A Varble	K Williams

April 2021



DISCLAIMER

This report was prepared as an account of work sponsored by the U.S. Government. Neither the United States nor any agency thereof, nor any of their employees, makes any warranty, express or implied, or assumes any legal liability or responsibility for the accuracy, completeness, or usefulness of any information, apparatus, product, or process disclosed, or represents that its use would not infringe privately owned rights. Reference herein to any specific commercial product, process, or service by trade name, trademark, manufacturer, or otherwise, does not necessarily constitute or imply its endorsement, recommendation, or favoring by the U.S. Government or any agency thereof. The views and opinions of authors expressed herein do not necessarily state or reflect those of the U.S. Government or any agency thereof.

This report was produced by the Surface Atmosphere Integrated Field Laboratory (SAIL) science team. It is a review of the science goals for the SAIL campaign and the proposed strategies for addressing these goals. The Atmospheric Radiation Measurement (ARM) user facility is working closely with the SAIL science team to support these science goals; however, implementation details may evolve during the course of the campaign planning and execution.

This report is available on the U.S. Department of Energy Office of Scientific and Technical Information website, osti.gov, and the ARM user facility website, arm.gov.

Surface Atmosphere Integrated Field Laboratory (SAIL) Science Plan

D Feldman, Lawrence Berkeley National Laboratory (LBNL)
Principal Investigator

A Aiken, Los Alamos National Laboratory
W Boos, University of California, Berkeley
R Carroll, Desert Research Institute
V Chandrasekar, Colorado State University (CSU)
W Collins, LBNL
S Collis, Argonne National Laboratory (ANL)
J Deems, National Snow and Ice Data Center
P DeMott, CSU
J Fan, Pacific Northwest National Laboratory (PNNL)
A Flores, Boise State University
D Gochis, National Center for Atmospheric Research
J Harrington, Pennsylvania State University (PSU)
M Kumijian, PSU
LR Leung, PNNL
T O'Brien, Indian University
M Raleigh, Oregon State University
A Rhoades, LBNL
S McKenzie Skiles, University of Utah
J Smith, University of California, Irvine
R Sullivan, ANL
P Ullrich, University of California, Davis
A Varble, PNNL
K Williams, LBNL
Co-Investigators

April 2021

Prepared for the U.S. Department of Energy,
Office of Science, Biological and Environmental Research Program

Executive Summary

Mountains are the natural water towers of the world, effectively turning water vapor into readily available fresh water through precipitation, snowpack, and runoff. Unfortunately, Earth system models (ESMs) have persistently been unable to predict the timing and availability of water resources from mountains because the source(s) of model error are difficult to isolate in complex terrain with limited atmospheric or land-surface observations. Further complications arise from the gross scale mismatch between ESM grid box sizes and the relevant scales of mountainous hydrological processes. The mountain hydrometeorology community has repeatedly called for integrated atmospheric and land observations of water and energy budgets in complex terrain that span these scales to establish benchmarks against which scale-dependent models can be further developed.

The Surface Atmosphere Integrated field Laboratory (SAIL) campaign responds to these calls by deploying the U.S. Department of Energy (DOE) Atmospheric Radiation Measurement (ARM) user facility's second Mobile Facility (AMF2), additional ARM instrumentation, and an X-band scanning precipitation radar from Colorado State University to the East River Watershed near Crested Butte, Colorado. Integrated observations are key to the success of the SAIL campaign. Therefore, SAIL will collocate atmospheric observations with the long-standing collaborative resources including the ongoing surface and subsurface hydrologic observations from the DOE's Watershed Function Science Focus Area (SFA). It will also work closely with the U.S. Geological Survey (USGS) as part of its Next-Generation Water Observing System (NGWOS), the National Oceanic and Atmospheric Administration (NOAA)'s Study of Precipitation and Lower-Atmospheric impacts on Streamflow and Hydrology (SPLASH), and the Rocky Mountain Biological Laboratory.

SAIL's main science question is: Across a range of models from LES to mesoscale process to Earth system models, what level of atmospheric and land-atmosphere interaction process fidelity is needed to produce unbiased seasonal estimates of the surface energy and water budgets of mountainous watersheds in the Upper Colorado River Basin?

In order to answer that question, SAIL will collect data to address four key science sub-questions:

1. SSQ-1. How do multi-scale dynamic and microphysical processes control the spatial and temporal distribution, phase, amount, and intensity of precipitation?
2. SSQ-2. How strongly do aerosols affect the surface energy and water balance by altering clouds, precipitation, and surface albedo, and how do these impacts vary seasonally?
3. SSQ-3. What are the contributions of snow sublimation, radiation, and turbulent fluxes of latent and sensible heat to the water and energy balance of the snowpack?
4. SSQ-4. How do atmospheric and surface processes set the net radiative absorption that is known to drive the regional flow of water into the continental interior during the summer monsoon?

SAIL data will enable the quantification of the processes that need to be represented at the scale of mountainous watersheds, to help build a foundation for the robust process modeling required to advance the representation of mountain hydrology in ESMs.

The campaign will start on September 1, 2021 and end on June 15, 2023, allowing for observations of precipitation, aerosol, cloud, radiative, and surface processes as they impact mountainous hydrology across multiple seasonal cycles.

Acronyms and Abbreviations

3D	three-dimensional
ABL	atmospheric boundary layer
ACSM	aerosol chemical speciation monitor
AERI	atmospheric emitted radiance interferometer
AERIOE	Atmospheric Emitted Radiance Interferometer Optimal Estimation Value-Added Product
AGL	above ground level
AMF	ARM Mobile Facility
AOP	Aerosol Optical Properties Value-Added Product
AOS	Aerosol Observing System
AOSMET	AOS meteorological measurements
APS	aerodynamic particle sizer
ARM	Atmospheric Radiation Measurement
ASD	Analytical Spectral Devices
ASFS	Atmospheric Surface Flux Station
ASO	Airborne Snow Observatory
ASR	Atmospheric System Research
BC	black carbon
BCSD-CMIP5	Bias-Corrected, Spatially Disaggregated downscaled Coupled Model Intercomparison Project – Phase 5
BER	Biological and Environmental Research
BERAC	Biological and Environmental Research Advisory Committee
BL	boundary layer
BrC	brown carbon
CASTNET	Clean Air Status and Trends Network
CB	cloud base
CBAC	Crested Butte Avalanche Center
CBMR	Crested Butte Mountain Resort
CCN	cloud condensation nuclei, cloud condensation nuclei particle counter
CEIL	ceilometer
CERES	Clouds and the Earth’s Radiant Energy System
CIES	column-integrated energy source
CLAMPS	Collaborative Lower Atmospheric Mobile Profiling System
CO	carbon monoxide, carbon monoxide mixing ration system
CONUS	continental United States
CPC	condensation particle counter

CPCF	condensation particle counter-fine
CSPHOT	Cimel sunphotometer
CSU	Colorado State University
CWCB	Colorado Water Conservation Board
CWP	cloud water path
DEM	digital elevation model
DL	Doppler lidar
DLPROF	Doppler Lidar Profiles Value-Added Product
DOE	U.S. Department of Energy
DSM	digital soil mapping
EC	eddy covariance
ECOR	eddy correlation flux measurement system
EDW	elevation-dependent warming
EESM	Earth and Environmental System Modeling
EESSD	Earth and Environmental Systems Sciences Division
EM	electromagnetic
EPA	Environmental Protection Agency
ESM	Earth system model
ESS	Environmental System Science
ET	evapotranspiration
EVI	enhanced vegetation index
FT	free troposphere
GNDRAD	ground radiometer on stand for upwelling radiation
GPM	Global Precipitation Measurement
HRRR	High-Resolution Rapid Refresh
HSRL	high-spectral-resolution lidar
HTDMA	humidified tandem differential mobility analyzer
IFL	integrated field laboratory
IMPROVE	Interagency Monitoring of Protected Visual Environments
INP	ice-nucleating particle
IOP	intensive operational period
IRT	infrared thermometer
IWP	ice water path
JPL	Jet Propulsion Laboratory
KAZR	Ka-band ARM Zenith Radar
LAI	leaf area index
LBNL	Lawrence Berkeley National Laboratory
LDQUANTS	Laser Disdrometer Quantities Value-Added Product

LES	large-eddy simulation
LIDAR	light detection and ranging
MARCUS	Measurements of Aerosols, Radiation, and Clouds over the Southern Ocean
MASL	meters above sea level
MERRA-2	Modern-Era Retrospective analysis for Research Applications, Version 2
MET	surface meteorological instrumentation
MFRSR	multifilter rotating shadowband radiometer
MFRSRCOD	Multifilter Rotating Shadowband Radiometer Cloud Optical Depth Value-Added Product
MODIS	Moderate Resolution Imaging Spectroradiometer
MPL	micropulse lidar
MT-CLIM	Mountain Climate Simulator
MWR	microwave radiometer
MWR3C	microwave radiometer, 3-channel
MWRLOS	Microwave Water Radiometer: Water Liquid and Vapor along Line of Sight Path Value-Added Product
NADP	National Atmospheric Deposition Program
NAM	North American Monsoon
NAME	North American Monsoon Experiment
NARCCAP	North American Regional Climate Change Assessment Program
NASA	National Aeronautics and Space Administration
NCAR	National Center for Atmospheric Research
NCP	normalized coherent power
NDVI	normalized difference vegetation index
NEON	National Ecological Observatory Network
NEPH	nephelometer
NGWOS	Next-Generation Water Observing System
NOAA	National Oceanic and Atmospheric Administration
NOHRSC	National Operational Hydrologic Remote Sensing Center
NPF	new particle formation
NSF	National Science Foundation
OACOMP	Organic Aerosol Component Value-Added Product
OZONE	ozone monitor
PARS2	Parsivel2 disdrometer
PBL	planetary boundary layer
PCASP	passive cavity aerosol spectrometer
PH	Pumphouse
POPS	printed optical particle spectrometer

PPI	plan-position indicator
PRISM	Parameter-Elevation Regressions on Independent Slopes Model
PSAP	particle soot absorption photometer
QCECOR	Quality-Controlled Eddy Correlation Measurement Value-Added Product
RADFLUXANAL	Radiative Flux Analysis Value-Added Product
RADSYS	radiometer suite
RGB	red, green, blue
RGMA	Regional & Global Model Analysis
RHI	range-height indicator
RMBL	Rocky Mountain Biological Laboratory
RWP	radar wind profiler
SAIL	Surface Atmosphere Integrated Field Laboratory
SBR	Subsurface Biogeochemical Research
SEB	surface energy balance
SEBS	surface energy balance system
SFA	Science Focus Area
SKYRAD	sky radiometers on stand for downwelling radiation
SLR	Snow-Level Radar
SMPS	scanning mobility particle sizer
SNICAR	Snow-Ice and Aerosol Radiative Transfer
SNOTEL	Snow Telemetry
SO	science objective
SOA	secondary organic aerosol
SONDE	balloon-borne sounding system
SP2	single-particle soot photometer
SPLASH	Study of Precipitation and Lower-Atmospheric impacts on Streamflow and Hydrology
SQ	science question
SSQ	science sub-question
STAC	size- and time-resolved aerosol counter
STORMVEX	Storm Peak Lab Cloud Property Validation Experiment
SURFRAD	Surface Radiation Network
SWE	snow-water equivalent
TBS	tethered balloon systems
TES	Terrestrial Ecosystem Science
TOA	top-of-atmosphere
TRMM	Tropical Rainfall Measuring Mission
TSI	total sky imager

UAV	unmanned aerial vehicle
UHSAS	ultra-high-sensitivity aerosol spectrometer
USGS	U.S. Geological Survey
VAP	Value-Added Product
VARANAL	Constrained Variational Analysis Value-Added Product
VR-CESM	Variable-Resolution Community Earth System Model
WBPLUVIO2	Pluvio ² weighing bucket rain gauge
WFSFA	Watershed Function Scientific Focus Area
WRF	Weather Research and Forecasting
WU	Weather Underground
WUS	Western United States
XBPWR	X-band dual-polarimetric weather radar

Contents

Executive Summary	iii
Acronyms and Abbreviations	v
1.0 Background.....	1
1.1 Campaign Overview.....	4
1.2 Previous Campaigns.....	14
1.2.1 STORMVEX.....	14
1.2.2 NAME.....	15
2.0 Scientific Questions.....	16
2.1 Precipitation Processes.....	16
2.2 Aerosol Processes.....	19
2.3 Snow Processes.....	22
2.4 Warm-Season Processes.....	25
3.0 Scientific Objectives.....	26
3.1 Precipitation Process Characterization.....	27
3.2 Cold Snow-Season Processes.....	28
3.3 Aerosol Regimes and Radiation.....	30
3.4 Aerosol-Cloud Interactions.....	33
3.5 Surface Energy Balance.....	34
4.0 Measurement Strategies.....	36
4.1 AMF2 and XBPWR during Normal Operations.....	39
4.1.1 Strategies Supporting Science Objective 1.....	40
4.1.2 Strategies Supporting Science Objective 2.....	41
4.1.3 Strategies Supporting Science Objective 3.....	42
4.1.4 Strategies Supporting Science Objective 4.....	43
4.1.5 Strategies Supporting Science Objective 5.....	43
4.2 Collaborative Resources and Guest Instrumentation.....	44
4.3 Other ARM Resources.....	45
5.0 Project Management and Execution.....	47
6.0 Science.....	48
6.1 Precipitation Process Science.....	48
6.2 Snow Sublimation and Wind Redistribution Science.....	49
6.3 Aerosol Precipitation Interaction Science.....	51
6.4 Surface Energy Balance Science.....	52
6.5 Integrated Field Laboratory Science.....	52
6.6 Modeling Activities Science.....	53
7.0 Relevancy to the DOE Mission.....	55
8.0 References.....	56

Figures

1	Cartoon of the dominant atmospheric and surface processes in mid-latitude continental interior mountainous watersheds that impact mountainous hydrology and their interseasonal variability.....	3
2	The 640,000 km ² Colorado River Watershed and, on the right, the 300 km ² drainage that includes Coal Creek, the Slate River, Washington Gulch and the East River located within 20 km of Crested Butte, Colorado.....	4
3	Watershed boundaries of Coal Creek, Slate River, Washington Gulch, and the East River, along with tributary overlays.....	5
4	Map of the East River Watershed depicting the network of stream gauging/stream water sampling locations, meteorological stations, and other distributed and specialized measurement sites in the watershed.....	13
5	Seasonal cycle and range of interannual variability of monthly-mean GPCP (v7) precipitation over a 1x1-degree box centered on Crested Butte (left), and over the entire Colorado-Utah region (right).....	14
6	1981-2010 climatological average of the seasonal trajectory in measured total precipitation and snow-water equivalent at the Butte and Schofield Pass SNOTEL stations as a function of day in water year.....	14
7	Info-graphic showing precipitation micro- and macro-physical processes that contribute to precipitation in high-altitude complex terrain.....	17
8	ASO-measured snow depth around Crested Butte, Colorado in early April, 2019.....	18
9	Cartoon of a range of aerosol processes that impact radiation and precipitation and, ultimately, hydrology.....	19
10	Diagram of range of atmospheric aerosol processes and their impacts.....	21
11	Annual cycles of aerosol mass concentrations of fine organic and elemental carbon, and soil dust, at the White River Interagency Monitoring of Protected Visual Environments (IMPROVE) network site, located close to the proposed SAIL site, at 3413 m MSL, 39.1536 latitude, -106.8209 longitude. (b) INP concentrations via immersion freezing collected by several campaigns since 2000 in the Colorado Mountains.....	22
12	ASO Snow Water Equivalent Retrieval Comparison over the East River Watershed from (left) April 1, 2016, (center) March 30, 2018, and (right) May 24, 2018.....	23
13	Box-whisker plots (box spans 25-75th percentile and whiskers span the 5th to 95th percentiles) of ASO SWE as a function of elevation bin.....	23
14	Cartoon of three major areas where snow sublimation occurs: Over the snowpack, in the canopy, and at ridgelines in blowing snow plumes.....	24
15	NOHRSC estimates of (a) April 1, 2020 SWE, (b) April 1, 2019 SWE, (c) April 1, 2020 blowing-snow sublimation and (d) April 1, 2019 blowing-snow sublimation.....	25
16	Climatological June-August atmospheric column-integrated energy source, obtained by summing the surface sensible and latent heat flux and the column-integrated radiative flux convergence, as estimated from MERRA-2 reanalysis.....	26

17	XBPWR beam-blockage analysis from the Old Teocali Lift site showing radial coverage in (a) winter and (b) summer.....	28
18	Panoramic drone photo of Old Teocali Lift site looking towards Gothic, Colorado.....	28
19	ASO survey of the northern edge of the East River Watershed from April, 2019 showing variability of snowpack near ridgelines.....	29
20	Map of the radiative forcing by deposited aerosols in snow from the ASO flight over the East River Watershed in April, 2016.....	31
21	Diagram of impacts of impurities on the surface albedo of snow and associated snow-albedo and grain-size feedbacks.	33
22	Cartoon of range of aerosol-precipitation processes with the relative vertical positioning in the atmosphere and their length scales.	34
23	Perspective view looking north towards East River Watershed with the watershed boundary in red, the location for SAIL of the XBPWR in green, and the location of the AMF2 as a red marker.....	40
24	Three potential sites for TBS deployment: (1) RMBL Gothic Townsite in red, Kettle Ponds in yellow, and Mt. Crested Butte Boneyard in yellow.	46
25	(a) Topographic map of a 400x400-km domain surrounding the East River Watershed (outlined in black). (b) Domain-wide comparison of wintertime WRF simulations with PRISM for Calendar Year 2017. (c) Same as (b) but showing wintertime domain bias (WRF-Prism), (d) Same as (c) but showing summertime bias.	48
26	Two-pronged data assimilation to achieve snow process closure at the mesoscale.....	50
27	Example of determination of biological INPs based on thermal treatment of unamended aliquots of particles, and distinguishing total organic contributions of INPs through H ₂ O ₂ digestion.	51

Tables

1	List of SAIL AOS instruments including summary information.	7
2	List of SAIL cloud instruments including summary information.	8
3	List of SAIL wind instruments including summary information.	8
4	List of SAIL radiometry instruments including summary information.....	9
5	List of SAIL surface meteorology instruments including summary information.....	10

1.0 Background

The majority of worldwide water resources (60-90%) emerge from mountains (Huss et al. 2017). In North America, mountains comprise a quarter of the continent's land area, but store 60% of the snowpack (Wrzesien et al. 2018). However, these water towers of the world are threatened by many factors contributing to elevation-dependent climate warming (Barnett et al. 2005, Mote et al. 2018, MRI 2015, López-Moreno et al. 2017, Musselman et al. 2017), with deleterious implications for snow cover, water resources, and even atmospheric dynamics (Chen et al. 2017, MRI 2015, Mote et al. 2018). This warming is expected to induce modifications to snow accumulation, melt, and subsequent water budget partitioning and is expected to decrease streamflow (Clow 2010, Barnhart et al. 2016, Li et al. 2017, McCabe et al. 2017). Given the potential for water resource stress in the near and long term, there are clear societal needs for Earth system models (ESMs) to provide robust predictions of how water resources arising from, especially, mid-latitude mountain systems will evolve in a changing climate.

Unfortunately, across many generations of development, ESMs have shown persistent problems in the prediction of both trends in these resources and their availability across seasons. Across Earth's major mountain ranges, the amplification of warming trends at higher-elevations has been underestimated by models (Rangwala et al. 2012). This accelerated, elevation-dependent warming (EDW) has large implications for snow cover, water resources, and even atmospheric dynamics (Qian et al. 2011, MRI 2015, Huss et al. 2017, Mote et al. 2018). A number of mechanisms have been advanced to explain EDW, which range from surface albedo feedbacks to changes in downwelling longwave radiation from air temperature and surface humidity (Palazzi et al. 2017, 2019).

ESM performance on the seasonal scale also has significant room for improvement. In the winter and spring, ESMs exhibit an inability to capture the temporal dynamics of mountain snowpack in the western US (Frei et al. 2005, Rutter et al. 2009, Essery et al. 2009). Work by Chen et al. (2014), Wu et al. (2017), and Rhoades et al. (2016, 2018a,b,c), indicates that many ESMs exhibit a mode of common failure in the date of peak snowpack timing and in spring snowmelt rate within both the California Sierra Nevada and Colorado Rocky Mountains. In the summer, precipitation in the western and central U.S. has exhibited seasonal shifts on decadal time-scales, with significant implications for water resources and planning (Gochis et al. 2006, Grantz 2007), but again, model prediction of these trends and variability have much room for improvement (Liang et al. 2008, Castro et al. 2012, Sheffield et al. 2013, Clark et al. 2015a,b).

Recent work has revealed that process-specific details matter. Rhoades et al. (2018a) found that projected changes in western United States (WUS) mountainous snow-water equivalent (SWE) from before 2005 to 2045-2065 are -19% for North American Regional Climate Change Assessment Program (NARCCAP), -26% for the Bias-Corrected, Spatially-Disaggregated downscaled Coupled Model Intercomparison Project – Phase 5 (BCSD-CMIP5), -38% for Variable-Resolution Community Earth System Model (VR-CESM), and -69% for raw climate model fields for CMIP5. The NARCCAP provides an estimate of SWE changes in regional climate models, while BCSD-CMIP5 estimates those changes with statistical downscaling, and VR-CESM provides estimates from variable-resolution climate model simulations. All of these simulations have different inherent assumptions about how the processes significantly impact mountainous hydrology. Regional climate models contain parameterized processes that differ from their parent model, statistical downscaling techniques focus on capturing the myriad processes that impact mountainous hydrology through statistical analysis of observations, and variable-resolution simulations

have similar or identical parameterizations as their parent model. It should be noted that the largest decrease in SWE, as exhibited by the raw CMIP5 models, is also the most suspect. Due to their coarse resolution, numerous processes of relevance, especially related to the nonlinear interactions between complex terrain and the atmosphere, these raw simulations have the largest bias and exhibit almost no SWE during the historical observational period.

Efforts to fix these problems are hampered by questions of which model process representation(s) are contributing most to this error, and extreme heterogeneity in mass and energy fluxes in high-altitude complex terrain complicates efforts to transfer a limited set of observations to a broader understanding of the drivers of model errors in mountain hydrology. Given the gross scale mismatch between the size of a typical ESM grid cell (~100 km) and the spatial and temporal heterogeneity of atmospheric and land-surface hydrological processes (~1 km and ~10 m, respectively), and observational campaigns are often challenged in resolving these processes across their range of temporal and spatial scales. This has led to a breakdown of the traditional observation and modeling workflow in complex terrain. That is, the approach whereby researchers collect observational data in the mountains, confront models with those data, identify model skill and reveal model deficiencies, and make improvements to those models accordingly, is not straightforward because these systems are so under-observed that traditional atmospheric process models, such as convection-permitting Weather Research and Forecasting (WRF), are more reliable for forcing hydrological models than observational data sets like Parameter-Elevation Regressions on Independent Slopes Model (PRISM) (Lundquist et al. 2019). Consequently, the model improvement pathway is ill-posed: The ways in which a limited set of new observations can improve atmospheric process models are often not immediately clear.

This challenge is not insurmountable, however: A focus on the understanding and quantification of the processes across these scales can, with process model support, produce a data set whereby the process observations are transferable to ESMs. In this spirit, progress in ESM representation of seasonal mountain hydrology requires a focused effort to quantify the sub-grid land-atmospheric processes at appropriate scales. Figure 1 diagrams these processes in mid-latitude, continental interior watersheds.

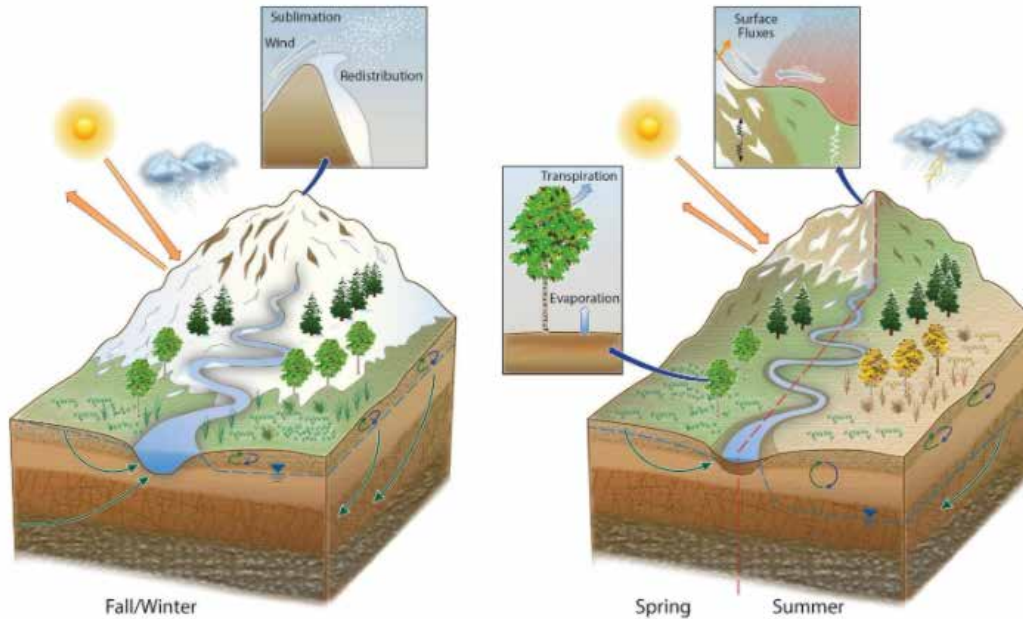


Figure 1. Cartoon of the dominant atmospheric and surface processes in mid-latitude continental interior mountainous watersheds that impact mountainous hydrology and their interseasonal variability including precipitation, radiation, snow sublimation, and wind redistribution in the fall-winter and evapotranspiration, dust-on-snow, advective flows, and convection in the spring/summer.

For these watersheds, several qualitatively understood processes impact hydrology and change dramatically across seasons, many of which are atmospheric in nature and several that involve surface-atmosphere interactions. Orographic precipitation in fall and winter, and occasionally spring and convective precipitation in summer, represent the dominant water inputs to these watersheds. The snowpack is influenced by a number of processes including sublimation losses and wind redistribution that occur principally in the atmosphere. Aerosols influence both the energetics of the snowpack and precipitation and clouds, while seasonally varying radiation strongly forces the snowpack. All of these are critical for setting the major driver for mountainous watershed availability: The snowpack's snow-water equivalent. Meanwhile, a major loss pathway for water in the spring, summer, and fall is evapotranspiration.

To understand the hydrology of these watersheds, a holistic understanding of these interwoven processes is necessary. Consequently, the mountain hydrometeorology community has long recognized the importance of simultaneous measurements in energy and water fluxes within complex terrain in order to manage and predict water resources through the understanding and quantification of relevant processes (Lundquist et al. 2003, Bales et al. 2006, Henn et al. 2016, Lundquist et al. 2016, Henn et al. 2018). The community has emphasized that integrated atmospheric and land observations can test how models represent both precipitation and surface processes (Viviroli et al. 2011, Rasmussen et al. 2012) and evaluate the accuracy of commonly used mountain reanalysis products (Henn et al. 2016, 2018). The mountain hydrometeorology community has declared that both a combination of land and atmosphere observations and targeted modeling studies are needed to improve understanding of the coupling between precipitation and hydrologic fluxes (Bales et al. 2006, Viviroli et al. 2011, Lundquist et al. 2015, Clark et al. 2015a,b). Furthermore, DOE's Biological and Environmental Research Advisory Committee

(BERAC) has specifically requested integrated field laboratories (IFLs), including those in mountainous watersheds, and suggested their prioritization to advance BER science (BERAC 2015). Finally, the 2019 ARM Mobile Facility Workshop Report has highlighted that Mountainous and Complex Terrain regions are a Region/Area of Interest because these AMF campaign data have the potential to inform science questions on turbulence, aerosols, and land-atmosphere interactions in order to improve and evaluate model parameterizations (U.S. DOE 2019).

Messerli et al. (2004) highlights those mountain ranges that are the most hydrologically significant and, for application purposes, helps prioritize their study. In North America, the Colorado River is the most hydrologically significant, draining an area of 640,000 km² with approximately 74 km³ of annual discharge (60 million acre-feet). These water resources enable ~53 gigawatts of electric power generation capacity, support ~\$1.3 trillion of economic activity annually, and provide ~15 million jobs (James et al. 2014), but water resources from this river have been dwindling – they have decreased by 9.3 % °C⁻¹ of warming over the past 100 years (Milly et al. 2020). Within this large watershed, there are areas of significant research and modeling focus, but one in particular stands out because it has been extensively studied with long-duration biological experiments and, more recently, it is the focus of sustained and intensive research activity. The left panel of Figure 2 shows the drainage area of the Colorado River Basin, highlighting the principal tributaries of the Colorado River (Gila, San Juan, and Gunnison).

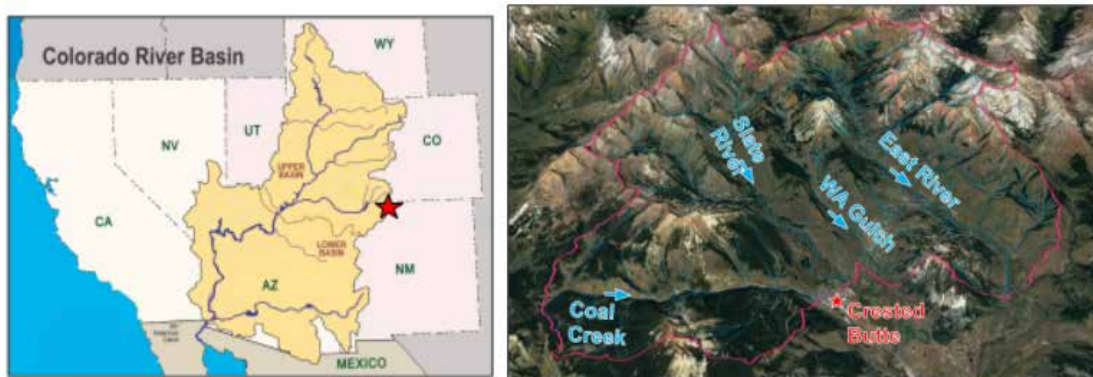


Figure 2. The 640,000 km² Colorado River Watershed and, on the right, the 300 km² drainage that includes Coal Creek, the Slate River, Washington Gulch and the East River located within 20 km of Crested Butte, Colorado.

The Gunnison River is one of the largest tributaries of the Colorado River. The right panel of Figure 2 shows that the Upper Gunnison Basin’s East River Watershed, located in the Elk Mountain range of the Rocky Mountains, is the central focus of the Watershed Function Scientific Focus Area (WFSFA) (<http://watershed.lbl.gov>). The WFSFA is supported by DOE’s Biological and Environmental Research (BER) Subsurface Biogeochemical Research (SBR) program to advance predictive watershed hydro-biogeochemistry (Hubbard et al. 2020).

1.1 Campaign Overview

SAIL is a field campaign that arose out of the repeated scientific community requests for integrated atmosphere-through-bedrock observations in mountainous watersheds. It will deploy the Second Mobile

Facility of DOE's ARM facility (AMF2) to the East River Watershed of the Upper Colorado River in southwestern Colorado. Most of the AMF2 instruments will be located just south of the Rocky Mountain Biological Laboratory at Gothic, Colorado.

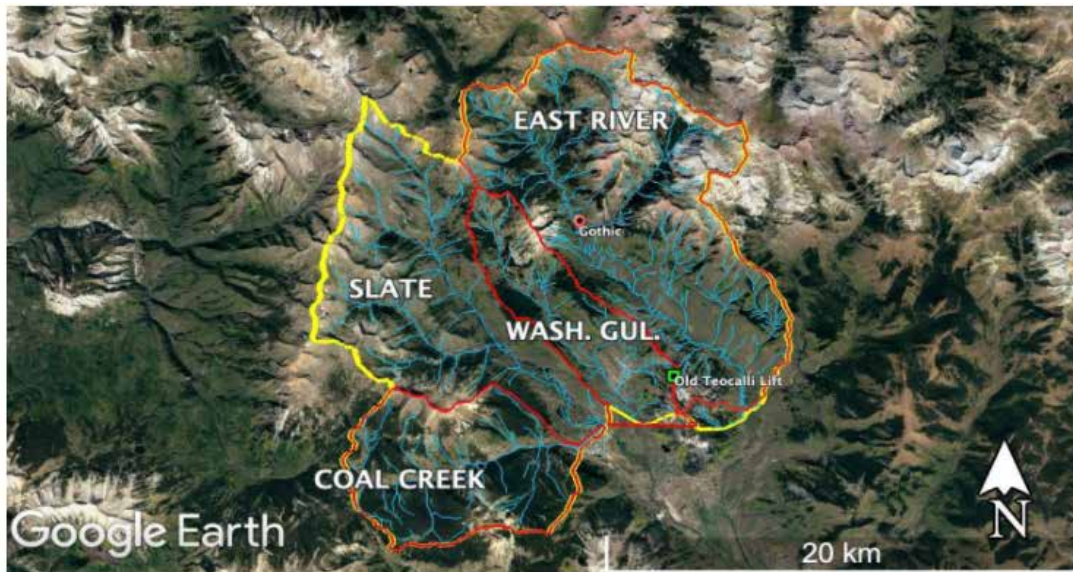


Figure 3. Watershed boundaries of Coal Creek, Slate River, Washington Gulch, and the East River, along with tributary overlays. The two principal sites of the SAIL deployment are indicated. Most AMF2 instruments will be located in Gothic, while the scanning precipitation radar and the AOS will be located at the Old Teocali Lift site.

The containerized instruments will be located adjacent to Gunnison County Road 317 (38°57'22.35"N, 106°59'16.66"W), while the field instruments will be located on an adjacent hill (38°57'22.99"N, 106°59'8.79"W). The containerized instruments will be located within the East River Valley at an elevation of ~2885 meters above sea level (MASL) with the instruments on the adjacent hill at ~2917 MASL. In addition to the AMF2, SAIL will also deploy a scanning, X-band dual-polarimetric weather radar (XBPWR) to provide observations of precipitation amount and type across the East River Watershed. Colorado State University (CSU) will provide the XBPWR and that institution will provide support for the development of precipitation retrievals. The XBPWR and the Aerosol Observing System (AOS) will be placed together at an elevated location on Crested Butte Mountain near the Old Teocali Lift (38°53'52.66"N, 106°56'35.21"W) at an elevation of ~3137 MASL. The XBPWR and AOS measurements will be separated by ~7.5 km from the AMF2.

For SAIL, the AMF2 instruments that will be deployed can be grouped into several categories:

1. Aerosol Observing System ([AOS](#)):
 1. Aerosol chemical speciation monitor ([ACSM](#))
 2. Aerosol Observing System meteorology station ([AOSMET](#))
 3. Ambient nephelometer ([NEPH](#))
 4. Carbon monoxide mixing ratio system ([CO](#))
 5. Ozone monitor ([O3](#))
 6. Cloud condensation nuclei counter ([CCN](#))

7. Condensation particle counter ([CPC](#))
 8. Humidified tandem differential mobility analyzer ([HTDMA](#))
 9. Ice-nucleating particle ([INP](#))
 10. Particle soot absorption photometer ([PSAP](#))
 11. Scanning mobility particle sizer ([SMPS](#))
 12. Single-particle soot photometer ([SP2](#))
 13. Ultra-high-sensitivity aerosol spectrometer ([UHSAS](#))
2. Cloud Properties:
1. Ceilometer ([CEIL](#))
 2. High-spectral-resolution lidar ([HSRL](#))
 3. Ka-band ARM Zenith Radar ([KAZR](#))
 4. Micropulse lidar ([MPL](#))
 5. Total sky imager ([TSI](#))
3. Radiometry:
1. Atmospheric emitted radiance interferometer ([AERI](#))
 2. Cimel sun photometer ([CSPHOT](#))
 3. Ground radiometers on stand for upwelling radiation ([GNDRAD](#))
 4. Infrared thermometer ([IRT](#))
 5. Multi-filter rotating shadowband radiometer ([MFRSR](#))
 6. Microwave radiometer 3-channel ([MWR3C](#))
 7. Microwave radiometer line of sight ([MWRLOS](#))
 8. Sky radiometers on stand for downwelling radiation ([SKYRAD](#))
4. Surface Meteorology/Fluxes:
1. Disdrometer ([PARS2](#))
 2. Eddy correlation flux measurement system ([ECOR](#))
 3. Surface energy balance system ([SEBS](#))
 4. Surface meteorology system ([MET](#))
 5. Weighing bucket precipitation gauge ([WBPLUVIO2](#))
5. Winds:
1. Doppler lidar ([DL](#))
 2. Radar wind profiler ([RWP](#))
 3. Radiosonde ([SONDE](#))

Tables 1-5 provides a description of the instrument dimensions, spatial and temporal resolution, range, and the geophysical variable(s) to which the fundamental measurements are sensitive for the SAIL datstreams.

Table 1. List of SAIL AOS instruments including summary information on specific instrument capabilities, dimension of observations, spatial and temporal resolution, range, and quantities that instruments observe.

Instrument	Dimensions	Spatial Resolution	Temporal Resolution	Range	Measurement
ACSM	Point Obs	N/A	30 minutes	N/A	Aerosol speciation
AOSMET	Point Obs	N/A	1 second	N/A	RH, T, winds
CO	Point Obs	N/A	1 minute	N/A	Carbon monoxide
CCN	Point Obs	N/A	1 second	N/A	Cloud condensation nuclei
CPC	Point Obs	N/A	1 second	N/A	Sub-micron aerosol particle number concentration
HTDMA	Point Obs	N/A	10 minutes	N/A	Aerosol particle hygroscopicity
INP	Point Obs	N/A	2x weekly	N/A	Immersion freezing temperature spectra of ice-nucleating particles
NEPH	Point Obs	N/A	5 seconds	N/A	Scattering and hemispheric backscatter of aerosols
O3	Point Obs	N/A	5 seconds	N/A	Surface atmospheric ozone concentration
PSAP	Point Obs	N/A	1 second	N/A	Bulk absorption of surface atmospheric aerosols
SMPS	Point Obs	N/A	TBD	N/A	Surface aerosol size distribution
SP2	Point Obs	N/A	1 minute	N/A	Surface atmospheric soot mass
UHSAS	Point Obs	N/A	10 seconds	N/A	Surface aerosol size distribution

Table 2. List of SAIL cloud instruments including summary information on specific instrument capabilities, dimension of observations, spatial and temporal resolution, range, and quantities that instruments observe.

Instrument	Dimensions	Spatial Resolution	Temporal Resolution	Range	Measurement
CEIL	Z	10 m	16 seconds	7.5 km	PBL, CB height, atmospheric backscatter
HSRL	Z	7.5 m	5 seconds	30 km	Vertical profiles of optical depth, backscatter cross-section, depolarization, and backscatter phase function
KAZR	Z	30 m	1 minute	20 km	Vertically-resolved cloud particle profiles of Doppler velocity, reflectivity, and spectral width at Ka band
MPL	Z	15 m	10 seconds	18 km	Aerosol and cloud location and scattering property profiles, hydrometeor phase
TSI	X, Y	<45 m	30 seconds	6 km	Horizontal distribution of cloud sky fraction

Table 3. List of SAIL wind instruments including summary information on specific instrument capabilities, dimension of observations, spatial and temporal resolution, range, and quantities that instruments observe.

Instrument	Dimensions	Spatial Resolution	Temporal Resolution	Range	Measurement
DL	X, Y, Z	30 m	30 seconds	10 km	3D radial wind velocities
RWP	Z	10 m	1 hour	10 km	Vertical wind profiles of speed and direction
SONDE	Z	100 m	6 hours	6 km	Atmospheric profiles of temperature and water vapor and wind speed and direction

Table 4. List of SAIL radiometry instruments including summary information on specific instrument capabilities, dimension of observations, spatial and temporal resolution, range, and quantities that instruments observe.

Instrument	Dimensions	Spatial Resolution	Temporal Resolution	Range	Measurement
AERI	Z, limited X,Y	100 m	30 seconds	10 km	RH and T profiles
CSPHOT	Point Obs	N/A	1 minute	N/A	Solar and sky irradiance
GNDRAD	Point Obs	N/A	1 minute	N/A	Shortwave and longwave broadband radiative flux
IRT	Point Obs	N/A	3 seconds	N/A	Equivalent blackbody brightness temperature in field of view
MFRSR	Point Obs	N/A	1 minute	N/A	Aerosol optical depth, diffuse and direct radiation, total water vapor derived from radiance at 6 channels from 415 nm to 940 nm
MWR3C	Point Obs	N/A	1 second	N/A	Total column liquid water in clouds and total column gaseous water vapor
MWRLOS	Point Obs	N/A	1 second	N/A	Total column liquid water in clouds and total column gaseous water vapor
SKYRAD	Point Obs	N/A	1 minute	N/A	Surface downwelling solar and infrared broadband radiation

Table 5. List of SAIL surface meteorology instruments including summary information on specific instrument capabilities, dimension of observations, spatial and temporal resolution, range, and quantities that instruments observe.

Instrument	Dimensions	Spatial Resolution	Temporal Resolution	Range	Measurement
PARS2	Point Obs	N/A	1 minute	N/A	Surface precipitating hydrometeor particle size and fall speed
ECOR	Point Obs	N/A	30 minutes	N/A	Turbulent fluxes of momentum, latent and sensible heat
SEBS	Point Obs	N/A	30 minutes	N/A	Surface upwelling and downwelling solar and infrared broadband radiation
MET	Point Obs	N/A	1 minute	N/A	Surface wind speed, wind direction, air temperature, barometric pressure, relative humidity, rain-rate
WBPLUVIO2	Point Obs	N/A	1 minute	N/A	Surface warm-season precipitation

Another instrument that is not part of the AMF2 package is the XBPWR. This dual-polarization scanning X-band radar measures reflectivity in horizontal polarization (Z_H), differential reflectivity (Z_{DR}), enhanced reflectivity (Z_{HV}), vertical polarization antenna voltage (V), radial wind velocity (W), correlation coefficient between horizontal and vertical co-

Digital elevation model: Of the East River and Washington Gulch drainages obtained using Light Detection and Ranging (LiDAR) QL1-grade measurements having a lateral resolution of <0.5 m.

Airborne Snow Observatory (ASO): This aerial resource was developed and operated by the NASA Jet Propulsion Laboratory (JPL), but it is now managed by ASO, Inc., a Colorado Public Benefit Corporation. Aircraft flights of the ASO were sponsored by a joint venture between the WFSFA and the Colorado Water Conservation Board (CWCB) and have mapped snow depth (3-m resolution) and snow-water equivalent (SWE) at 50-m resolution at peak SWE (early April) and at intermediate melt (mid-May) across the WFSFA extended domain (2500 km²). The supporting ground campaign includes 20 snow pits to measure 10-cm vertically resolved temperature, SWE, density, and isotopic signature, and bulk chemistry (anions, cations, carbon, trace metals). Crystal structure and dust layers are identified. Five flights have been flown to date (April 2016, April 2018, May 2018, April 2019, June 2019). Additional resources are being investigated to continue flights beyond 2020.

National Ecological Observatory Network (NEON): And its Airborne Observation Platform was flown late June 2018 as a partnership between the National Science Foundation (NSF), Stanford University and Lawrence Berkeley National Laboratory (LBNL). The flight mapped 370 km² in the East River with a hyperspectral imaging spectrometer (sampling interval 5 nm, 380-2510 nm), full waveform and discrete return LiDAR, and a high-resolution RGB camera. Data was collected at 1-m spatial resolution. Derived data include total biomass, vegetation indices (enhanced vegetation index [EVI], normalized difference vegetation index [NDVI]), ecosystem structure (vegetation type, heterogeneity, height and leaf area index [LAI]), canopy chemistry (lignin, nitrogen, water content, xanthophyll cycle), digital elevation modeling (DEM), and digital soil mapping (DSM). Intensive ground campaigns occurred to calibrate/validate. Supplementing this data set are unmanned aerial vehicle (UAV)-based measurements of plant functional types and canopy structure using multispectral imaging and photogrammetry, respectively.

Surface and airborne geophysics: To identify variations in bedrock lithology, structural heterogeneity, depth of weathering, fracture density, and matrix porosity as they pertain to groundwater storage. Data collected include electromagnetic (EM) soundings and self-potential over surface grids. Airborne EM data collected in October 2017 was used to generate a 370-km² subsurface structural rendering of the watershed to depths of 300 m at 10-m spatial resolution.

Stream network: Contains seven gauges with transducers providing 10-min pressure and temperature data, with rating curves developed using acoustic Doppler velocity meter and salt dilution tracer techniques (Carroll and Williams 2019). Five additional USGS gauges and four gauges to be installed by Co-Investigator Carroll in 2020 reside along the East River but outside the proposed domain. Three auto-samplers are deployed to sample riverine solutes and isotopes of water daily to constrain streamflow source (snowmelt versus groundwater). Grab samples for water chemistry are done weekly to twice monthly at all other locations.

Shallow and deep monitoring wells: Consist of a network of 50+ shallow (<10 m) and 10+ deep (>10 m) groundwater monitoring wells used to track seasonal variations in groundwater elevation and their relationship to annual precipitation totals. These wells are also used to obtain samples for geochemical and microbiological analysis to link hydrologic processes with subsurface biogeochemical reactions of interest to BER.

Rocky Mountain Biological Laboratory (RMBL): With Berkeley Laboratory support, RMBL operates a meteorological network of five stations that span an elevation gradient from 3500-2400m, and a sixth site downriver. Each station includes: Air temperature/relative humidity; barometric pressure; wind speed/direction; photosynthetically active radiation (up/down fluxes); longwave/shortwave radiation (up/down fluxes); snow depth; precipitation; solar radiation (up and down); 10m air temperature; five depth-resolved soil moisture/temperature probes; logger/communications with radio/solar panel/multiplexor for real-time data telemetry. Additionally, 10 wind-shielded precipitation gauges are available for disbursement within the study domain to address specific science questions.

Eddy covariance (EC) flux tower: Located in the East River Watershed at Pumphouse (PH) and consists of sub-hourly measurements of vertical flux of heat, water, and gases calculated by a covariance of deviations in vertical wind speed and tracer species using a 3D sonic anemometer, gas analyzer (open and closed), and thermocouple. It is currently offline but may be rebuilt if funds are available.

Crested Butte Avalanche Center (CBAC): Provides daily snowpack analysis, avalanche forecasting, and risk assessment as functions of aspect and elevation. Four weather stations operated in cooperation with Irwin Guides and the Crested Butte Mountain Resort (CBMR) are in close proximity to SAIL, with stations spanning elevations from 3110 3660 m. All stations collect temperature, relative humidity, and wind data. Select stations collect snowfall/accumulation, SWE, and incoming solar radiation.

Environmental Protection Agency (EPA) currently operates a Clean Air Status and Trends Network (CASTNET) monitoring station in the townsite of Gothic, Colorado. The station is part of the National Atmospheric Deposition Program (NADP) that assesses trends in pollutant concentrations, atmospheric deposition, and ecological effects due to changes in air pollutant emissions. The station collects meteorological data (e.g., temperature, solar radiation, precipitation, etc.), as well as both wet and dry deposited aerosols.

Weather Underground (WU) stations are scattered throughout the area. Nine stations are close to the town of Crested Butte (elev. 2626-2929 m) and an additional 11 stations are located within the Upper Gunnison River Basin. Sub-hourly data are collected for temperature, barometric pressure, dew point, wind, and precipitation (hourly). The SFA currently scrubs data from six WU stations for ingestion into its database.

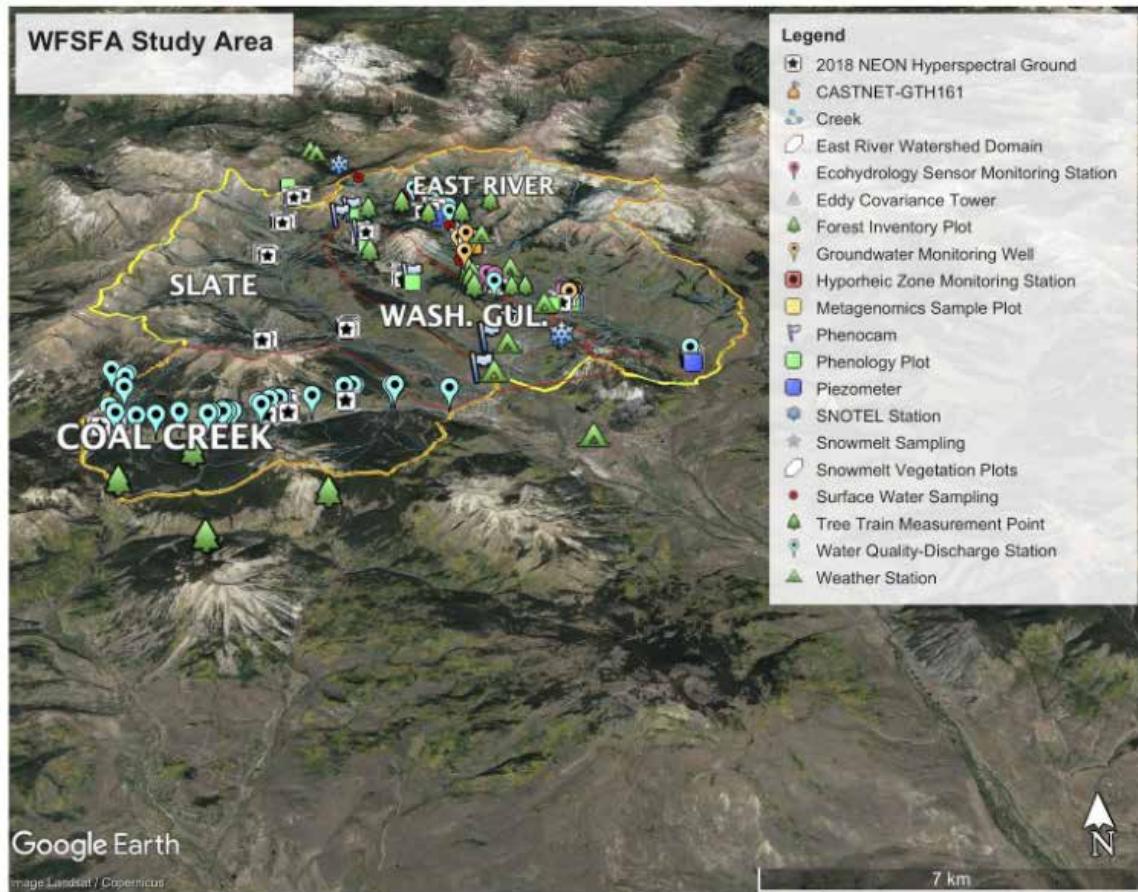


Figure 4. Map of the East River Watershed depicting the network of stream gauging/stream water sampling locations, meteorological stations, and other distributed and specialized measurement sites in the watershed. Continuous measurements of snow-water equivalent (SWE) are made at the two Snow Telemetry (SNOTEL) locations and at one of the meteorological stations.

Figures 5 and 6 show aspects of this variability. Precipitation occurs throughout the year in this region, though at higher elevations most of the precipitation occurs in the form of snowfall and preferentially occurs in the winter. Figure 6 shows two SNOTEL stations: The Schofield Pass station to the north and the Butte station to the south. Figure 6 shows a climatology of total precipitation and SWE measured at those two stations, indicating that Schofield Pass receives nearly double the precipitation of Butte. There is also significant variability in dust-on-snow events: While not shown here, most of the dust received in the area occurs during the spring in a few events, but there is significant interannual variability in dust concentration, with deposition occurring preferentially in alpine, as opposed to sub-alpine, conditions.

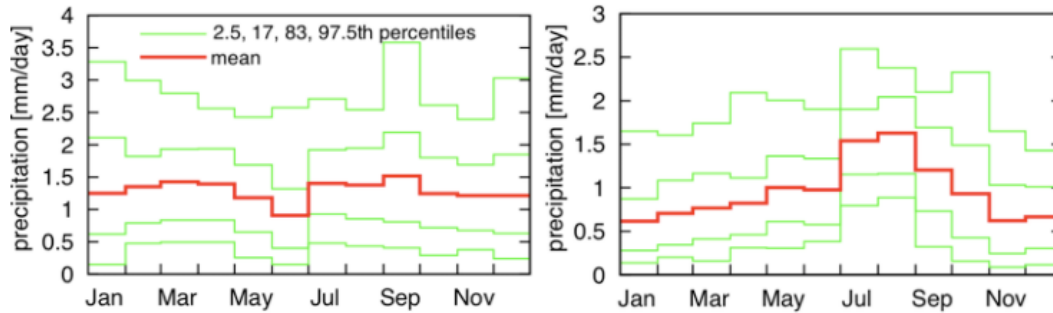


Figure 5. Seasonal cycle and range of interannual variability of monthly-mean GPCP (v7) precipitation over a 1x1-degree box centered on Crested Butte (left), and over the entire Colorado-Utah region (right).

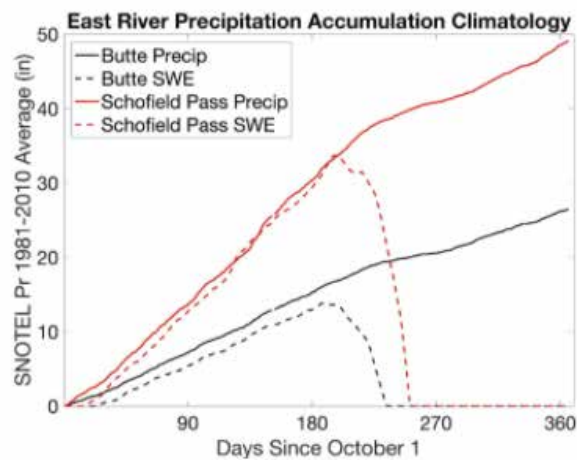


Figure 6. 1981-2010 climatological average of the seasonal trajectory in measured total precipitation and snow-water equivalent at the Butte and Schofield Pass SNOTEL stations as a function of day in water year.

1.2 Previous Campaigns

While many previous field experiments have been conducted in the Rocky Mountains, we note two specific campaigns, since SAIL is intended to complement and build off of their findings.

1.2.1 STORMVEX

The Storm Peak Lab Cloud Property Validation Experiment (STORMVEX) around Steamboat Springs, Colorado in 2010-2011 provides numerous opportunities to compare and contrast results with SAIL. Given the geographic proximity of the STORMVEX measurements to those of the proposed SAIL site, the types of clouds observed and the roles of aerosols in clouds and precipitation at the two sites can and should be compared.

Surprises associated with STORMVEX included the striking finding of a large contribution of coarse-mode aerosols to both aerosol microphysical and bulk optical properties (Kassianov et al. 2017) and a substantial contribution of ice-crystal orientation to the 95 GHz radar backscatter

(Marchand et al. 2013). Observations from SAIL can therefore be compared against STORMVEX to determine the spatial and temporal consistency of the STORMVEX findings.

For the coarse-mode aerosol finding, SAIL will have similar instrumentation as STORMVEX, including the multifilter rotating shadowband radiometer (MFRSR) to determine aerosol optical depth, and also the scanning mobility particle sizer (SMPS), the aerodynamic particle sizer (APS), and the nephelometer to jointly determine total particle light absorption and scattering and the contribution of large particles to light absorption and scattering. Data from SAIL can also test the ice-crystal orientation finding from STORMVEX using the XBPWR and the KAZR to look at ice-crystal orientation through SAIL's multiple winter seasons.

The comparison of SAIL and STORMVEX can only go so far, however, since the STORMVEX deployment measured over wintertime and early springtime conditions. First and foremost, the purpose of STORMVEX centered around retrievals of geophysical quantities in complex terrain, while SAIL is focused on mountainous hydrology, and therefore focuses on different processes and observations from STORMVEX, leverages long-duration, distributed networks as part of the Watershed Function SFA, and covers all seasons.

Specifically, the extended duration of observations as part of SAIL would capture the changes in precipitation amount and phase, cloud type, aerosols, and cloud-aerosol and aerosol-precipitation interactions during the transition from a winter mid-latitude baroclinic wave regime to a summer North American monsoonal regime. SAIL would also measure throughout the springtime, which generally include most dust events (Skiles et al. 2015). SAIL observations will enable numerous opportunities to establish whether these variables are modulated by aerosols and whether differences between the two campaigns can be explained with existing process models.

1.2.2 NAME

The North American Monsoon Experiment (NAME), which included extensive field observations and associated research activities in northern Mexico and the southwestern U.S. in 2004, started to break down the paradigm that monsoon precipitation is entirely moisture-driven (Higgins and Gochis 2007). For example, Douglas and Englehart (2007) showed that transient synoptic systems are surprisingly common during the monsoon season, and that their presence strongly modulates precipitation intensity. None of the studies associated with NAME (or any others neither observational nor modeling as far as we are aware) have sought to explicitly and quantitatively evaluate the relative importance of moisture versus uplift in monsoon precipitation. Furthermore, results from NAME are largely inapplicable for understanding the hydroclimatology of the Upper Colorado River Basin, since NAME gathered measurements far to the southwest of the region of interest for SAIL and only during monsoonal flows. Observational deployments in the NAME 2004 campaign were focused on the NAME's "Tier 1" region, which is centered on northern Mexico, and so the northernmost observations in NAME 2004 were limited to central Arizona and New Mexico.

Additionally, the NAME campaign largely focused on warm-season meteorology and did not include a robust surface hydrological observation network (e.g., soil moisture, groundwater, streamflow, and surface energy fluxes). While a few measurements of this type were made, they were not coordinated in an integrated fashion to permit quantitative analysis and modeling of catchment-to-river-basin-scale water fluxes, storages, and residence times. The SAIL campaign will directly address these shortcomings.

2.0 Scientific Questions

The state of mountainous hydrology science and opportunities within the East River Watershed motivate the overarching science question for the SAIL campaign: Across a range of models from LES to mesoscale process to Earth system models, what level of atmospheric and land-atmosphere interaction process fidelity is needed to produce unbiased seasonal estimates of the surface energy and water budgets of mountainous watersheds in the Upper Colorado River Basin?

This overarching science question enables the campaign to establish metrics for success. Principally, SAIL will succeed if the measurements that it collects enable a demonstration that a necessary and sufficient amount of information has been collected regarding the dominant atmospheric and land-atmosphere interaction processes to drive hydrological models such that it can be shown that errors in those models are not dominated in drivers of surface energy and mass balance (from uncertainties in precipitation, radiation, aerosols, snow sublimation and redistribution, and evapotranspiration).

The rationale here is that such a demonstration would provide a level of benchmarking for mountainous hydrological modeling that has yet to be achieved and serve as a robust observational foundation for model development ranging in complexity and domain from process models to Earth system models. An effort to develop this ambitious demonstration motivates a number of science sub-questions that, in turn, drive the campaign's science objectives. The sub-questions focus on a set of intertwined processes that ultimately set the surface energy and mass balances.

2.1 Precipitation Processes

1. How do multi-scale dynamic and microphysical processes control the spatial and temporal distribution, phase, amount, and intensity of precipitation?

Because SAIL focuses on hydrology, it must first focus on precipitation processes, since precipitation is known to exhibit first-order heterogeneity in space and time. The heterogeneity is driven by processes that range from the synoptic to the microphysical scale that are highly impacted by the surface, including terrain, and the distribution of energy and water at the surface.

The surface water balance in mountainous terrain is strongly modulated by the amount and phase of precipitation (e.g., Hamlet et al. 2007, Berghuijs et al. 2014, Li et al. 2017, Musselman et al. 2017, 2018). However, the detailed characterization of precipitation in mountainous environments is extremely poor in comparison to less topographically-complex locations (Henn et al. 2018). Operational weather radar coverage in the mountainous regions of the continental United States is exceedingly sparse due to radar beam blockage (Maddox et al. 2002, National Research Council 2002). The actual time-varying precipitation amount and phase across much of the Rocky Mountains currently is estimated from a series of point observations, or from precipitation satellites such as the Tropical Rainfall Measuring Mission (TRMM) and Global Precipitation Measurement (GPM). Unfortunately, there is a strong potential for biases from point observations since steep slopes, high elevations, and forested sites are underrepresented in the measurement network (e.g., Sevruk 1997, Frei and Schär 1998, Henn et al. 2018), and gauge undercatch of precipitation is ubiquitous, particularly for snowfall (e.g., Pan et al. 2003, Rasmussen et al. 2012). Interpolating between point observations has been found to depend strongly on the number, type, and spatial/elevational distribution of observations (Zhang et al. 2017) and to be

possibly the most important source of rainfall/runoff model errors (Moulin et al. 2009). Meanwhile, satellite precipitation estimates in complex terrain can also have significant biases (Prat and Barros 2010), particularly for winter orographic precipitation.

During the cold season, most precipitation is orographically produced. Several key processes control orographic precipitation properties, as depicted in Figure 7. They evolve during a storm life cycle as described in Stoelinga et al. 2013 including:

1. Precipitation growth of liquid droplets from collision/coalescence, and of ice particles from deposition, aggregation, riming, and secondary ice formation.
2. Precipitation loss from sublimation and evaporation.
3. The interaction of microphysics with orographic flows, including how microphysics varies with channeled flow, blocking, gravity waves, and small-scale turbulence.
4. The seeder-feeder process for enhancing low-level orographic precipitation from high-level precipitation driven by larger-scale circulations.

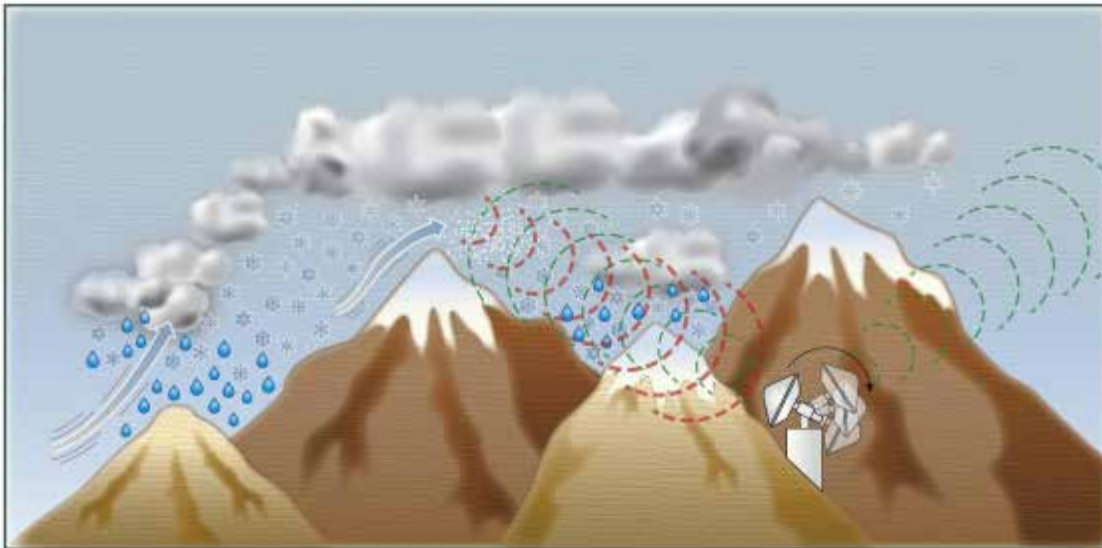


Figure 7. Info-graphic showing precipitation micro- and macro-physical processes that contribute to precipitation in high-altitude complex terrain. Mechanical, upslope airflow induces a wide range of processes as described by Stoelinga et al. 2013.

During the warm-season, most precipitation comes from moist convection driven by thermally-driven upslope flow and the larger-scale North American Monsoon (NAM), which transports water vapor into the continental interior from the Gulf of California and Gulf of Mexico (Adams and Comrie 1997). The (Zhu et al. 2005) but influences of localized land surface conditions (e.g., soil moisture) need to be considered. Several studies have suggested an inverse relationship between winter snow accumulation and summer rainfall, with decreased snow accumulation driving reduced soil moisture such that less energy is needed to heat the land surface and this enhances the onset of rains (Gutzler 2000, Lo and Clark 2002, Zhu et al. 2005), while in contrast, a positive soil moisture and rainfall feedback has been found by others

(e.g., Vivoni et al. 2009), and work by Carroll et al. (2020) pointed to the delicate and intertwined relationship between summer precipitation and winter snowfall.

In the East River Watershed, there is widespread, though indirect, evidence of variability in the spatial and temporal distribution, phase, amount, and intensity of precipitation. Weather stations show a large range of cold-season precipitation and ASO surveys (https://nsidc.org/data/ASO_3M_SD/versions/1), as highlighted in Figure 8. The ASO surveys measure the snow-depth at the end of the accumulation season, which suggests far more precipitation in the mountains to the west of the East River Watershed, with Crested Butte Mountain receiving relatively far less precipitation. While the ASO surveys measure a quantity that is integrated over many snow processes, their SWE measurements are the single best predictor of water resources during the water year and the role of precipitation is dominant (Oaida et al. 2019).

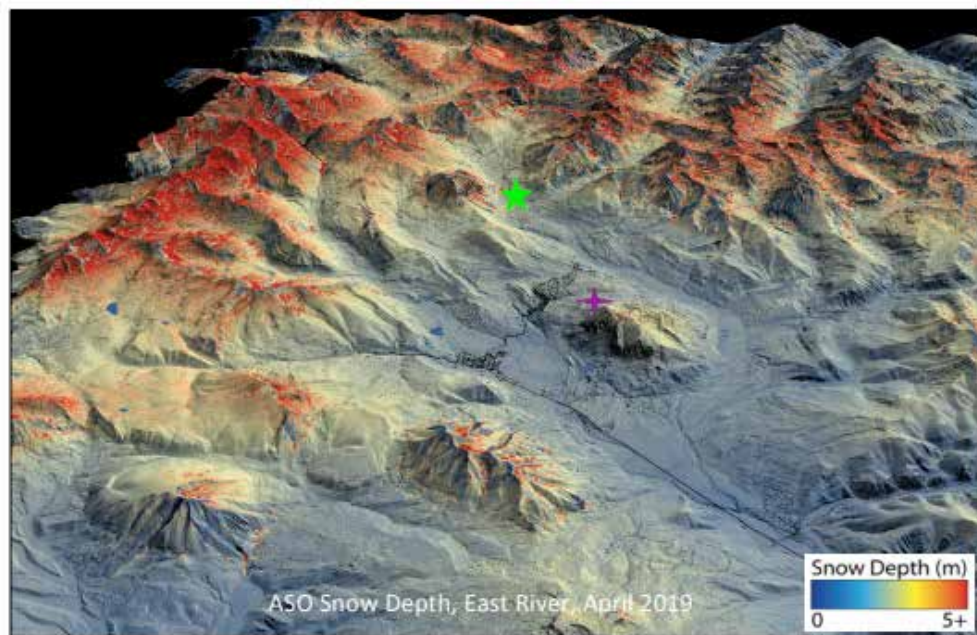


Figure 8. ASO-measured snow depth around Crested Butte, Colorado (green star denotes AMF2 location; purple cross denotes XBPWR and AOS location) in early April, 2019.

Dynamics from the synoptic- to the field-scale, along with microphysical processes described above may be influencing these patterns. SAIL seeks to develop data sets to disentangle cold- and warm-season precipitation processes, as they comprise the dominant hydrologic input to mountainous watersheds (Lundquist et al. 2018). The East River Watershed is currently very limited in terms of data on the spatiotemporal distribution of precipitation phase, amount, and intensity. Efforts to model precipitation are not able to resolve the micrometer-scale processes that control precipitation, so representations of those processes at the kilometer-scale are needed and are represented with bulk microphysics. Several different microphysics schemes seek to capture bulk microphysical state and evolution and co-evolving impacts in complex terrain to develop unbiased estimates of water resources. These schemes seek to develop a simplified description of microphysical evolution with large- and small-scale atmospheric conditions, though often with limited application to ice-cloud microphysics (Harrington et al. 2013). SAIL observations of this evolution will help reveal the strengths and deficiencies of each scheme.

In order to answer SSQ#1, SAIL will measure the spatial and temporal distribution of precipitation phase, amount, and intensity, as well as a number of ancillary data sets, to gain insights into the dynamic and microphysical processes spanning field-to-watershed scales.

2.2 Aerosol Processes

2. How strongly do aerosols affect the surface energy and water balance by altering clouds, precipitation, and surface albedo, and how do these impacts vary seasonally?

There are numerous processes by which aerosol particles, which include secondary organic aerosol (SOA), inorganic particles such as dust, and light-absorbing particles comprised of brown and black carbon, impact the atmospheric and surface precipitation and radiative environments. Figure 9 depicts the long-range effects of aerosols by showing a large number of processes, some of which occur at low altitudes. SAIL's interest arises because these processes impact surface energy and water at high altitudes.

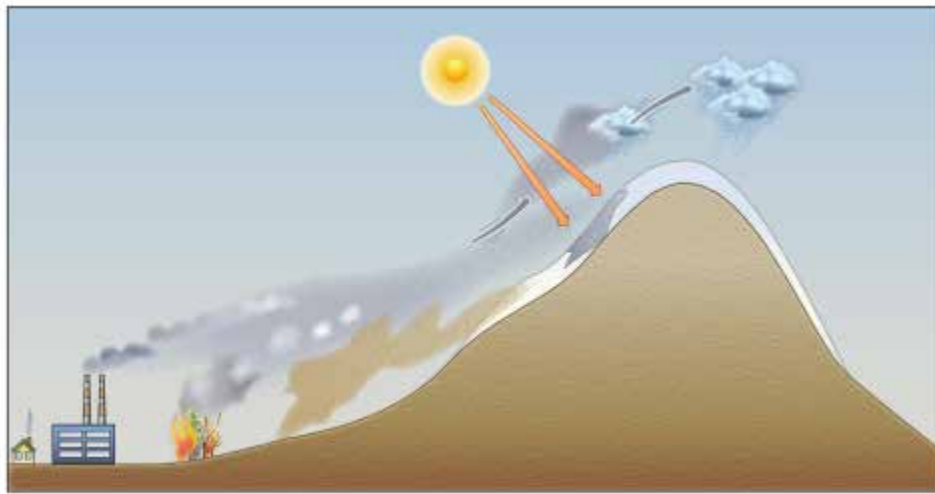


Figure 9. Cartoon of a range of aerosol processes that impact radiation and precipitation and, ultimately, hydrology.

Absorbing particles enhance snowmelt rates by lowering surface albedo, directly in the visible wavelengths and indirectly in the near infrared wavelengths by enhancing snow grain growth (Painter et al. 2007). While this impact has been studied previously, a more holistic view of the role of atmospheric particles that includes radiative impacts of absorbing and scattering aerosol in the air in addition to particles deposited on snow surfaces is required to fully understand the role of aerosols on mountain hydrology. For example, as the primary absorber of visible light in the atmosphere, atmospheric black carbon (BC), a product of incomplete combustion, can both reduce the amount of incident irradiance at the snow surface when present in aerosol and increase the amount of absorbed solar radiation when present at the snow surface. Snow-deposited absorbing particles tend to decrease atmospheric stability and increase turbulent fluxes, while entrained absorbing aerosols will tend to produce the opposite effect (Flanner et al. 2009, Hansen and Nazarenko 2004, Kaspari et al. 2011, Ramanathan and Carmichael 2008). Brown carbon (BrC) aerosols have been implicated as major drivers for cryospheric melt in high-altitude terrain, but are severely understudied (Wu et al. 2016). SOA has an important role to play as a precursor to BrC aerosols and in CCN formation, the latter of which is

discussed in detail in SO#4. Unfortunately, despite the radiative importance of atmospheric particles, both suspended in air as aerosols and deposited on snow surfaces, their energetic impacts are poorly constrained by observations and have been primarily informed to date by models (i.e., Bond et al. 2013).

Key to understanding the impacts of aerosols on radiation at the surface or in the atmosphere is obtaining a comprehensive set of observations of relevant aerosol properties that provide insights into the life cycle (formation, growth, and removal) of aerosol particles in Colorado. For example, observations at the Storm Peak Laboratory (Hallar et al. 2011, Kassianov et al. 2017), which is geographically proximal to the proposed deployment location for SAIL, suggest that long-range transported dust particles, while important aerosol constituents, do not deposit enough mass to visibly darken the snow surface (Gannet Hallar, Pers. Comm. 2018) and therefore these events may alter the energy flux in the atmosphere but not at the surface. In contrast, the regional dust events from the southern Colorado Plateau/Great Basin clearly impact snow albedo, snow melt rates, and regional hydrology (Painter et al. 2010, 2018).

Given their regional and short-lived nature, the relative importance of atmospheric radiative forcing by these episodic events is not clear. Measurements of aerosols performed at mountaintop stations show frequent new particle formation (NPF) events, often associated with intrusions of free tropospheric air and its interactions with boundary-layer trace gases (Kerminen et al. 2018). In several high-altitude sites, NPF was found to be strongly associated with upslope valley winds bringing air from lower altitudes, plausibly from the boundary layer (BL) (Weber et al. 1995, Shaw 2007, Nishita et al. 2008, Venzac et al. 2008, Rodriguez et al. 2009, Shen et al. 2016). Those upslope winds likely provide precursors such as reduced nitrogen compounds that lead to the formation of secondary BrC (Nguyen et al. 2013). In addition, biomass burning is an important source of primary black and brown carbon (Laskin et al. 2015), which can change atmospheric temperature and moisture profiles and affect cloud formation. The range of these processes is depicted in more detail in Figure 10.

Another key part of SSQ#2 concerns aerosol impacts on precipitation over mountainous regions. These impacts depend on atmospheric conditions, particularly relative humidity and cloud temperature (Lynn et al. 2007, Saleeby et al. 2009, Fan et al. 2014), aerosol properties (Givati and Rosenfeld 2004, Fan et al. 2014, 2017), and the terrain features such as mountain height and cross-mountain width (Mühlbauer and Lohmann 2006, 2008). There are qualitative differences in orographic precipitation between a low CCN and very high CCN conditions. The spillover factor of precipitation (i.e., the precipitation ratio over the leeward to windward side) was found to be enhanced via increases in cloud condensation nuclei (Mühlbauer and Lohmann 2006, Saleeby et al. 2011). Cloud phase – particularly the mixed-phase regime – could be very sensitive to ice-nucleating particles (INPs) such as long-range transported dust, leading to a large impact of aerosols on snow precipitation (Fan et al. 2017). The cloud microphysics feedback to dynamics through aerosol-cloud interactions was shown to change the mountain-valley circulation and enhance orographic mixed-phase clouds and precipitation (Fan et al. 2017). For light-absorbing aerosols such as black and brown carbon, through radiative effects aerosols can redistribute the moist static energy between the mountain and associated plain region and cause extreme precipitation over the mountains under a warm and moist synoptic condition over Southwest China (Fan et al. 2015), but suppress mountain-valley circulation and reduce the precipitation in a dry condition over Mt. Hua (Yang et al. 2016).

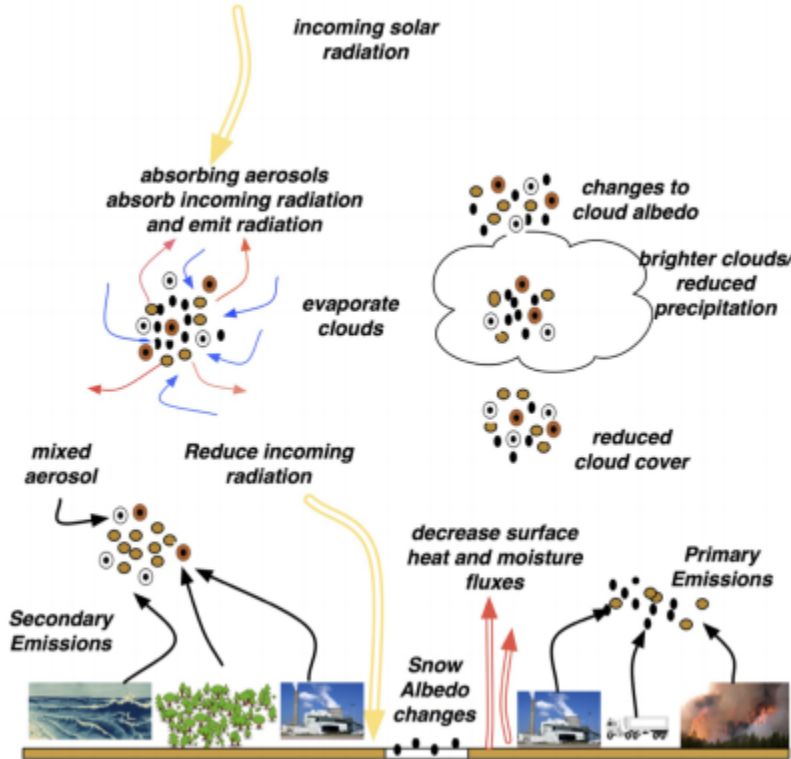


Figure 10. Diagram of range of atmospheric aerosol processes and their impacts.

Over the complex terrain of Colorado, Saleeby et al. (2011) found that the spillover effect is higher in the high mountains like the San Juan Range where high cloud water path (CWP) and ice water path (IWP) co-exist and is relatively lower in central high mountains because of less supercooled liquid water content. The synoptic scale flow and environmental factors like humidity largely control aerosol effects on the orographic precipitation. Therefore, aerosol impacts on the distribution and magnitude of precipitation over orography may vary by season.

Long-term records of INP concentrations in the Rocky Mountains are notably lacking, but the limited data that do exist, as shown in Figure 11a, are consistent with lower aerosol loadings overall in winter, and especially the lack of soil particle or organic and biological INP sources that may be elevated over higher-altitude forest regions during wet periods and summer convective storm events (Huffman et al. 2013, Prenni et al. 2013). Summer biomass burning may also potentially influence INPs in this region (McCluskey et al. 2014), as measurements during fires along the Colorado Front Range indicate INP concentrations exceeding ambient values near fire regions and falling near the upper bound of measurements in various campaigns in Figure 11b.

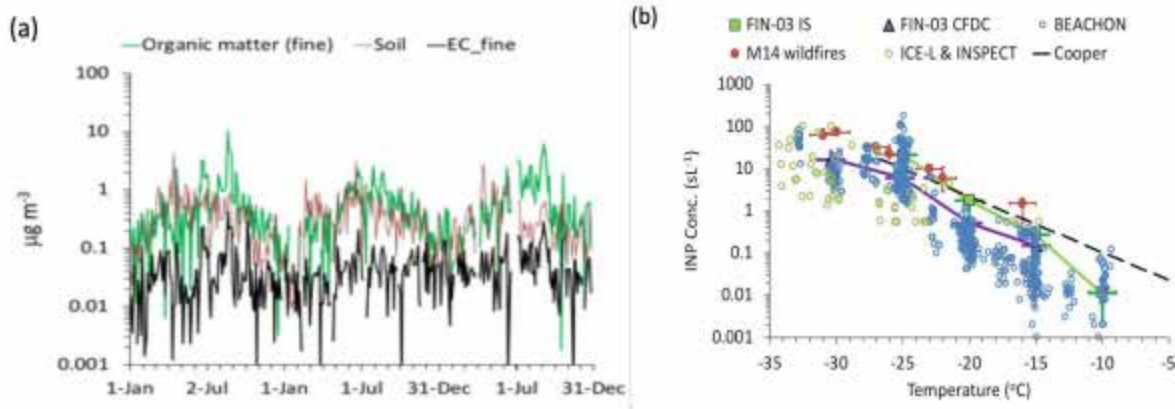


Figure 11. Annual cycles of aerosol mass concentrations of fine organic and elemental carbon, and soil dust, at the White River Interagency Monitoring of Protected Visual Environments (IMPROVE) network (Malm et al. 1994) site, located close to the proposed SAIL site, at 3413 m MSL, 39.1536 latitude, -106.8209 longitude. (b) INP concentrations via immersion freezing collected by several campaigns since 2000 in the Colorado Mountains.

In order to answer SSQ#3, SAIL will bring together observations of aerosols at the surface and in the atmosphere, along with measurements of clouds and precipitation for nearly two complete seasonal cycles.

2.3 Snow Processes

3. What are the contributions of radiation, turbulent fluxes of sensible and latent heat, and snow sublimation to the water and energy balance of the snowpack?

Several snow processes are key to understanding the hydrology of the East River Watershed, including snow sublimation, downwelling and upwelling shortwave and longwave radiation, and non-radiative energy fluxes of sensible and latent heat, and all of these are parameterized in atmospheric and surface process models.

In the wintertime, nearly continuous snow cover yields a high surface albedo and low surface upwelling longwave radiation, while clouds generally decrease surface downwelling shortwave radiation while increasing surface downwelling longwave radiation. Turbulent latent and sensible heat fluxes are generally smaller than radiative fluxes on seasonal time-scales (Willis et al 2002, Hock 2005), but these fluxes can exceed net radiation for brief periods of hours to days (Anderson et al. 2010). In the spring, the relative roles of radiation, the influence of clouds, and turbulent sensible and latent heat fluxes can change from winter and can vary spatially and temporally. The surface albedo generally becomes much more heterogeneous with patches of unfrozen and frozen surfaces, darker snow from melting and impurities, and this can induce advective heat fluxes (e.g., Liston 1995). During this season, the presence of persistent clouds generally produce a net negative effect (cooling) on surface radiation and can determine whether the surface melt energy for snow is dominated by radiation or turbulent or latent heat fluxes.

Figure 12 shows that patterns of SWE measured by ASO from 2016 to 2018 are similar at the end of the accumulation season (around April 1) across the watershed, but that the SWE at higher elevations was

more variable. Observations in late spring showed the impact of rapid decay of the snowpack with increased radiation and warming temperatures in the spring. The ASO survey in late May, 2018 shows only isolated pockets of remaining snow compared to April, and that the snow melt occurs preferentially at lower elevations. The change in distributions of SWE is strongly driven by radiative processes.

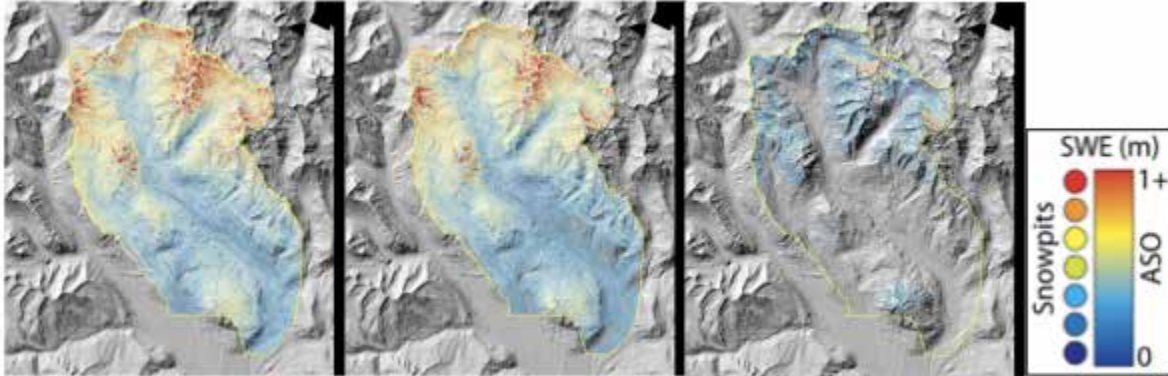


Figure 12. ASO Snow Water Equivalent Retrieval Comparison over the East River Watershed from (left) April 1, 2016, (center) March 30, 2018, and (right) May 24, 2018.

Meanwhile, radiation and turbulent fluxes of sensible and latent heat are modulated by solar angle and surface and atmospheric conditions. Figure 13 shows a schematic of fluxes and how they vary dramatically between the winter and the spring.

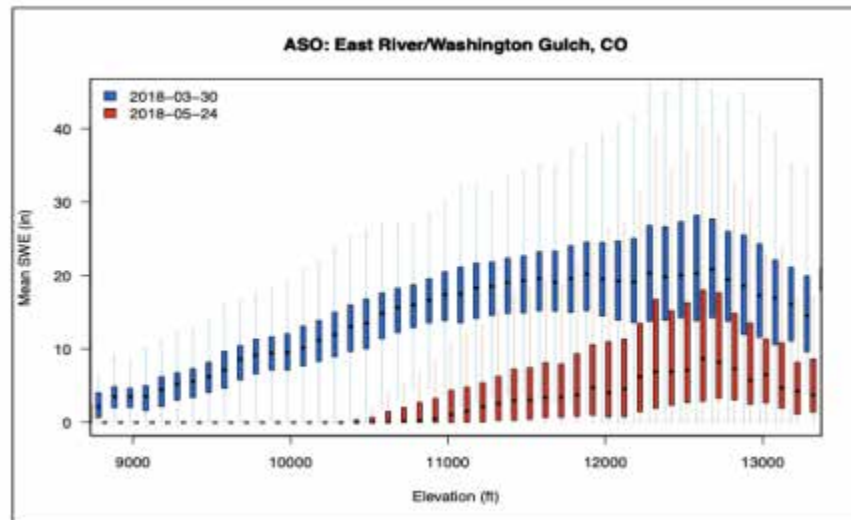


Figure 13. Box-whisker plots (box spans 25-75th percentile and whiskers span the 5th to 95th percentiles) of ASO SWE as a function of elevation bin.

Finally, snow sublimation processes have been estimated to reduce seasonal snowpack by over 20% (Mott et al. 2018), but there is large uncertainty in that estimate, with some studies showing a 0.1% effect (Groot Zwaafnick et al. 2013) and others showing a 25% effect (Liston and Sturm 2002). The central challenge for estimating sublimation is that such an estimation requires more than just measuring sublimation tendencies governed by atmospheric temperature and humidity, because most sublimation (~78%) occurs in lofted snow particles (Vionnet et al. 2014) due to the vast increase in surface area of

those particles. Therefore, the sublimation process depends both on winds, atmospheric thermodynamics, and entrainment particularly in the near-surface environment (Jennings et al. 2018).

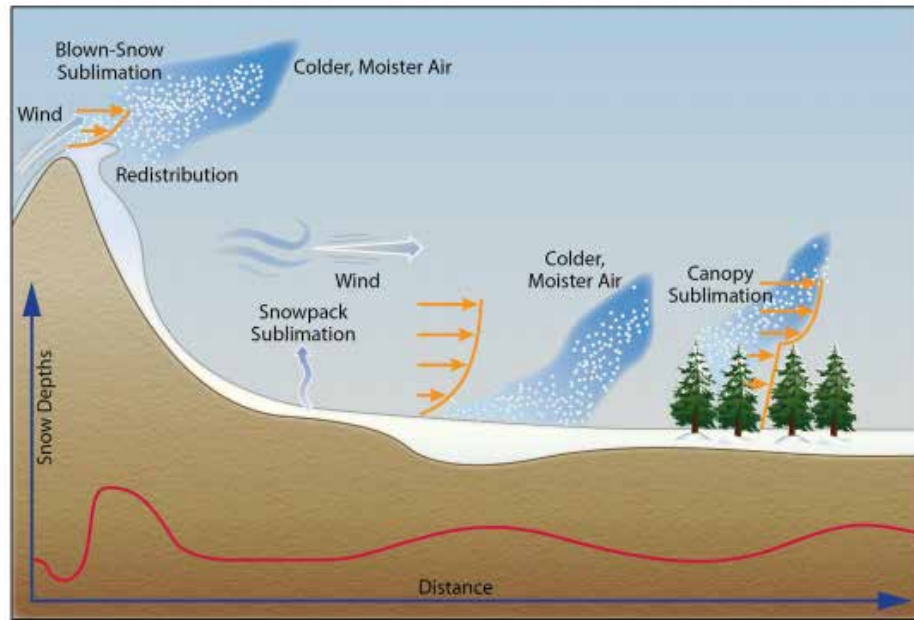


Figure 14. Cartoon of three major areas where snow sublimation occurs: Over the snowpack, in the canopy, and at ridgelines in blowing snow plumes. Also depicted is the latent heat associated with sublimation phase-change.

While microphysical sublimation is well understood and can be modeled as a diffusive transport of water vapor from a snow crystal (Jambon-Puillet et al. 2018), macrophysical sublimation is much more difficult to constrain outside of the laboratory. Sublimation is almost exclusively calculated by, and is highly dependent on, unconstrained assumptions. Canopy sublimation loss estimates depend on assumptions of how temperature and humidity vary in the canopy along with the amount of snow intercepted by the canopy and within-canopy turbulent fluxes. Blowing-snow sublimation loss estimates for an individual plume depend on assumptions of within-plume temperature and humidity estimates and the concentration and size distribution of blowing snow particles, and all of these terms are unconstrained (Svoma 2016).

Calculations of annual sublimation losses based on field observations and modeling in Germany, for example, indicate the dominance of blowing-snow sublimation and its preferential occurrence at higher elevations near ridgelines. Figure 15 shows calculations performed by the National Operational Hydrologic Remote Sensing Center (NOHRSC) over the Colorado Rocky Mountains and Crested Butte, highlighting the spatiotemporal variability of SWE and blowing-snow sublimation. While both processes vary spatially, SWE varies slowly with time, punctuated by storm events, though blowing-snow sublimation varies with winds and atmospheric thermodynamics on faster timescales.

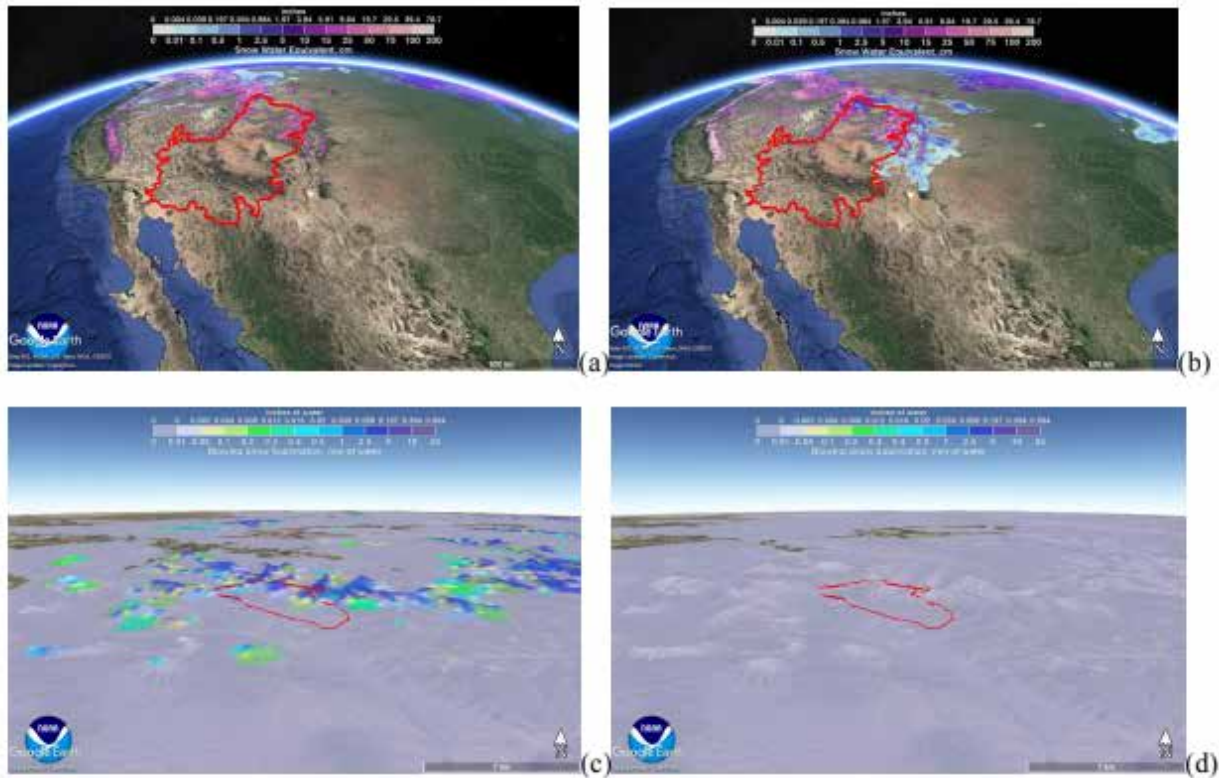


Figure 15. NOHRSC estimates of (a) April 1, 2020 SWE, (b) April 1, 2019 SWE, (c) April 1, 2020 blowing-snow sublimation and (d) April 1, 2019 blowing-snow sublimation.

Radiation, turbulent fluxes of sensible and latent heat, and sublimation are marked by their spatial heterogeneity and challenges associated with making field-scale observations and extrapolating from sparse observations to larger domains. Given this situation, answering SSQ#3 requires the development of objectives that recognize the need for supporting modeling activities and use observations to address the largest sources of uncertainty in those activities.

In order to answer SSQ#3, SAIL will collect direct measurements of radiation and the turbulent fluxes of sensible and latent heat over the time-varying snowpack across two accumulation and melt seasons. Observational constraints on snowpack, canopy, and blowing-snow sublimation will also be developed with the campaign.

2.4 Warm-Season Processes

4. How do atmospheric and surface processes set the net radiative absorption that is known to drive the regional flow of water into the continental interior during the summer monsoon?

During the summer, the local radiative forcing becomes increasingly important for large-scale circulation, driving low-level flow that transports water vapor into the continental interior from the Gulf of California and Gulf of Mexico (Adams and Comrie 1997). Radiative fluxes in the Rockies are thus crucial for controlling regional-scale winds and precipitation in summer; these fluxes produce a column-integrated energy source (CIES) that is positive over all of North America in summer and is particularly strong over

western orography (Figure 21). The poleward extent of North American monsoon rainfall is set by a balance between this net, continental-scale energy source and the advection of low-energy air from the cold, mid-latitude ocean (Chou and Neelin 2003, Neelin 2007).

At the local level, the details of the intensity, duration, and frequency of summertime convective events are of hydrologic importance. Here, the evolution of the warm boundary layer in complex terrain involves a wide range of meteorological processes dependent on local and regional conditions. At the local level, a number of qualitatively known atmospheric and surface-state quantities control the CIES. These include the time-varying distributions of atmospheric water vapor, clouds, soil moisture, evapotranspiration, and turbulent fluxes of sensible and latent heat. The complexity of atmospheric flow increases in complex terrain, and most of these flow regimes can be resolved locally with SAIL data. As shown in Figure 16, the CIES has high spatial autocorrelation on seasonal and regional scales, but at the local level there is spatial and temporal heterogeneity. Characterizing how these heterogeneities relax into spatially autocorrelated CIES will have broad applicability for modeling regional-monsoonal flows.

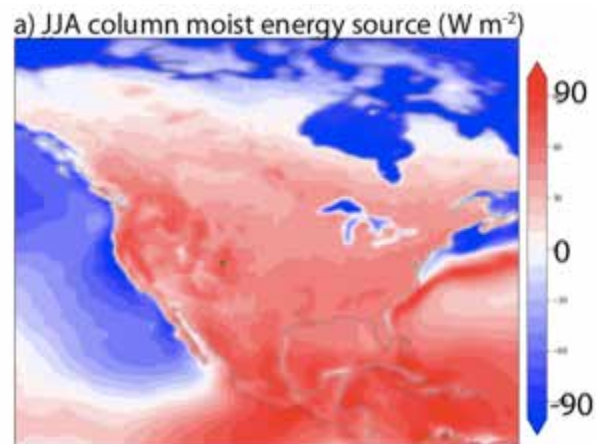


Figure 16. Climatological June-August atmospheric column-integrated energy source, obtained by summing the surface sensible and latent heat flux and the column-integrated radiative flux convergence, as estimated from the Modern-Era Retrospective analysis for Research Applications, Version 2 (MERRA-2) reanalysis.

In order to answer SSQ#4, SAIL will collect direct measurements of boundary-layer evolution, radiation, and the turbulent fluxes of sensible and latent heat over one warm season, along with highly detailed observations of the time-varying cloud and precipitation fields.

These data can then be analyzed to identify and enumerate the processes contributing to these time-varying fields and whether or not the relationships between warm-season processes and warm-season observables are captured by atmospheric process models.

3.0 Scientific Objectives

In order to address SSQs#1-4, SAIL has five interrelated, achievable science objectives (SO#1-SO#5) for high-altitude complex terrain that use both ARM facilities and collaborative resources. The science objectives are discussed below.

3.1 Precipitation Process Characterization

1. Characterize the spatial distribution of orographic and convective precipitation processes on diurnal-to-seasonal time-scales and how those processes interact with large-scale circulation.

This science objective primarily addresses SSQ#1, and SAIL will achieve this SO#1 by establishing a baseline set of observations of this precipitation principally from the XBPWR. CSU will use data from the XBPWR to return several data products (ZH, ZDR, ZHV, V, W, HV, NCP, DP, KDP, R) and CSU will provide precipitation amount and hydrometeor classification retrievals at ~100-meter spatial resolution, 5-minute temporal resolution, with a range of 50 km where beams are not blocked.

Precipitation retrievals will be checked against disdrometer data and are expected to achieve a nominal uncertainty of 15% for rainfall (Chandrasekar et al. 2018) and 30% for snowfall (von Lerber et al. 2017).

From these datastreams, the XBPWR will provide detailed precipitation structure information that will be useful for observing embedded convective structures in wintertime storms (e.g., Kumjian et al. 2014), precipitation-type transitions, warm-season orographic convection, and transport of hydrometeors across mountain ridges. Doppler-derived wind fields will also provide useful information on airflow structures (Jackson et al. 2019) over multi-directional ridgelines surrounding the East River basin and the AMF2, which have been documented in other, more limited-duration X-band radar deployments in Colorado (e.g., Gochis et al. 2016). In addition, coordinated range height indicator (RHI) scans from the XBPWR with the KAZR at the AMF2 site will yield multi-wavelength polarimetric radar observations above the AMF2 to probe how hydrometeor microphysics and dynamics interact in the vicinity of that site.

Figure 17 shows a summary of beam-blockage analysis for the XBPWR system for different elevation angles, using the closest GPM measurements in winter and summer to determine the elevations at which precipitation is likely to occur for those seasons and masking the range of the XBPWR accordingly. This figure, along with Figure 18, show that XBPWR measurements will provide excellent coverage over the East River Watershed and the AMF2 throughout the SAIL campaign and will provide extended coverage to a radius of 20 km in winter at 40 km in summer. The radar's location on Crested Butte Mountain is designed to enable measurements of incoming storms and is blocked to the south and southeast because few precipitation events come from that direction.

Previous work with XBPWR in high-altitude complex terrain has shown that radar observations coupled with flow modeling can produce a remarkable amount of insight into precipitation processes. Mott et al. (2014) showed that, at least for a single winter storm in Switzerland, XBPWR data and analysis showed that orographic effects of snow deposition effects could be largely attributed to the seeder-feeder process. Since ice microphysical processes such as vapor deposition, riming, and aggregation have observable “fingerprints” in polarimetric radar data (e.g., Schrom et al. 2015, Moisseev et al. 2015, Schrom and Kumjian 2016, Kumjian and Lombardo 2017), SAIL can follow the approach of Mott et al. (2014) to produce a much more comprehensive characterization and assessment of the relative importance of microphysical processes over the East River Watershed. This can be especially useful for understanding how vertical gradients in precipitation are more pronounced in some parts of the watershed as compared to others, with implications for what is being missed by the lack of radar observations in complex terrain.

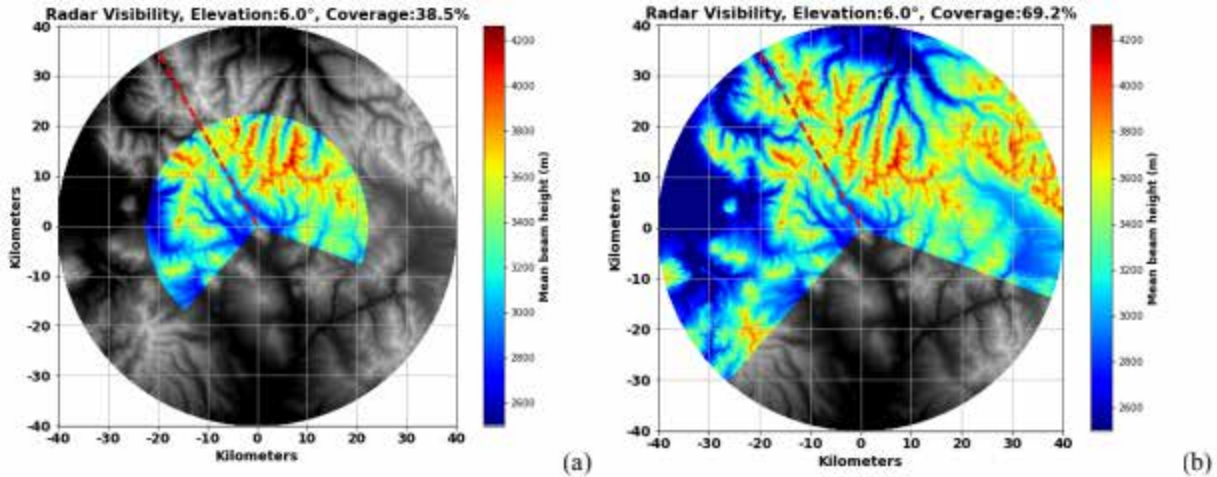


Figure 17. XBPWR beam-blockage analysis from the Old Teocali Lift site showing radial coverage in (a) winter and (b) summer. Color indicates beam height of likely measurement of precipitation based on nearest GPM precipitation height retrievals. Red-dashed line connects radar site to AMF2 site.



Figure 18. Panoramic drone photo of Old Teocali Lift site looking towards Gothic, Colorado. Acquired February 19, 2021 by Dr. Ian Breckheimer. Horizontal line indicates approximate height of XBPWR antenna.

During the warm season, convective clouds and precipitation will be measured along with radiative forcing to help address SSQ#4 and develop relationships between column energy sources and large-scale convection. The connection of precipitation processes to regional-scale atmospheric flow patterns that is an integral part of SSQ#1 will be achieved through integration of measurements with reanalyses and constrained variational analyses (e.g., Tang et al. 2016).

3.2 Cold Snow-Season Processes

2. Quantify cold-season land-atmosphere interactions that alter snowpack mass balance through wind redistribution and sublimation and the spatial scaling of those processes.

Winds impact mountainous hydrology by redistributing snowpack in ways that can have significant hydrological consequences, including carrying snow over a mountain crest and into or out of the watershed of interest (Mott et al. 2018). For example, in the East River Watershed, the observed distribution of snowpack from the ASO, as shown in Figure 18, suggests that deposition occurs on windward slopes, yet winds may be redistributing snow from windward to leeward slopes.

For this science objective, SAIL will develop observationally constrained estimates of the impacts of wind-redistribution and sublimation on the snowpack across the East River Watershed. While direct observations of these processes are not possible, observational constraints on the terms needed to

calculate sublimation, including the co-evolution of the spatiotemporal distribution of blowing-snow occurrence, thermodynamics, and radiation, can be developed with SAIL.

The campaign will collect a series of observations to estimate the sublimation and blowing-snow redistribution to develop a detailed picture of (1) the atmospheric wind-field across the East River Watershed, (2) atmospheric temperature and humidity for sublimation tendencies, and (3) snow entrainment and deposition.

A variety of datastreams will build a detailed picture of the three-dimensional distribution of wind speeds and directions both at the surface, throughout the boundary layer, and into the free troposphere. These include vertical winds from the balloon-borne sounding system (SONDE) and the radar wind profiler (RWP). Surface wind observations will be provided by the AMF2 surface meteorology package and will be supplemented by the six existing Watershed Function SFA meteorological stations, the latter of which are distributed across alpine, sub-alpine, and montane terrains as shown in Figure 5. Finally, SAIL will use the Doppler Lidar (DL) WIND Value-Added Product, which will provide horizontal wind structure speed and direction in the lowest 3 km of the atmosphere to a maximum horizontal range of 9.6 km from the AMF2 at 30-m resolution depending on signal attenuation by condensates.

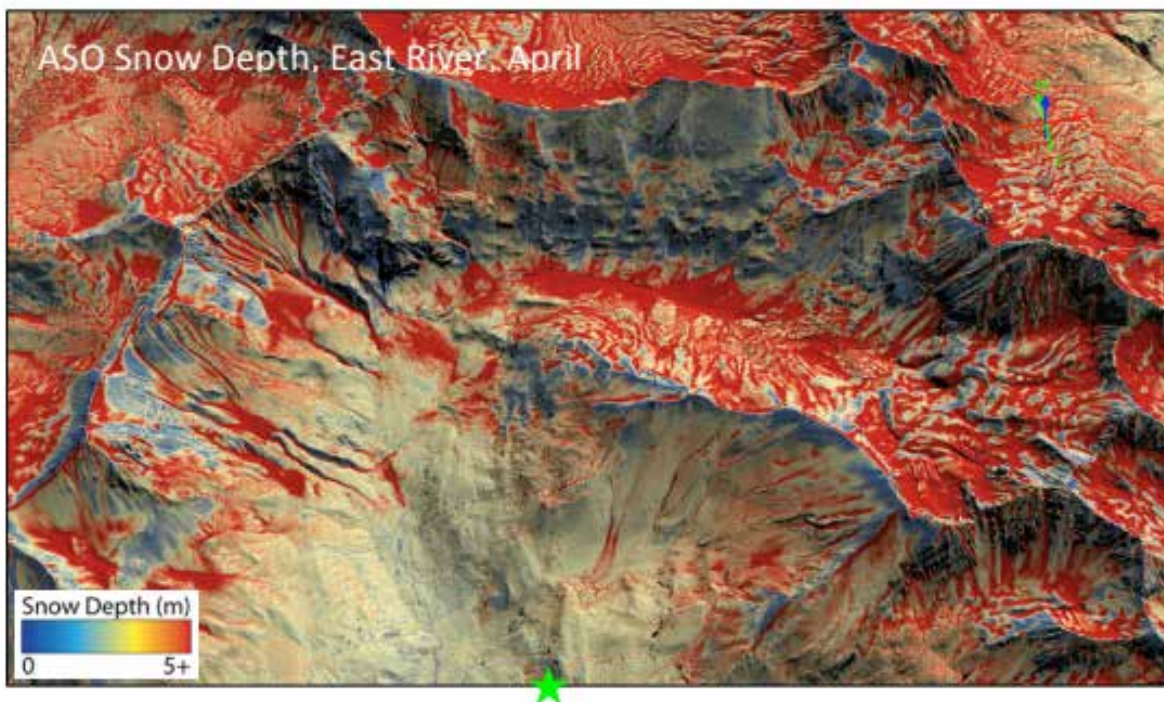


Figure 19. ASO survey of the northern edge of the East River Watershed from April, 2019 showing variability of snowpack near ridgelines. Green star indicates the location of the AMF2 for SAIL.

Atmospheric temperature and humidity conditions will be measured with the surface meteorology stations package from the AMF2 and the Watershed Function SFA meteorology stations, vertically above the AMF2 with the SONDE. Higher frequency of the SONDE launches would better characterize the diurnal evolution of atmospheric thermodynamics. From AERI retrievals in clear-sky conditions every few minutes, supplemented with microwave radiometer (MWR) column water vapor constraints

(e.g., Blumberg et al. 2015), SAIL will leverage the marine AERI's capabilities of scanning across zenith angles between 45 and 135 degrees to assess horizontal variability in temperature and humidity near the AMF2.

Together, these instruments will provide continuous field measurements of the thermodynamic tendency of sublimation, especially from blowing snow. SAIL will establish the spatial variability in sublimation spatial tendencies of mountains at a scale beyond those established from previous, more limited field campaigns (Mott et al. 2018). Given that numerical models predict large spatiotemporal variability in sublimation (Strasser et al. 2008, Groot Zwaaftink et al. 2011, Vionnet et al. 2014), these observations can provide a new level of detail of sublimation's impact, including when and where it occurs, on the seasonal snowpack by resolving blowing snow events. The DL and radar are specifically sensitive to winds in non-precipitating and precipitating events, respectively, and can thereby develop wind redistribution information by observing the location and frequency of wind erosion and deposition.

3.3 Aerosol Regimes and Radiation

3. Establish aerosol regimes, the processes controlling the life cycle of aerosols in those regimes, and quantify the impacts of aerosols in those regimes on the atmospheric and surface radiative budget.

A picture of aerosols that may be observed in SAIL can be seen in Figure 11a, which shows the annual cycle of some relevant particle types at a site from the IMPROVE network (Malm et al. 1994), which lies 25 km northeast of the center of the East River Watershed (but in a different watershed). Organic carbon mass concentrations follow an annual cycle of winter minima and summer maxima that appear driven both by biogenic particle formation and episodic biomass burning events (wildfires). Soil mass concentrations are driven by both episodic regional (e.g., Southwest U.S.) and long-range (Asian) transport of mineral dust in spring (Skiles et al. 2015, Kassianov et al. 2017). Figure 20 shows the preferential deposition of dust at higher elevations that is consistent with long-range transport. Elevated dust concentrations persist through dry summers and reach minimum values from mid-November to mid-February. Elemental carbon has a weak annual cycle, though tending to mimic that for organic matter. Coarse-particle mass follows the organic matter and soil peaks (not shown). These observations indicate that, while there are limited atmospheric aerosol measurements within the East River Watershed, those collected by SAIL can be grouped into regimes.

With this science objective, SAIL will observe and develop a better understanding of the source(s) (long-range transported versus formed in situ via NPF), evolution (e.g., chemical processing such as reactions with reduced nitrogen compounds such as ammonia that leads to secondary BrC formation), and loss pathways such as dry and wet deposition of aerosols in the vicinity of the East River Watershed, and then understand the importance of different aerosol types for the surface and atmospheric radiative environment.

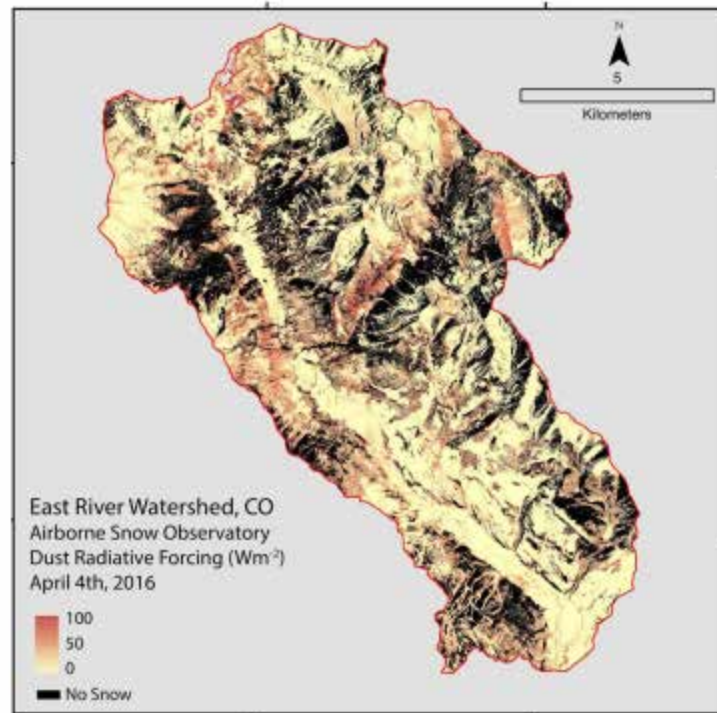


Figure 20. Map of the radiative forcing by deposited aerosols in snow from the ASO flight over the East River Watershed in April, 2016.

Within SO#3, the SAIL campaign will address the following scientific questions:

1. What are the dominant regimes of seasonal aerosol transport, formation, growth, and removal processes in the region?
2. Within these regimes, how do aerosol particles redistribute radiant energy, including warming the atmosphere and/or the surface radiative forcing?

To address SO#3-Q1, SAIL will collect data to enable the categorization of different aerosol regimes sampled across the seasons, such as periods impacted by transported urban pollution (high BC and CO), long-range transported dust events (submicron, supermicron, light-absorbing), biomass burning, clean forest conditions, anthropogenically impacted periods, and stratospheric intrusions. This science objective requires chemical composition data from the aerosol chemical speciation monitor (ACSM) for aerosol composition with sulfate as a marker for long-range transport and from the Organic Aerosol Component Value-Added Product (OACOMP) to distinguish fresh primary organics from secondary and aged organic species. The single-particle soot photometer (SP2) for black carbon and the AOS carbon monoxide (CO) detector will enable measurements that define periods impacted by BC and BrC and urban emission sources as well as local impacts potentially from the town of Crested Butte. With the SP2 and AOP VAP, periods impacted by other absorbing species, including absorbing dust and brown carbon, can be directly identified and will benefit from cloud condensation nuclei (CCN) and ice-nucleating particle (INP) data.

Here the data will enable researchers to look at measured water uptake data to understand whether bulk kappa data can be used from the CCN to represent aerosol water uptake properties within complex mountainous terrain. A higher-order goal to delve further into aerosol water uptake properties will rely

upon humidified tandem differential mobility analyzer (HTDMA) data to understand the impacts of bimodal aerosol regimes as identified by the scanning mobility particle sizer (SMPS), indicating different aerosol sources and chemistries. The aerodynamic particle sizer (APS) will provide additional information beyond the datastreams listed above by identifying periods impacted by supermicron species, often dominated by dust species. A broader correlative analysis of INP data versus aerosol distribution, hygroscopicity, and chemical composition can also be examined.

To address SO#3-Q2, SAIL will develop a detailed characterization of atmospheric radiative properties. AOS observations will be critical to answer SO#3-Q2 by measuring aerosol optical properties, nephelometer, gas-phase CO, and ozone, to determine when the aerosols that are impacted by transported sources are light absorbing. By using SP2 and PSAP data, it will be possible to determine when the measured aerosols are dominated by BC versus other light-absorbing species, such as BrC and dust. These observations will enable closure studies to determine water-uptake data from the CCN and HTDMA to verify predicted kappas by chemical composition. If supplemented by the APS, size distribution measurements can also be used to help identify coarse-mode dust sources. In the absence of an APS, light absorption and scattering can be used from the nephelometer data and compared when sampling submicron-versus-supermicron data with the different impactor size cuts available within the AOS.

The SAIL campaign, through collaborative resources, plans to characterize the radiative effects of deposited aerosols on the snow. As seen in Figure 20 and diagrammed in Figure 21, observations to date from the ASO suggest wind-driven spatial variability in deposited aerosol impacts on snow albedo. Ongoing data collected from snow pits, following Skiles and Painter (2017b) as part of the Watershed Function SFA, can characterize snowpack radiative forcing, because snow pit data reveal the time-evolution of deposition during the accumulation season (See Section 4.0 for details). Once completed, the result of SO#3 will be a detailed, quantitative data set of the relationships between aerosol regimes and their radiative forcing in the atmosphere and at the surface.

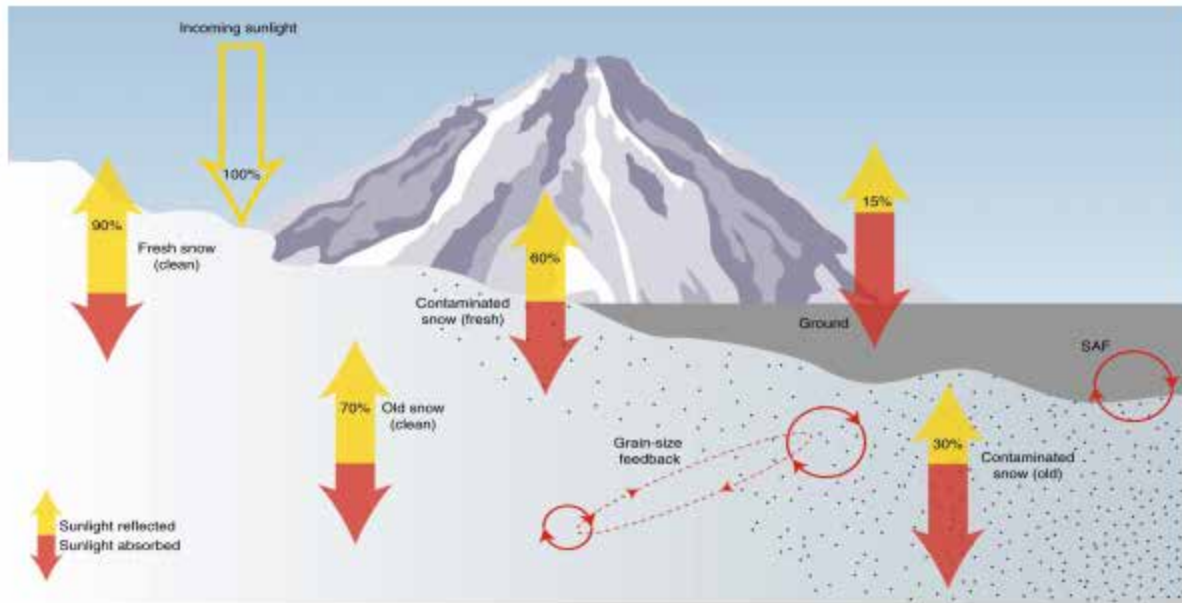


Figure 21. Diagram of impacts of impurities on the surface albedo of snow and associated snow-albedo and grain-size feedbacks.

3.4 Aerosol-Cloud Interactions

4. Quantify the sensitivity of cloud phase and precipitation to cloud condensation nuclei (CCN) and ice-nucleating particle (INP) concentrations.

The SAIL campaign recognizes the impacts of aerosols on precipitation, as it seeks to address SSQ#2. This science objective pertains to characterizing and developing observational constraints for the processes by which CCN and INP impact cloud phase and precipitation. Figure 20 highlights the vertical positioning and length-scales of these processes.

To address SO#4, SAIL will focus on addressing the following sub-questions:

1. Do new particle formation events control the variability of aerosol hygroscopicity and CCN concentrations, and their subsequent impacts on precipitation?
2. What are the contributions of biological particles, wildfires, and long-range transported dust to INP concentrations, do they vary seasonally, and are they linked strongly to precipitation efficiency of clouds?
3. How does the aerosol-precipitation relationship vary with different aerosol regimes, and atmospheric dynamic and thermodynamic conditions?

To address SO#4-Q1, aerosol size distribution from a few nanometers to a few micrometers, composition, hygroscopicity, and CCN concentrations will be obtained mainly from AOS measurements including the SMPS, UHSAS, passive cavity aerosol spectrometer (PCASP), condensation particle counter-fine (CPCF), HTDMA, and CCN instruments. The continuous 18-month measurements of these aerosols' properties will allow us to understand the variability of aerosol regimes.

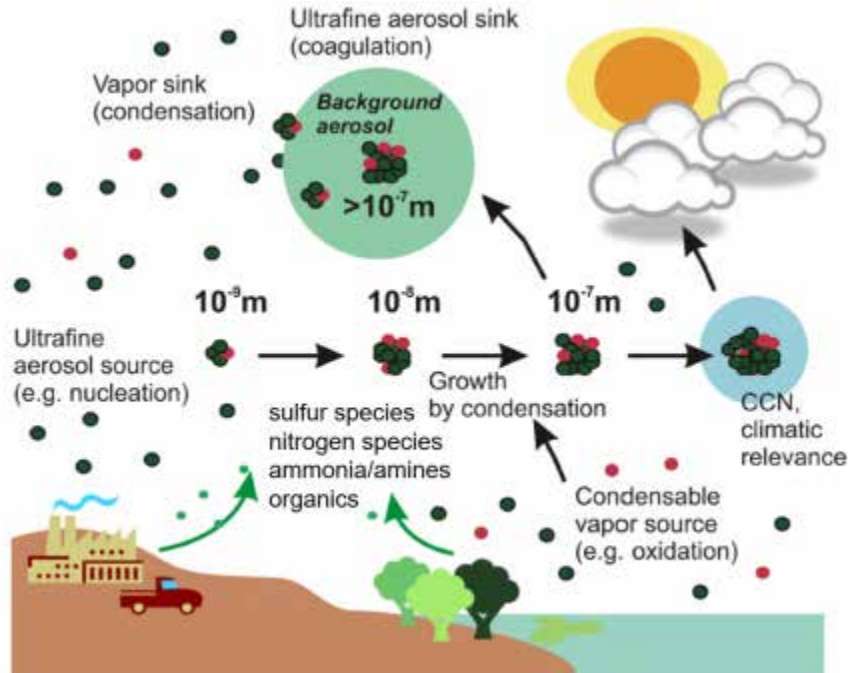


Figure 22. Cartoon of range of aerosol-precipitation processes with the relative vertical positioning in the atmosphere and their length scales.

To address SO#4-Q2, the AOS measurements of aerosol size distribution, hygroscopicity, and CCN characteristics will need to be complemented by INP measurements in order to understand cloud properties and precipitation efficiency of orographic clouds.

To address SO#4-Q3, besides the measurements described for SO#4-Q1 and SO#4-Q2, the measurements of atmospheric meteorology to classify the typical meteorological conditions are essential. It is also important to obtain enough samples for each typical meteorological condition.

Cloud and precipitation measurements are essential to address all three questions above, especially SO#4-Q3. The vertical evolution of hydrometeors and cloud kinematics can be retrieved from the vertically pointing radar. The cloud phase and precipitation information can be obtained from the XBPWR. Surface precipitation rate and surface raindrop size distribution can be measured from rain gauges and disdrometers. With XBPWR data, SAIL can also conduct some process-level analysis of aerosol impacts on the microphysical processes such as vapor deposition, riming, and aggregation, and then precipitation.

3.5 Surface Energy Balance

5. Quantify the seasonally-varying surface energy balance, the land-surface and atmospheric factors controlling it, and the spatial variability in those factors.

In the high-altitude complex terrain of the East River Watershed, the surface energy balance varies dramatically with season. In the winter and spring, it exerts control on the evolution of the frozen surface state and local dynamics, and in the summer, it exerts control on regional dynamics. However, closing the

snow energy balance has proven challenging, even with collocated observations of shortwave and longwave radiation components, ground heat flux, and latent heat fluxes (Helgason and Pomeroy 2012).

For SO#5, SAIL will develop a set of observations that can decompose and understand primary controls on the terms of the seasonally-varying surface energy balance (SEB). A detailed, mechanistic understanding of the land-surface and atmospheric factors controlling SEB enables informed interrogation of process models. SAIL will also evaluate the spatial variability in those factors to characterize this balance in the East River Watershed through the following questions:

1. What are the contributions of clouds, aerosols, humidity, and surface reflection to shortwave and longwave surface radiation and are 3D effects significant?
2. What are the controls on the turbulent fluxes of sensible and latent heat of snow cover and soil moisture?
3. What are the dominant factors controlling the CIES and what are the spatial correlations of those factors in the warm season?

With observations from the AMF2, SAIL can answer these questions by measuring the fluxes of radiation, sensible and latent heat, and the factors controlling them. Radiative fluxes will be provided by the surface energy balance system (SEBS), sky radiometer on stand for downwelling radiation (SKYRAD), and ground radiometer on stand for upwelling radiation (GNDRAD), with observations from the total sky imager (TSI) and AERI scanning across zenith angles from 45 to 135 degrees indicating horizontal heterogeneity in shortwave and longwave surface fluxes, respectively. If observations from cloud stereo cameras can be available in summertime, those observations will characterize the simultaneous heterogeneity in the cloud vertical and horizontal structure to show how cloud type and vertical structure impact surface radiation and other heat fluxes.

Surface radiative fluxes will be supplemented by shortwave and longwave fluxes measured at the meteorological stations maintained by the Watershed Function SFA. Factors controlling these fluxes include atmospheric thermodynamics, clouds, aerosols, and surface albedo. Measurements of atmospheric temperature and humidity (from SONDE/MWR and AERI), (3) surface albedo (from SEBS), (4) the impact of aerosols on radiation (derived from the MFRSR and Cimel sunphotometer [CSPHOT]), and (5) the impact of clouds on radiation (from the micropulse lidar [MPL] and KAZR) provide estimates of these factors. Turbulent fluxes of latent and sensible heat will be measured by the eddy correlation flux measurement system (ECOR), and Co-Investigator Gochis' guest eddy covariance tower, with the three-dimensional structure of boundary-layer turbulence characterized by the DL. Additionally, these fluxes can be estimated from net radiation, temperature, and humidity measurements distributed across the watershed following Sullivan et al. (2019a,b) in order to quantify the spatial heterogeneity in the fluxes.

For SO#5-Q1, collocated observations of atmospheric and surface state and their spatiotemporal distributions will be collected. Additionally, the importance of 3D effects can be analyzed observationally.

For SO#5-Q2, observations of the relationships between turbulent fluxes of sensible and latent heat and the distribution of snow cover and soil moisture will be collected. The former can be derived from visual inspections and ongoing satellite measurements such as the Moderate Resolution Imaging Spectroradiometer (MODIS) and the latter is derived observationally from the Watershed Function SFA's

ongoing measurements of surface volumetric soil moisture at six sites across the East River Watershed. Through widely used parameterizations, we can establish how surface states impact these turbulent fluxes in complex terrain.

For SO#5-Q3, SAIL data will develop the CIES by using observing surface radiative fluxes, turbulent fluxes of sensible and latent heat, and supplemental top-of-atmosphere (TOA) observations using 3-hourly estimates of TOA shortwave and longwave fluxes from the Clouds and the Earth's Radiant Energy System (CERES) synoptic product. Matching the difference in scales between the surface and TOA data will require follow-on science activities discussed in Section 6.

4.0 Measurement Strategies

Instruments

The science objectives of SAIL motivate a range of measurements and measurement strategies using the campaign instruments and linking SAIL observations to collocated measurements from collaborative resources.

First, however, we delineate the relevance and importance of SAIL AMF2 and XBPWR measurements to achieving the campaign's science objectives. This sets the priority for measurement strategies and also the priority to ensure continuity in data throughout the campaign. The following list details this information:

1. **ACSM**: Priority: **Critical**; science objectives: 3, 4; rationale: Aerosol speciation measurements are needed to detect sulfate as a marker for long-range transport, ammonium and nitrate for aerosol processing, and primary and secondary organic aerosol via the OACOMP VAP.
2. **AERI**: Priority: **Critical**; science objectives: 2, 4, 5; rationale: Vertical profiles of temperature and humidity and their horizontal variability are needed for sublimation rate and radiation sensitivity studies.
3. **AOSMET**: Priority: **Important**; science objectives: 2, 3; rationale: Secondary surface meteorology conditions are important for constraining sublimation rates and ambient atmospheric conditions for aerosols.
4. **CCN**: priority: **Critical**; science objectives: 3, 4; rationale: Cloud condensation nuclei are needed to understand relationships between observed cloud and aerosol properties.
5. **CEIL**: priority: **Important**; science objective: 3; rationale: Ceilometer data are important for determining clear-sky and/or aerosol-free conditions.
6. **CO**: priority: **Important**; science objective: 3; rationale: Carbon monoxide measurements are important for determining when observed aerosols may be the result of combustion.
7. **CPC**: priority: **Important**; science objectives: 3, 4; rationale: Condensation particles observations are important for measuring fine and ultrafine aerosol particle modes.
8. **CSPHOT**: priority: **Important**; science objectives: 3, 5; rationale: Aerosol optical depth measurements are important for constraining aerosol radiative effects.
9. **DL**: priority: **Critical**; science objectives: 2, 5; rationale: Wind measurements are critical for determining snow erosion/deposition and contextualizing ECOR observations.

10. **ECOR**: priority: **Critical**; science objective: 5; rationale: Eddy covariance measurements are critical for determining turbulent fluxes of sensible and latent heat.
11. **GNDRAD**: priority: **Critical**; science objective: 5; rationale: Surface shortwave and longwave radiation components are needed to understand surface energy balance.
12. **HSRL**: priority: **Critical**; science objectives: 2, 3; rationale: These observations are needed to understand the scattering properties of particles including aerosols and blowing snow.
13. **HTDMA**: priority: **Important**; science objective: 3; rationale: These observations will support a higher-order goal of understanding the impacts of bimodal aerosol regimes as identified by the SMPS.
14. **INP**: priority: **Critical**; science objective: 4; rationale: These observations are needed to understand aerosol controls on cloud phase and the impacts on snowfall, and to differentiate aerosol sources.
15. **IRT**: priority: **Nice to have**; science objectives: 1, 5; rationale: Surface radiative temperature can help constrain observed surface longwave radiation.
16. **KAZR**: priority: **Critical**; science objectives: 1, 4; rationale: Vertical cloud properties are critical for constraining cloud/precipitation microphysics and cloud susceptibility to aerosols.
17. **MET**: priority: **Critical**; science objectives: 2, 4, 5 rationale: Primary surface meteorology conditions are critical for constraining sublimation rates and ambient atmospheric conditions for aerosols.
18. **MFRSR**: priority: **Critical**; science objectives: 3, 4; rationale: Ambient aerosol amount measurements are critical and help constrain aerosol optical depths for understanding their radiative impacts.
19. **MPL**: priority: **Critical**; science objectives: 3, 5 rationale: These observations are critical for measuring the impact of clouds, aerosols, and surface radiation.
20. **MWR3C**: priority: **Important**; science objectives: 2, 4, 5; rationale: Primary observations on column water vapor and cloud water are important for constraining water vapor profiles and cloud radar measurements.
21. **MWRLOS**: priority: **Nice to have**; science objectives: 2, 5; rationale: Secondary observations of column water vapor and cloud water help constrain water vapor profiles and cloud radar measurements.
22. **NEPH**: priority: **Important**; science objectives: 3, 4; rationale: Light absorption and scattering data can be compared when sampling sub- versus super-micron data with different impactor size cuts.
23. **OZONE**: priority: **Critical**; science objective: 3; rationale: Ozone surface concentrations are needed for determining potential sources of transported aerosols.
24. **PARS2**: priority: **Critical**; science objective: 1; rationale: Surface precipitating or entrained hydrometeor particle size and fall speed are critical for validating XBPWR retrievals, especially for snow.
25. **PSAP**: priority: **Critical**; science objectives: 3, 4; rationale: These data are critical for working in conjunction with SP2 to determine when aerosols are dominated by BC versus other light absorbing species, such as BrC and dust.
26. **RWP**: priority: **Critical**; science objectives: 2, 3, 5; rationale: Continuous vertical wind profiles are needed in non-precipitating conditions to resolve wind gradients in BL and free troposphere (FT).

27. **SEBS**: priority: **Critical**; science objective: 5; rationale: Surface energy and simultaneous soil moisture data are critical for interpreting products derived from ECOR data.
28. **SKYRAD**: priority: **Critical**; science objective: 5; rationale: Downwelling shortwave and longwave radiation are critical for complementing GNDRAD and providing validation and heterogeneity data.
29. **SMPS**: priority: **Critical**; science objectives: 3, 4; rationale: These data are critical to provide size-resolved, indirect measurements of particle composition and new particle formation and growth in ambient aerosols, in conjunction with HTDMA data.
30. **SONDE**: priority: **Critical**; science objectives: 2, 4, 5; rationale: These data are critical for determining atmospheric thermodynamic profiles for sublimation and radiation.
31. **SP2**: priority: **Critical**; science objective: 3; rationale: Critical for identifying BC aerosols, for combining with PSAP to determine dominant aerosol species, and for combining with the Aerosol Optical Properties (AOP) VAP to identify when absorbing aerosols are dominated by absorbing dust and BrC.
32. **TSI**: priority: **Important**; science objective: 5; rationale: Hemispherically resolved cloud fraction is important for understanding heterogeneity in cloud radiative forcing.
33. **UHSAS**: priority: **Important**; science objectives: 3, 4; rationale: Surface aerosol size distribution information is important and will complement other AOS measurements.
34. **XBPWR**: priority: **Critical**; science objectives: 1,4; rationale: Spatial and temporal distribution of precipitation is necessary to characterize the topographic and microphysical drivers of precipitation variability.
35. **WBPLUVIO2**: priority: **Nice to have**; science objective: 1; rationale: Surface warm-season precipitation observations are useful for validating XBPWR precipitation retrievals.

Value-Added Products

Building from the measurements, several VAPs would also advance SAIL's science objectives. Below we list the VAPs that will be developed for SAIL, the science objectives they will support, and rationales for their inclusion.

1. **AERIOE**: science objectives: 2, 5; rationale: Atmospheric thermodynamic profiles are needed to support SO#2-Q1, SO#2-Q2, SO#5-Q1, and SO#5-Q3.
2. **AOD**: science objectives: 3, 5; rationale: Aerosol optical is needed to calculate aerosol radiative forcing to support SO#3-Q1.
3. **AOP**: science objectives: 3; rationale: Identifies periods impacted by absorbing species besides black carbon, including absorbing dust and brown carbon to support SO#3-Q1.
4. **DLPROF**: science objectives: 2, 5; rationale: Wind fields are needed to support SO#2-Q1, SO#2-Q2, and SO#5-Q2.
5. **LDQUANTS**: science objective: 1; rationale: Processed laser disdrometry data will support ground validation efforts of radar-based precipitation estimates from SO#1-Q1.
6. **MFRSRCLDOD**: science objectives: 3; rationale: Cloud optical depth is needed to calculate radiative effect from clouds for SO#5-Q1.

7. **OACOMP**: science objectives: 3; rationale: Distinguish between fresh primary organics from secondary and aged organic species to support SO#3-Q1.
8. **QCECOR**: science objectives: 5; rationale: Eddy correlation corrections and additional quality controls need to be applied to the ECOR-derived turbulent fluxes of sensible and latent heat in support of SO#5-Q2.
9. **RADFLUXANAL**: science objectives: 3, 5; rationale: Radiative fluxes are needed to quantify the contributions of aerosols and clouds to the surface energy budget to support SO#3-Q2 and SO#5-Q1.
10. **VARANAL**: science objectives: 2, 5; rationale: The relationship between large-scale wind fields and SAIL direct observations is needed to support SO#2-Q2 and SO#5-Q2.

Given the contributions of individual and collective SAIL measurements to the campaign's science objectives, we have developed measurement strategies for:

1. The AMF2 and XBPWR instruments during normal operations.
2. Collaborative resources and guest instrumentation.
3. Other ARM-deployable resources.
4. Intensive operational periods (IOPs).

4.1 AMF2 and XBPWR during Normal Operations

The overarching science question of SAIL motivates comprehensive, exhaustive measurements of the processes that dominate the uncertainty budget in hydrological modeling, but these processes exhibit first-order spatial and temporal heterogeneity. Therefore, there is a direct relationship between the physical location of the instruments within the East River Watershed and the information that these instruments will be providing to help answer the science question, its sub-questions, and its science objectives. Careful considerations are needed to ensure that the measurements provide an unbiased characterization of that process heterogeneity. This motivated the selection of two locations for instrument deployment, motivated by the following factors:

1. Provide mountain and valley end-members for atmospheric processes in the East River Watershed.
2. Enable complementary, overlapping, wide-ranging coverage for remote-sensing and in situ instruments.
3. Enable many studies of collocated datastreams that would be precluded with more sites.

Figure 23 shows the two sites selected. Most of the AMF2 instruments, with the exception of those in the AOS (ACSM, AOSMET, CO, CCN, CPC, HTDMA, INP, O3, PSAP, SMPS, SP2, UHSAS) will be located in a valley location at the RMBL. This site is much closer to the higher terrain surrounding the upper portion of the watershed where precipitation and snowpack are significantly enhanced. The RMBL site enables the AMF2 instruments to capture the thermodynamic and dynamic information related to the processes associated with that enhancement within generally understudied mountain valley environments. Radiative flux, precipitation, and vertically profiling atmospheric state, cloud, and aerosol measurements in this location will be the most useful for characterizing atmospheric conditions that directly connect with pre-existing surface hydrologic measurements in the watershed. The area around RMBL is accessible by road in the warm season and ski/snowshoe in winter from the CBMR base.

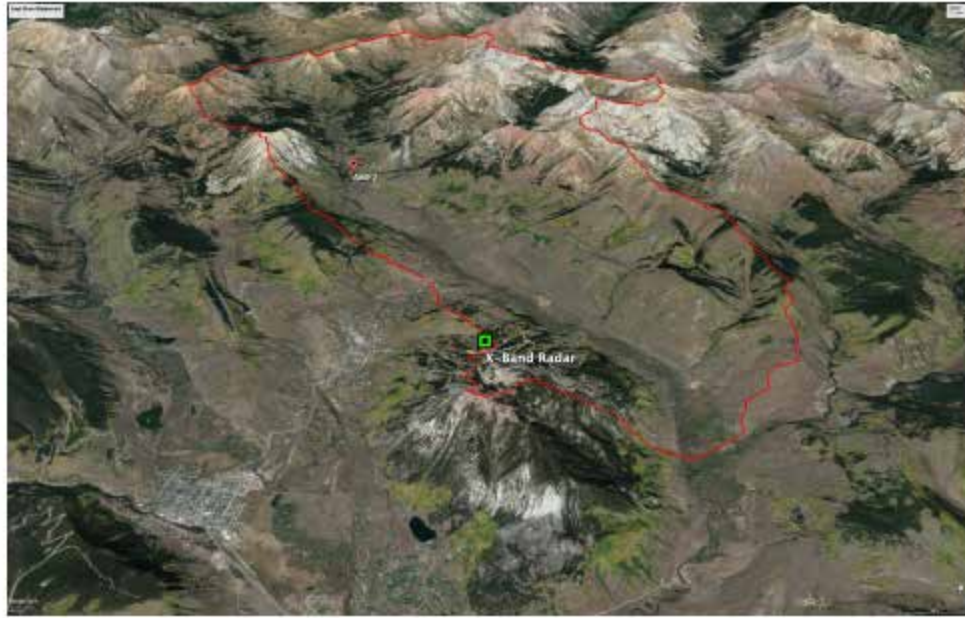


Figure 23. Perspective view looking north towards East River Watershed with the watershed boundary in red, the location for SAIL of the XBPWR in green, and the location of the AMF2 as a red marker.

The second site is on Crested Butte Mountain. This elevated, prominent location was selected to enable both radar and AOS measurements to sample a broader area, including beyond the East River Watershed. While there are tradeoffs with separating a subset instruments from AMF2, including the preclusion of many direct comparisons between their respective measurements, the emplacement of the AOS at Crested Butte Mountain advances SAIL science objectives because in situ aerosol property measurements at higher elevations increases the likelihood that those instruments will be collecting data on long-range transported aerosols along with a more detailed assessment of how aerosols interact with clouds and precipitation.

4.1.1 Strategies Supporting Science Objective 1

The achievement of SO#1 depends on developing a detailed picture of the spatial and temporal heterogeneity of precipitation, as well as the underlying processes that establish that heterogeneity. Therefore, measurement strategies for this science objective focus on maximizing the coverage of the XBPWR measurements. The emplacement of the XBPWR at a prominent, relatively elevated location with as minimal beam-blockage as possible is therefore of primary strategic interest, since it enables the instrument to view precipitation amount, type, and intensity at low-elevation angles, thereby capturing near-ground-level precipitation in wintertime and elevated precipitation in summertime at a single location. While logistical limitations such as the need for access and power for the XBPWR instrument must be considered, the site selected for the XBPWR enables nearly complete coverage of the East River Watershed and beyond, as shown in Figure 17. The XBPWR will be located at the southern edge of the East River Watershed and the northernmost edge of the watershed is less than 17 km away from the XBPWR, allowing that instrument to easily collect measurements across the entire watershed and beyond.

In fact, the XBPWR measurements will be very sensitive to detailed precipitation structures within the East River Watershed as well as upwind and downwind.

With the XBPWR located on Crested Butte Mountain, another key strategic consideration is for that instrument to be able to simultaneously sample the same volume that is being sampled by the KAZR instrument and other vertically sampling instruments from the AMF2. The collection of precipitation and thermodynamic data within the same air volume simultaneously develops a wide range of micro- and macrophysical data including on hydrometeor phase, size distribution, velocity, and the time-evolving processes that contribute to precipitation. It would yield multi-wavelength polarimetric radar observations that can be used to constrain precipitation microphysics evolution within orographically forced or convectively forced precipitation events.

Thermodynamic measurements from radiosondes will provide in situ sampling and insight into the underlying processes that contribute to precipitation vertical structure. The campaign will launch at least two radiosondes per day to capture different radiation regimes, but increased frequency of radiosonde launches to four times per day, where possible, will enable a resolution of precipitation events where event lengths that can be represented by a gamma distribution are often less than 24 hours long in the winter (Serreze et al., 2001) and only a few hours long in the summer (Gochis et al. 2003).

A final strategic consideration is the scan strategy of the XBPWR because it has direct implications for achieving SAIL's SO#1. While measurements of the XBPWR using plan-position indicator (PPI) scans enable surveying of precipitation across the East River Watershed and beyond to understand the variability across the area, there is scientific value in focusing scans in the sector where the AMF2 resides to better understand processes contributing to variability in the vertical structure of storms. Range-height indicator (RHI) scans, regularly (~15 minutes) interspersed with PPI scans, are needed during storms, in particular, to capture the time evolution of processes above the AMF2.

4.1.2 Strategies Supporting Science Objective 2

The achievement of SO#2 depends on making detailed measurements of observational constraints on the wind redistribution and sublimation of snow. The former term requires detailed measurements of wind fields and their spatial gradients, especially where there are strong gradients of suspended snow relative to surface stress.

For wind redistribution of snow, the XBPWR will measure Doppler radial velocities of particles, whether precipitating or suspended, and its measurements will be able to characterize hotspots of wind redistribution, especially at ridgelines, as well as redistribution during and outside of precipitation events (Walter et al. 2020). Where measurements of wind fields overlap with the scanning DL, we will have opportunities to characterize wind redistribution statistics and wind vectors. Scan strategies for these two instruments can achieve a combined greater sensitivity to wind fields.

Snow sublimation can be inferred and potentially quantified from a variety of SAIL data sources, including:

1. Vertical attenuation of radar reflectivity during precipitation (Walter et al. 2020).
2. Eddy covariance measurements of latent heat fluxes (Stigter et al. 2018).

3. Thermal and thermodynamic signatures of latent heat in blowing snow plumes (Taylor 1998).
4. Mass-balance investigations using snow-making equipment (Eisel et al. 1988).

Measurements of vertical wind structure and vertical atmospheric thermodynamic structure are central to characterizing snowpack and blowing-snow sublimation tendencies. The radiosonde measurements are key to characterizing the thermodynamic profile of temperature and humidity, and at least two radiosonde launches will occur daily. This will enable characterization of changes in these profiles across the day, while being supplemented by continuous AERI retrievals of these quantities. The AERI has zenith-scanning capabilities between 45 and 135 degrees, which can capture spatial variability in temperature and humidity and, where the instrument is able to scan towards and away from ridgelines with blowing snow plumes, how those quantities vary in and around those plumes.

Measurements from tethered balloon systems (TBS) can provide important constraints on snow processes. With the imaging configuration of that platform, which contains visible and thermal imaging capabilities, observations of the snow extent and temperature can be collected. These data can provide an important time-series of spatiotemporal snow evolution across the East River Watershed and fill the gap between continuous station observations that have limited or no spatial coverage at all and aerial snow surveys such as from ASO that provide highly spatially detailed snow depth measurements but with no temporal resolution.

4.1.3 Strategies Supporting Science Objective 3

The standard data collection approaches for the AOS are highly supportive of SO#3. That being said, the primary strategic decision to enable the achievement of SO#3 is its emplacement at an elevated location. While the AOS is typically collocated with other AMF2 instruments, SAIL will separate the AOS from the other AMF2 instruments and locate it with the XBPWR instrument. Reasons for this decision include:

1. To obtain aerosol (and trace gas) measurements representative of the region, SAIL needs a location with minimal local contamination sources. These local sources, including from the dirt road near RMBL during the summer and inversions in the winter, would skew observations and not be relevant for assessing aerosol impacts on clouds from a more regional standpoint.
2. The location of the AOS and XBPWR instruments on Crested Butte Mountain at the Old Teocali Lift site does not see significant ski or foot traffic. It is therefore less likely to be influenced by local mountain operations such as from snow cats and snow guns.
3. The location has a more open footprint, meaning less localized obstructions such as from trees that could impact the measurements (e.g., AOS wind speed).

The TBS measurements can provide important constraints on aerosol processes. The TBS has an aerosol concentration configuration that includes a printed optical particle spectrometer (POPS) and a condensation particle counter (CPC). These instruments should be used to measure aerosol size distribution and total aerosol concentration, respectively, during a range of aerosol loadings across seasons, which can be assessed with AOS measurements, principally, to characterize vertical profiles of aerosols to better understand regimes and radiation.

4.1.4 Strategies Supporting Science Objective 4

The primary strategic consideration for SO#4 is to ensure that direct measurements of aerosol properties and precipitation are collocated in space and time. The collocation of the XBPWR and the AOS instrument package ensures that AOS measurements are sampling air masses relevant to precipitation on elevated terrain.

While the AOS instruments provide highly detailed surface measurements, they do not provide aerosol profile measurements to characterize the relationship between ground-based measurements and those experienced in clouds. Therefore, aerosol profile measurements to obtain aerosol properties near cloud bases are important, and can be achieved with TBS measurements, so that platform represents an important aspect of the measurement strategy supporting science objective 4. The TBS measurements therefore should extend from the surface to an altitude that can sufficiently characterize aerosol-cloud and aerosol-precipitation interactions. Measurements at least 1 km above ground level (AGL), and preferably closer to 1.5 km AGL, can likely capture much of the boundary layer, even though the height of the boundary layer across seasons in this area is not known. The TBS has an aerosol composition configuration that includes a size- and time-resolved aerosol counter (STAC) and a POPS that should be used during a range of aerosol loadings across seasons, which can be assessed with AOS measurements, principally, to measure the range of aerosol-cloud and aerosol-precipitation interactions.

4.1.5 Strategies Supporting Science Objective 5

The primary strategic consideration for SO#5 is to collect surface radiative fluxes and turbulent fluxes of sensible and latent heat at end-members that support the unbiased estimation of these quantities across the East River Watershed. Previous measurements at an energy-limited end-member in a riparian zone of the East River (near the Pumphouse) can be contrasted against a shrub environment that alternates between water and energy limitations for turbulent fluxes of sensible and latent heat. Surface radiation measurements will capture the effects of the atmosphere, including gaseous constituents and condensates, and the effects of terrain on surface radiation.

The key strategic consideration for the radiation, sensible, and latent heat measurements is to ensure that the measurements sample the range of atmospheric and terrain effects. While the impacts of terrain on both shortwave and longwave radiation are understood and amenable to modeling (Lee et al. 2015, Plüss and Ohmura 1997), the intersection of impacts between terrain-induced radiative effects and associated changes in sensible and latent heat in complex terrain is just starting to be explored (Everard et al. 2020).

While a single ECOR instrument will be deployed with the AMF2, there is an option for an additional instrument at a location south of the AMF2 in Gothic. The Kettle Ponds site is 2 km south and represents an open rangeland environment that will be a distinct end-member from the AMF2 and other surface flux measurement locations. The Pumphouse location is 4 km south and represents a riparian habitat. It is an energy-limited end-member, where observations will set an upper bound on the evapotranspiration (ET) of the entire watershed.

4.2 Collaborative Resources and Guest Instrumentation

In addition to the wide range of collaborative resources associated with the WFSFA listed in Section 1.1, several additional resources impact SAIL measurement strategies.

First, there is potential for the deployment of an AmeriFlux Rapid Response surface flux measurement system to measure fluxes over a forested site. Such measurements would provide a forested end-member for understanding ET, and sensible and latent heat fluxes over deciduous or coniferous sites. Decisions and logistics support for that system are pending, as of this writing. If selected, that system will contribute directly to SO#5.

Second, NOAA will be deploying a wide range of atmospheric and surface measurements associated with the Study of Precipitation and Lower-Atmospheric impacts on Streamflow and Hydrology (SPLASH), led by Dr. Gijs de Boer of the Physical Sciences Laboratory. This campaign will start in September of 2021 and extend for one year.

It will provide one or more of the following instruments:

1. Atmospheric Surface Flux Station (ASFS)
2. Disdrometer
3. Atmospheric Boundary Layer (ABL) Profiler
4. Vertically Pointing Snow-Level Radar (SLR)
5. Mobile Surface Radiation Network (SURFRAD) station
6. Radiometer suite (RADSYS)
7. Surface energy balance tower
8. Collaborative Lower Atmospheric Mobile Profiling System (CLAMPS) with the following:
 - a. Doppler lidar
 - b. AERI
 - c. Microwave radiometer

The SPLASH instrumentation will be located within the East River Watershed at locations separate from, and complementary to, the SAIL locations. (1) at Avery Picnic ~2 km north of the RMBL in Gothic, (2) at Kettle Ponds ~2km south of RMBL, (3) at the Pumphouse ~4 km south of RMBL, and (4) at Brush Creek ~ 10 km south of RMBL, adjacent to the south side of Crested Butte Mountain. Given the breadth and depth of the SPLASH instrumentation, the SPLASH campaign will advance all SAIL science objectives.

SAIL may also benefit from additional guest instrumentation. Co-Investigator Skiles will loan an additional SP2 instrument to complement SAIL's SP2. This will provide measurements at AMF2 to capture spatial gradients in BC, and advance SO#3 and SO#4.

Snow pits will also be a key collaborative resource. Snow pit observation and sampling will occur in the following order: (1) collect spectral snow albedo over the pit site; (2) excavate pit, record snow depth, and collect 10-cm temperature profile along shaded pit wall, noting visual snow and dust stratigraphy; (3) measure snow density in 10-cm increments using a density cutter and field scale; and (4) gravimetric sampling for dust/aerosol stratigraphy in 3-cm increments in the top 30 cm of the snow column. Spectral snow albedo and surface effective grain size will be retrieved with an Analytical Spectral Devices field spectroradiometer (i.e., spectrometer; FieldSpec4).

Snow samples will be kept frozen until analysis in Skiles' lab at the University of Utah, at which point they will be melted, weighed, a 50-mL aliquot drawn off for black carbon analysis, and then filtered and dried for deposited aerosol mass and concentration, which is typically strongly dominated by dust.

Single laser light diffraction (Malvern Instruments; Mastersizer 2000E) from a subset of snow samples containing dust layers introduced directly using a wet dispersion system. The reflectance of filtered aerosols, when optically thick, will be measured with the same field spectrometer mentioned above coupled to an Analytical Spectral Devices (ASD) RTS-3ZC integrating sphere. The 50-mL aliquots will be analyzed for BC using the same SP2 deployed in the field, which will return to the lab in the summer, by coupling the instrument with an ultrasonic nebulizer (A5000T; Cetac). Sample analysis procedure for dust and BC in snow is described in detail in Skiles and Painter (2017); we will follow the same methodology.

For additional logistical support for guest instrumentation, there is an established process by which users can [submit ARM field campaign requests](#).

4.3 Other ARM Resources

In addition to the AMF2 instrumentation, there may be opportunities to deploy TBS during SAIL. This platform provides visible and thermal imaging instrumentation, atmospheric profiling of temperature, water vapor, and winds along the tether, and cloud and aerosol properties, as well as allowing for hosting guest instrument payloads, where applicable.

The TBS can provide unique, aerial information that is highly complementary to other SAIL data sets. It makes measurements on a regular basis and can capture the evolution of the surface and atmospheric environments during its deployment windows. The science value of TBS deployment depends on the season during which it is deployed, but generally enables the following:

During winter, TBS instrumentation can characterize the spatial distribution and evolution of snow cover and the spatial distribution of the thermal environment, as well as provide information on cloud and aerosol properties. Making measurements before and after storms, if they happen, would constrain precipitation rain/snow transitions and wind scouring, processes that occur during storms.

During spring, regular measurements at the start and end of the snow melt-out would enable the tracking of the evolution of snow cover and the thermal conditions on the ground, and the aerosol measurements would provide critical information on the vertical distribution of dust-on-snow events. Making measurements pre- and post- rain-on-snow events, if they happen, would characterize the response of the snowpack to more rapid melt events.



Figure 24. Three potential sites for TBS deployment: (1) RMBL Gothic Townsite in red, Kettle Ponds in yellow, and Mt. Crested Butte Boneyard in yellow.

During summer, the TBS would be able to characterize the conditions that favor or disfavor the development of convective events locally, including how regional flow patterns impact the evolution of the boundary layer during the summer.

During fall, the TBS would be able to characterize the change in snow cover at the onset of the accumulation season and associated impacts on the thermal environment.

Another key organizing activity will be to focus research and data collection activities in IOPs, which can augment the scope of the science that SAIL can achieve. In particular, IOPs can help advance efforts to address SAIL’s overarching science question by developing numerous datastreams at an even higher level of process detail. Collaborative activities that can serve as the focal points for IOPs include, but are not limited to:

1. Snow survey flights
2. TBS deployments
3. WFSFA, SPLASH, NGWOS, or SnowEx intensive data-collection periods.

Here are some examples for potential IOP activities. In the cold season, IOPs provide opportunities to study the connection between precipitation, aerosols, snow atmospheric and snowpack processes, and radiation with focused experiments to track the change in snow before, during, and after storms. During the spring, IOPs provide opportunities to track aerosols from the atmosphere to the snowpack and their

subsequent impact on snowpack energetics, while also targeting how the emergence of snow-free areas change local atmospheric dynamics. Finally, IOPs provide opportunities to study boundary-layer evolution, the development of convection, and its impact on the land surface moisture and energetics.

In addition to any potential guest instrumentation for an IOP, IOPs can include additional radiosonde launches. These activities enable a greater, detailed resolution of the diurnal development of atmospheric thermodynamics in mountain valleys. For programmable instruments such as the XBPWR and DL, careful considerations and dynamic adaptive scan strategies are needed to sample the evolution of precipitation and winds where they are occurring.

5.0 Project Management and Execution

Given the scope of SAIL, including as the first integrated field laboratory (IFL), organization of the campaign is central to the resulting science. At a high level, SAIL has and will continue to reach out to key scientific partners within BER including, but not limited to, the Atmospheric System Research (ASR), Environmental System Science (ESS), Earth and Environmental System Modeling (EESM), Regional & Global Model Analysis (RGMA), and Subsurface Biogeochemical Research (SBR) programs. The campaign also has and will continue to reach out to key agency partners with USGS, primarily through its Next-Generation Water Observing System (NGWOS); NOAA, primarily through the SPLASH campaign; NASA, primarily through the SnowEx mission; and the National Center for Atmospheric Research (NCAR), primarily through the Research Applications Laboratory. State and local scientific partners are invaluable to the scientific success of SAIL and include, but are not limited to, RMBL, Western Colorado University, and the Upper Gunnison Water Conservancy District. Other, more detailed aspects of SAIL management and execution are listed below.

IFL: SAIL necessarily requires active communication between the points of contact for the ARM facilities being requested and the large number of existing collaborative resources in the East River Watershed, many of which are associated with the Watershed Function SFA. The SAIL PI team regularly meets and Co-Investigators Carroll, Gochis, Raleigh, Skiles, and Williams contribute substantially to that SFA and provide needed links to those WFSFA resources. The data from these collaborative resources will be publicly available and are described in the Data Management Plan.

Website: SAIL has a website (<https://sail.lbl.gov>) to centralize logistics for the deployment along with planning information for project participants. SAIL also has an [ARM-hosted Campaign Website](#) that describes the campaign at a high level, including associated official publications and activities. It will provide evergreen links to the location of the SAIL data that will be hosted on [ARM Data Discovery](#). It will also provide evergreen links to the locations of WFSFA data so that researchers can find atmosphere-through-bedrock observations at a centralized location.

Reviews and Reporting: In coordination with the AMF personnel, SAIL will produce periodic status reports in the preparation, execution, and conclusion of the campaign to ensure SAIL is planned, managed, and executed to meet its science objectives. The campaign expects that external investigators will seek to develop IOPs in conjunction with the deployment, and will work with IOP proposers to ensure maximum science benefit. At the conclusion of the campaign, the SAIL science team will conduct post-project reviews at the ARM/ASR Science Team meetings.

6.0 Science

This section presents some science opportunities that SAIL data enable. Merely a subset of opportunities that the campaign seeks to enable through broad community-wide participation, it should be considered a starting set of activities.

6.1 Precipitation Process Science

Over the upper Colorado River watershed, it has been shown that cloud-system-resolving WRF simulations produce 20-30% more cold-season precipitation than reanalyses with biases that increase with elevation (Wrzesien et al. 2018) and are highly sensitive to the choice of cloud microphysics (Liu et al. 2011). Further, owing to a lack of observational or laboratory constraints, most existing cloud microphysics schemes have substantial deficiencies in their representations of ice processes (e.g., Harrington et al. 2013). Figure 25 shows a comparison of WRF simulations with the PRISM reanalysis (Daly et al. 2008) over southwestern Colorado, with very different precipitation bias patterns between summer and winter, and generally an overprediction of precipitation by WRF in both means and extremes. Resolving the differences between WRF and PRISM requires a close inspection of the physical processes that contribute to these biases.

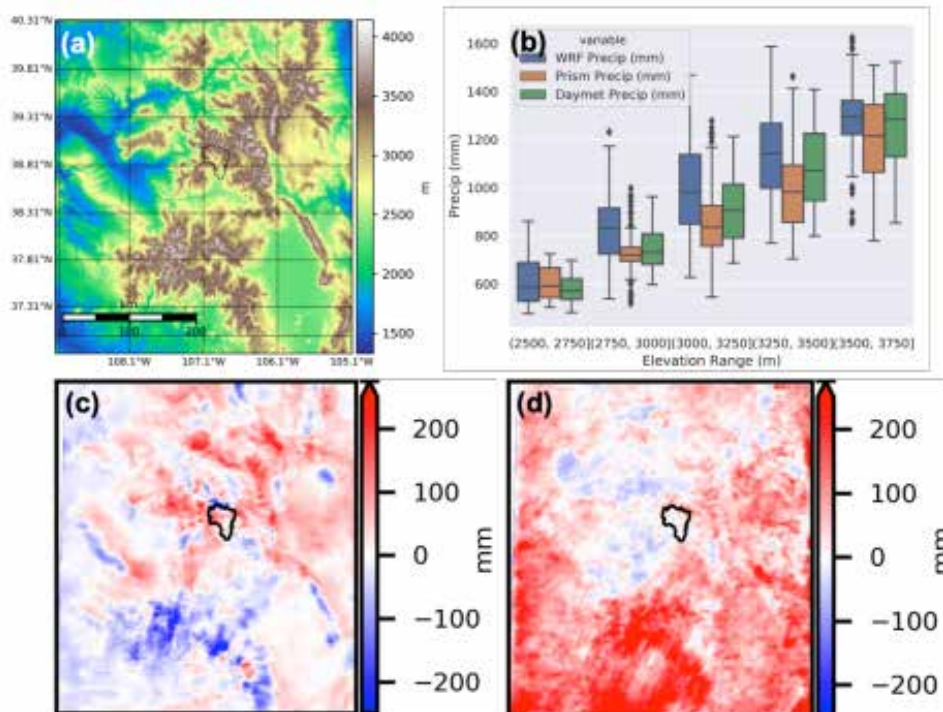


Figure 25. (a) Topographic map of a 400x400-km domain surrounding the East River Watershed (outlined in black). (b) Domain-wide comparison of wintertime WRF simulations with PRISM for calendar year 2017. (c) Same as (b) but showing wintertime domain bias (WRF-Prism), (d) Same as (c) but showing summertime bias.

This motivates the following questions:

1. What roles do terrain features have in generating winter precipitation within different stability, flow, temperature, humidity, and large-scale vertical motion conditions?
2. What cloud and sub-cloud processes control phase and accumulation at the surface?
3. How does sublimation/evaporation in the lee of terrain features and topographic height influence surface accumulation?
4. How do meteorological conditions impact ice habit, amount, aggregation, breakup, and riming, and how does this impact surface accumulation?
5. How do topographically affected winds and turbulence affect transport of hydrometeors and precipitation accumulation?

Each of these questions can be addressed using SAIL data, in conjunction with reanalysis information on the synoptic flows through this environment.

With detailed XBPWR, KAZR, and SONDE data, process models can be evaluated following the framework suggested by Lundquist et al. (2019). SAIL data form the basis both for developing gridded precipitation products directly and for evaluating the errors produced in the creation of gridded data from point gauge network observations.

The SAIL data will also enable the creation of fingerprints of liquid, ice, and mixed-phase precipitation processes such as aggregation, riming, and seeder feeder from a combination of radar, satellite, surface, and profiling observations with the aid of measurement simulators applied to cloud-scale models. After controlling for possible meteorological errors, these fingerprints can then be linked to periods and locations with model errors to determine which processes will be targeted for further parameterization sensitivity testing with the goal of improving parameterizations and prediction of precipitation. All of these analyses will collectively characterize the ability of state-of-the-art multi-scale models and parameterizations to predict a variety of precipitation processes in mountainous terrain that strongly impact local and regional hydrology.

6.2 Snow Sublimation and Wind Redistribution Science

Many SAIL datastreams impose observational constraints on the terms for snow sublimation. The XBPWR, DL, RWP, SONDE, and MET will measure wind fields and snow redistribution, while SONDES will measure atmospheric temperature and humidity.

Together, these measurements will directly quantify the thermodynamic tendency for snow sublimation and where and when this tendency overlaps with blowing snow events during precipitating and non-precipitating conditions. SAIL can use these measurements to build bottom-up observationally based estimates of sublimation by quantifying the contributions of sublimation from the snowpack surface and sublimation from blowing snow to the loss of snowpack across the accumulation and melt seasons.

These measurements will also help quantify the spatial distribution of the wind redistribution of snow during and outside of precipitating events, including where wind erosion and deposition occur and the

relative importance of this redistribution in precipitating and non-precipitating events and how that relationship varies with antecedent snow conditions.

Finally, the combination of precipitation, sublimation tendency, and wind redistribution observations help develop a snow process closure experiment. This experiment is diagrammed in Figure 26 and will create a multi-pronged set of constraints for snow processes that most impact the snowpack at the mesoscale. SAIL data can be assimilated into a wind-downscaling solution at the mesoscale, while targeted snow surveys can be assimilated into snow dynamics models. These two combined approaches would assimilate data at the small spatial scales of relevance to snow accumulation and redistribution process models and the large spatial scales of relevance to atmospheric process models to develop an optimal solution for snowpack evolution at the mesoscale that is cognizant of snow processes at the scale of tens of meters. Furthermore, this two-pronged assimilation approach can produce an optimal solution with uncertainty estimates.

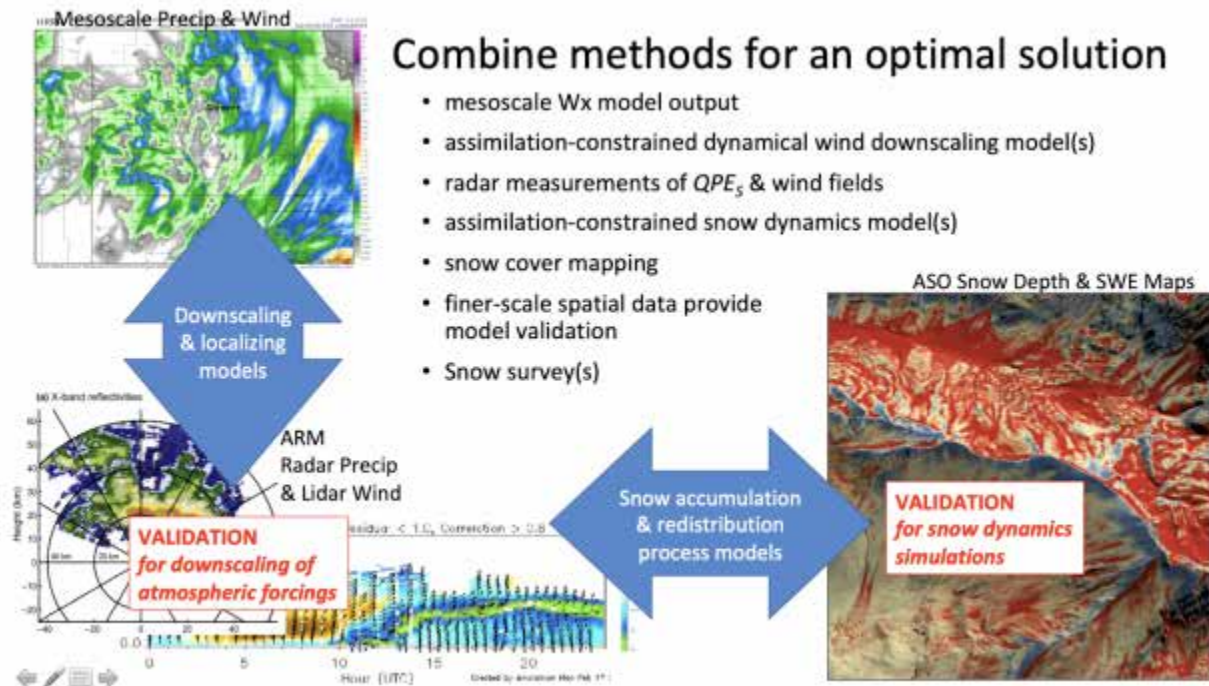


Figure 26. Two-pronged data assimilation to achieve snow process closure at the mesoscale.

SAIL will observe radiative properties of aerosols in the atmosphere and other atmospheric state variables (thermodynamics and clouds) as inputs to well-established radiative transfer routines to calculate the radiative forcing of these quantifiers and their variability by aerosol regime.

These provide information to inform surface radiative calculations. To determine the unique and combined impacts of dust and BC, relative and total concentrations will be used as inputs for individual runs of the Snow-Ice and Aerosol Radiative Transfer (SNICAR) model. This addresses one of the largest uncertainties in the assessment of the role of light absorbing aerosols in snow, as studies have typically focused on one aerosol type (i.e., BC; Bond et al. 2013). Such a data set can be used to directly uncover model errors in aerosol radiative forcing (e.g., Jones et al. 2017).

6.3 Aerosol Precipitation Interaction Science

To address SO#4-Q1, SAIL will collect data to identify the significant new-particle nucleation events and examine the associated environmental conditions. Data on the aerosol characteristics (e.g., size distribution, composition, and hygroscopicity) and their relationship with CCN under different aerosol scenarios will be collected. These will enable studies of how new-particle growth affects CCN concentrations, cloud droplet number concentration, ice microphysical processes such as vapor deposition, riming and aggregation, and precipitation.

For SO#4-Q2, SAIL data will enable investigations of how different aerosol sources such as wildfires, long-range transported dust, and biological particles contribute to INP concentrations. This is particularly important where INP data can be correlated with aerosol composition, cloud microphysics properties such as ice water content, cloud phase, and hydrometeor type, and snow precipitation under different meteorological conditions. SAIL data also enable the quantification of INP-precipitation efficiency based on meteorological conditions and aerosol scenarios, motivated by previous studies showing that temperature and moisture exert a large control of aerosol effects on the orographic precipitation (Fan et al. 2017, Saleeby et al. 2011).

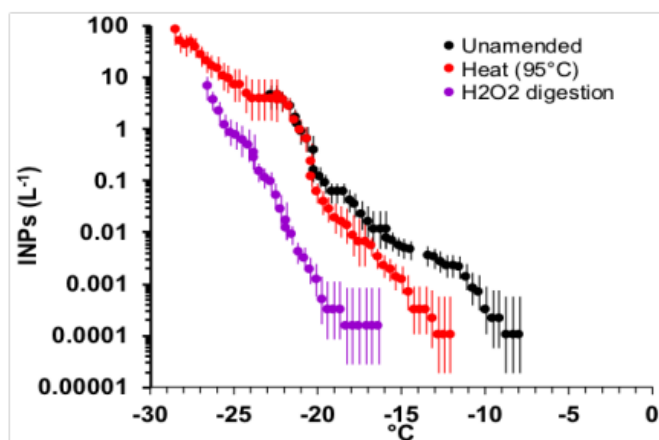


Figure 27. Example of determination of biological INPs based on thermal treatment of unamended aliquots of particles, and distinguishing total organic contributions of INPs through H₂O₂ digestion. It is not unusual for biological INPs to be expressed at temperatures > -20 °C, and for organic INPs to dominate to quite low temperatures in certain environments. These data are from the Measurements of Aerosols, Radiation, and Clouds over the Southern Ocean (MARCUS) deployment, emphasizing biological and organic INPs present in oceanic emissions from sea spray.

To address SO#4-Q3, SAIL data will enable the identification of typical aerosol and meteorological scenarios. SAIL will allow researchers to identify relationships between aerosol characteristics, including both CCN and INP, and cloud properties such as CWP, IWP, cloud phase, and precipitation for each scenario. Associated modeling studies can focus on the most common aerosol scenarios. For each scenario, hypotheses about the major mechanisms leading to observed relationships can be posed, then real-case WRF model simulations with bin microphysics at the LES scale can be conducted to test the hypotheses.

For example, in case of wildfires, the emitted black and brown carbon may change the local circulation through aerosol radiative effect, which would impact orographic clouds and precipitation more dramatically compared with CCN effects. In the case of hygroscopic aerosols (CCN effect), literature shows inconsistent results: Borys et al. (2003) showed that increasing CCN suppresses riming and lead to reduced snowfall rate, but opposite results were seen in Saleeby et al. (2011) and Fan et al. (2017). The inconsistency might be due to different mountain width and height, and different meteorological conditions. Since the meteorological conditions vary strongly with seasons over this region, this analysis will be conducted for different seasons, and aerosol impacts on snowfall is of particular interest.

6.4 Surface Energy Balance Science

For SO#5-Q1, the observational data will form inputs to radiative transfer models. They will enable the development of radiative closure studies (e.g., Mlawer et al. 2002, 2003, McFarlane et al. 2011, 2016) to systematically quantify contributions to the observed shortwave and longwave upwelling and downwelling radiation. These studies will specifically isolate the roles of humidity, clouds, and aerosols in contributing to the surface energy balance.

For SO#5-Q2, modeling support needs to be coupled to SAIL data to understand turbulent fluxes of sensible and latent heat across the East River Watershed. Since these fluxes are generally difficult to measure across terrain, they have been parameterized, typically with a bulk aerodynamic model (e.g., Anderson et al. (2010). However, Schlögl et al. (2017) showed that this is inappropriate in complex terrain due to the violation of the mandatory assumptions of stationarity and horizontal homogeneity. SAIL expects that these fluxes may vary with snow cover, soil moisture, and vegetation type and density and heterogeneities thereof (Wu et al. 2015, Gevaert et al. 2018, Meng et al. 2014). With SAIL, as the melt season progresses, we will measure these fluxes and their variation with wind speed and surface temperature, snow, and soil moisture changes throughout the East River Watershed and directly quantify bulk aerodynamic model parameterization errors and how they vary with surface conditions. Because bulk aerodynamic models are widely used, SAIL data can quantify how appropriate this model is, and critically when and where it is biased, for parameterizing the role of sensible and latent heat fluxes for contributing to surface-melt and warm-season fluxes. For these cases, WFSFA's network of soil moisture measurements, and meter-scale mapping of vegetation across the East River Watershed (Carroll et al. 2018, Hubbard et al. 2018), will be leveraged.

From SO#5-Q3, SAIL will build up a climatology of the controls on CIES. These can be compared against convection-permitting, data-constrained simulations of the region to quantitatively position the atmospheric states realized over East River Watershed in the broader distribution of states achieved over the Rockies, with NOAA's High-Resolution Rapid Refresh (HRRR) model provides an hourly, 3-km horizontal resolution atmospheric state estimate over the continental United States (CONUS).

6.5 Integrated Field Laboratory Science

The collocation of atmospheric, surface, and sub-surface field activities in the East River Watershed is specifically designed to enable science activities that are driven by questions with answers that require simultaneous, overlapping measurements, as part of an IFL.

In addition to the science questions and objectives specific to SAIL, this campaign may yield other co-benefits due to its detailed observations of both land and atmosphere that can be used by these two communities. For the atmospheric science community, scientific opportunities are enabled by existing data sets associated with the WFSFA. First, the network of existing meteorological observations, including SNOTEL, can be used to directly calibrate the relationships between precipitation radar measurements and precipitation phase and amount, since these relationships depend on microphysics and can thus vary both spatially and temporally. Second, the distributed network of ongoing field measurements, as shown in Figure 4, can at the very least provide spatial and temporal context to those data collected at the AMF2 central facility as part of SAIL. There are four Snow Telemetry (SNOTEL) sites that have collected data between 9 and 38 years, and 25 additional stations that have been collecting temperature, humidity, barometric pressure, and wind speed data, with select stations also collecting solar and infrared radiation, snow depth, precipitation, soil moisture and soil temperature, and the EPA Clean Air Status and Trends Network (CASTNET) collecting wet and dry deposition. These data can be used to characterize elevation gradients and variability on synoptic-to-interannual timescales in these observed variables. Furthermore, measurements of the snowpack chemistry can provide information about the spatial and elevational dependence of, in particular, aerosol deposition and can establish the representativeness of the detailed aerosol measurements at the AMF2 in complex terrain.

For the existing WFSFA, the uncertainties in the spatiotemporal distribution of (1) precipitation and phase, (2) temperature, and (3) radiative fluxes greatly complicate surface and subsurface hydrologic model development efforts, since their inputs are characterized by sparse meteorological station inputs that may not be capturing relevant spatiotemporal and/or elevational gradients. Precipitation amount and phase observations would therefore greatly advance SBR-funded research, and would extend BER's investments in bedrock-through-canopy infrastructure to address significant gaps in atmospheric inputs.

6.6 Modeling Activities Science

SAIL campaign data can support a wide range of modeling activities. For process models, SAIL observational data sets are necessary to allow benchmark evaluation of integrated process model skill in mountainous terrain when simulated in a free-running state bounded (or periodically updated), using SAIL-like observations as constraints, and, finally, in a degraded state whereby more complicated parameterizations in the integrated process model are swapped and validated with those more commonly used in Earth system models. Thus, integrated process models allow for a framework in which one can assess and isolate the direct effect of swapping model parameterization sophistication (e.g., rain-snow partitioning, boundary-layer scheme, microphysics, etc.) and the sensitivities to horizontal, vertical, and time-step resolution.

This framework of a hierarchy of integrated process model experiments can then be used to interrogate important process-level choices in modeling mountainous environments such as:

- 1) Precipitation phase-partitioning – land-surface models in most Earth system models crudely assume that precipitation phase and snow density are only dictated by a distinct range of surface temperatures. Jennings et al. (2018) have shown that due to the hydrometeor energy balance theory, where low ambient relative humidity promotes evaporative cooling via exchanges in latent heat,

environments. This therefore highlights the need to update these parameterizations to account for not only surface temperature, but, at least, relative humidity as well.

- 2) Boundary-layer processes – the implications of boundary-layer scheme bulk-parameterization choice (e.g., aerodynamic roughness length) has been a longstanding topic in land-surface and snowpack model literature because the choice of how these processes are generalized can lead to a decoupling of the atmosphere-land interface and a rapid cooling effect that may lead to large biases in surface temperature, particularly in the winter season (Slater et al. 2001).
- 3) Snowpack bulk-density and snow cover (from satellites and Watershed Function SFA surveys) parameterizations – akin to precipitation phase-partitioning, the snow model components of Earth system models often assume that the density of snowpack is dictated by a distinct set of temperature ranges (e.g., >2 C, 0 C to -15 C, and <-15 C) and, until recently, had not accounted for the importance of wind redistribution (van Kampenhout et al. 2017). This is important because snow cover affects albedo and surface energy. This is an often underestimated and poorly observed process that can lead to much different late-winter to early-spring distributions of snowpack in mountainous regions. In addition, grid-cell-based snow cover parameterizations in Earth system models are often represented by hyperbolic tangent functions that relate snowpack bulk characteristics such as the density of new snow, the momentum roughness length, and a tuning coefficient (e.g., Oleson et al. 2013), which may not be sufficient in representing the true snowline, particularly during the melt season.
- 4) Shortwave and longwave feedbacks in complex terrain – neither the atmospheric dynamical core nor the land-surface models in most Earth system models account for the influences of terrain on shortwave and longwave energy exchange. The interaction of complex terrain, particularly shortwave shading due to cliff faces and variability (i.e., slope) and mountain range orientation (i.e., aspect) have a profound impact on the spatial heterogeneity and lifetime of snowpack pockets into late-spring and early summer. The addition of these two processes appear to be a low-hanging fruit and relatively easy subgrid-scale parameterization to implement into Earth system models.
- 5) Microphysics in complex terrain – the spatiotemporal distribution of precipitation amount and phase has been poorly explored to date because spatially continuous observations of both have been sorely lacking for decades in mountainous environments (Bales et al. 2006, Kinar and Pomeroy 2015). This has led to a recent collision course between convection-permitting climate modeling (Currier et al. 2017, Prein et al. 2015) and geospatial statistics (Daly et al. 2008) as both attempt to convince the mountain research communities that they can provide better spatiotemporal estimates of mountain precipitation. Given that radar measurements are proven means to estimate the spatiotemporal evolution of precipitation (Lundquist et al. 2008, Mott et al. 2014), SAIL provides a middle ground in which the added value of microphysics schemes commonly used in climate models can be juxtaposed with the methods employed by reanalysis product generation (e.g., the Mountain Climate Simulator [MT-CLIM] used in Livneh – <http://www.ntsg.umt.edu/project/mt-clim.php>).

Data from SAIL can be used in Earth system model development. Earth system model representation of mountain snowpack has largely been hampered by the distinct scale mismatch between common Earth system model resolutions (~100km) and snow models (~10m-1km) (Frei et al. 2005, Rutter et al. 2009, Essery et al. 2009, Chen et al. 2014, Wu et al. 2017, Rhoades et al. 2016, 2018). The path forward may be the use of intermediate scale (~1-10km) integrated process models (e.g., WRF fully coupled with a snow model). This is because integrated process models are more tractable as they are computationally less expensive, can more realistically represent important model lower boundary features (e.g., topography and land-surface cover) and can be more easily bounded (or periodically updated) by observations.

This list is not exhaustive, yet provides a sampling of the possible process representation exploration that can be enabled by both the establishment of an integrated process model coupled with a SAIL observational campaign and their combined potential to abate longstanding Earth system model modes of failure, particularly in mountainous regions (Rhoades et al. 2016, 2018). A secondary benefit of this work is that after the integrated process model has been optimized (or can be bounded by periodic observations), it can then provide a more physics-based means to spatially interpolate between intermittent observations in both space and time.

7.0 Relevancy to the DOE Mission

The SAIL deployment of the AMF2 is highly relevant to, and specifically supports, the BER Earth and Environmental Systems Sciences Division (EESSD) mission. First, the 2019 Workshop Report for the ARM Mobile Facility (U.S. DOE 2019) indicates that mountainous and complex terrain regions “were identified by the workshop organizers as the highest priority for discussion.” Within complex terrain, the report notes that: “Observations could support studies to improve the significant understanding gaps in the areas of convection, extreme precipitation and weather, and interactions between atmospheric circulation, radiation, and land-surface conditions.” The report further identifies clouds and precipitation, aerosols, and land-atmosphere interactions as key science topics. By measuring clouds, precipitation, aerosols, and land-atmosphere interactions using ARM observations and existing surface observations from the Watershed Function SFA within the context of an integrated field laboratory, the SAIL campaign is directly responsive to the science needs identified in that report.

The Workshop Report also highlighted potential collaborations with other DOE programs with the following language: “Mountains provide an organizing theme for studying atmospheric and terrestrial processes, so the deployment of the AMF in mountains may foster collaborations between ARM/ASR and Terrestrial Ecosystem Science (TES) and SBR programs to improve understanding and modeling of earth system processes.” Finally, SAIL may be able to complement the upcoming deployment of the AMF3 to the Southeastern U.S. by providing upstream data on aerosols and eastward-propagating atmospheric phenomena.

SAIL will contribute to EESSD’s Strategic Plan Goal 2, Supporting Objective 6 by addressing the couplings between water and energy in a mountainous watershed and thus will “advance understanding and process representation of the couplings involving energy and water cycles, and improve dynamical representations of these cycles to better represent climate forcings at the interfaces of terrestrial, aquatic, and urban systems.”

By involving the ARM user facility in an Integrated Field Laboratory and by responding to BERAC’s recommendation for an IFL and the repeated requests by the mountain hydrometeorology community for integrated surface and atmospheric observations, the SAIL deployment would directly advance EESSD’s Strategic Plan Goal 4, supporting Objective 4 of “advanc[ing] capabilities and aggressively exploit[ing] the unique DOE facilities that provide critical detailed observations necessary to understand cloud, aerosol, and radiative properties over land, sea, and ice.”

With respect to the ARM Decadal Vision, SAIL observations will provide a clear path towards advancing the scientific understanding and Earth system model representation in regions of complex topography wherein models are consistently problematic and uncertain in their representation of processes

contributing to precipitation and snowmelt. SAIL further supports the ARM Decadal Vision that identifies “regions influenced by significant orography” as priorities for using the AMF to advance DOE high-priority science. Finally, the SAIL deployment, when coupled to ongoing terrestrial science observations as part of the Watershed Function SFA, support the strategic goals for the next-generation ARM facility by “strengthen[ing] interactions with the user community” and “enhanc[ing] data products and processes.”

8.0 References

- Adams, DK, and AC Comrie. 1997. “The North American Monsoon.” *Bulletin of the American Meteorological Society* 78(10): 2197–2213, [https://doi.org/10.1175/1520-0477\(1997\)078<2197:TNAM>2.0.CO;2](https://doi.org/10.1175/1520-0477(1997)078<2197:TNAM>2.0.CO;2)
- Anderson, B, A Mackintosh, D Stumm, and SJ Fitzsimons. 2010. “Climate sensitivity of a high-precipitation glacier in New Zealand.” *Journal of Glaciology* 56(195): 114–128, <https://doi.org/10.3189/002214310791190929>
- Bales, RC, NP Molotch, TH Painter, MD Dettinger, R Rice, and J Dozier. 2006. “Mountain hydrology of the western United States.” *Water Resources Research* 42(8): W08432, <https://doi.org/10.1029/2005WR004387>
- Barnett, TP, JC Adam, and DP Lettenmaier. 2005. “Potential impacts of a warming climate on water availability in snow-dominated regions.” *Nature* 438: 303–309, <https://doi.org/10.1038/nature04141>
- Barnhart, TB, NP Molotch, B Livneh, AA Harpold, JF Knowles, and D Schneider. 2016. “Snowmelt rate dictates streamflow.” *Geophysical Research Letters* 43(15): 8006–8016, <https://doi.org/10.1002/2016GL069690>
- BERAC. 2015. https://science.osti.gov/-/media/ber/berac/pdf/Reports/BERAC_IFL_Response.pdf
- Berghuijs, WR, RA Woods, and M Hrachowitz. 2014. “A precipitation shift from snow towards rain leads to a decrease in streamflow.” *Nature Climate Change* 4: 583–586, <https://doi.org/10.1038/nclimate2246>
- Bond, TC, SJ Doherty, DW Fahey, PM Forster, T Berntsen, BJ DeAngelo, MG Flanner, S Ghan, B Karcher, D Koch, S Kinne, Y Kondo, PK Quinn, MC Sarofim, MG Schultz, M Schulz, C Venkataraman, H Zhang, S Zhang, N Bellouin, SK Guttikunda, PK Hopke, MZ Jacobson, JW Kaiser, Z Klimont, U Lohmann, JP Schwarz, D Shindell, T Storelvmo, SG Warren, and CS Zender. 2013. “Bounding the role of black carbon in the climate system: A scientific assessment.” *Journal of Geophysical Research: Atmospheres* 118(11): 5380–5552, <https://doi.org/10.1002/jgrd.50171>
- Borys, RD, DH Lowenthal, SA Cohn, and WOJ Brown. 2003. “Mountaintop and radar measurements of anthropogenic aerosol effects on snow growth and snowfall rate.” *Geophysical Research Letters* 30(10): 1538, <https://doi.org/10.1029/2002GL016855>

- Carroll, RWH, LA Bearup, W Brown, W Dong, M Bill, and KH Williams. 2018. “Factors controlling seasonal groundwater and solute flux from snow-dominated basins.” *Hydrological Processes* 32(14): 2187–2202, <https://doi.org/10.1002/hyp.13151>
- Carroll, RWH, and KH Williams. 2019. Discharge data collected within the East River for the Lawrence Berkeley National Laboratory Watershed Function Science Focus Area (Water years 2015-2018). ESS-DIVE. <https://doi.org/10.21952/WTR/1495380>
- Carroll, RWH, D Gochis, and KH Williams. 2020. “Efficiency of the summer monsoon in generating streamflow within a snow dominated headwater basin of the Colorado River.” *Geophysical Research Letters* 47(23): e2020GL090856, <https://doi.org/10.1029/2020GL090856>
- Castro, CL, H Chang, F Dominguez, C Carrillo, J Schemm, and HH Juang. 2012. “Can a Regional Climate Model Improve the Ability to Forecast the North American Monsoon?” *Journal of Climate* 25(23): 8212–8237, <https://doi.org/10.1175/JCLI-D-11-00441.1>
- Chandrasekar, V, H Chen, and B Philips. 2018. “Principles of High-Resolution Radar Network for Hazard Mitigation and Disaster Management in an Urban Environment.” *Journal of the Meteorological Society of Japan* 96A: 119–139, <https://doi.org/10.2151/jmsj.2018-015>
- Chen, F, M Barlage, M Tewari, R Rasmussen, J Jin, D Lettenmaier, B Livneh, C Lin, G Miguez-Macho, G-Y Niu, L Wen, and Z-L Yang. 2014. “Modeling seasonal snowpack evolution in the complex terrain and forested Colorado Headwaters region: A model intercomparison study.” *Journal of Geophysical Research Atmospheres* 119(24): 13,795–13,819, <https://doi.org/10.1002/2014JD022167>
- Chen, X, Y Liu, and G Wu. 2017. “Understanding the surface temperature cold bias in CMIP5 AGCMs over the Tibetan Plateau.” *Advances in Atmospheric Sciences* 34: 1447–1460, <https://doi.org/10.1007/s00376-017-6326-9>
- Chou, C, and JD Neelin. 2003. “Mechanisms limiting the northward extent of the northern summer monsoons over North America, Asia, and Africa.” *Journal of Climate* 16(3): 406–425, [https://doi.org/10.1175/1520-0442\(2003\)016<0406:MLTNEO>2.0.CO;2](https://doi.org/10.1175/1520-0442(2003)016<0406:MLTNEO>2.0.CO;2)
- Clark, MP, B Nijssen, JD Lundquist, D Kavetski, DE Rupp, RA Woods, JE Freer, ED Gutmann, AW Wood, LD Brekke, JR Arnold, DJ Gochis, and RM Rasmussen. 2015a. “A unified approach for process-based hydrologic modeling: 1. Modeling concept.” *Water Resources Research* 51(4): 2498–2514, <https://doi.org/10.1002/2015WR017198>
- Clark, MP, B Nijssen, JD Lundquist, D Kavetski, DE Rupp, RA Woods, JE Freer, ED Gutmann, AW Wood, DJ Gochis, RM Rasmussen, DG Tarboton, V Mahat, GN Flerchinger, and DG Marks. 2015b. “A unified approach for process-based hydrologic modeling: 2. Model implementation and case studies.” *Water Resources Research* 51(4): 2515–2542, <https://doi.org/10.1002/2015WR017200>
- Clow, DW. 2010. “Changes in the Timing of Snowmelt and Streamflow in Colorado: A Response to Recent Warming.” *Journal of Climate* 23(9): 2293–2306, <https://doi.org/10.1175/2009JCLI2951.1>

- Currier, WR, T Thorson, and JD Lundquist. 2017. “Independent Evaluation of Frozen Precipitation from WRF and PRISM in the Olympic Mountains.” *Journal of Hydrometeorology* 18(10): 2681–2703, <https://doi.org/10.1175/JHM-D-17-0026.1>
- Daly, C, M Halbleib, JI Smith, WP Gibson, MK Doggett, GH Taylor, J Curtis, and PP Pasteris. 2008. “Physiographically sensitive mapping of climatological temperature and precipitation across the conterminous United States.” *International Journal of Climatology* 28(15): 2031–2064, <https://doi.org/10.1002/joc.1688>
- DeMott, PJ, AJ Prenni, X Liu, MD Petters, CH Twohy, MS Richardson, T Eidhammer, SM Kreidenweis, and DC Rogers. 2010. “Predicting global atmospheric ice nuclei distributions and their impacts on climate.” *Proceedings of the National Academy of Sciences of the United States of America* 107(25): 11217–11222, <https://doi.org/10.1073/pnas.0910818107>
- de Wekker, SFJ, and M Kossmann. 2015. “Convective Boundary Layer Heights over Mountainous Terrain—A Review of Concepts.” *Frontiers in Earth Science*, <https://doi.org/10.3389/feart.2015.00077>
- Douglas, AV, and PJ Englehart. 2007. “A climatological perspective of transient synoptic features during NAME 2004.” *Journal of Climate* 20(9): 1947–1954, <https://doi.org/10.1175/JCLI4095.1>
- Eisel, LM, KD Mills, and CF Leaf. 1988. “Estimated Consumptive Loss from Man-Made Snow.” *Journal of the American Water Resources Association* 24(4): 815–820, <https://doi.org/10.1111/j.1752-1688.1988.tb00932.x>
- Essery, R, N Rutter, J Pomeroy, R Baxter, M Stahli, D Gustafsson, A Barr, P Bartlett, and K Elder. 2009. “SNOWMIP2: An Evaluation of Forest Snow Process Simulations.” *Bulletin of the American Meteorological Society* 90(8): 1120–1136, <https://doi.org/10.1175/2009BAMS2629.1>
- Everard KA, HJ Oldroyd, and A Christen. 2020. “Turbulent Heat and Momentum Exchange in Nocturnal Drainage Flow through a Sloped Vineyard.” *Boundary-Layer Meteorology* 175: 1–23, <https://doi.org/10.1007/s10546-019-00491-y>
- Fan, J, LR Leung, PJ DeMott, JM Comstock, B Singh, D Rosenfeld, JM Tomlinson, A White, KA Prather, P Minnis, JK Ayers, and Q Min. 2014. “Aerosol impacts on California winter clouds and precipitation during CalWater 2011: Local pollution versus long-range transported dust.” *Atmospheric Chemistry and Physics* 14(1): 81–101, <https://doi.org/10.5194/acp-14-81-2014>
- Fan, J, D Rosenfeld, Y Yang, C Zhao, LR Leung, and Z Li. 2015. “Substantial contribution of anthropogenic air pollution to catastrophic floods in Southwest China.” *Geophysical Research Letters* 42(14): 6066–6075, <https://doi.org/10.1002/2015GL064479>
- Fan, J, LR Leung, D Rosenfeld, and PJ DeMott. 2017. “Effects of cloud condensation nuclei and ice nucleating particles on precipitation processes and supercooled liquid in mixed-phase orographic clouds.” *Atmospheric Chemistry and Physics* 17: 1017–1035, <https://doi.org/10.5194/acp-17-1017-2017>
- Flanner, MG, CS Zender, PG Hess, NM Mahowald, TH Painter, V Ramanathan, and PJ Rasch. 2009. “Springtime warming and reduced snow cover from carbonaceous particles.” *Atmospheric Chemistry and Physics* 9(7): 2481–2497, <https://doi.org/10.5194/acp-9-2481-2009>

- Frei, C, and C Schär. 1998. “A precipitation climatology of the Alps from high-resolution rain-gauge observations.” *International Journal of Climatology* 18: 873–900, [https://doi.org/10.1002/\(SICI\)1097-0088\(19980630\)18:8<873::AID-JOC255>3.0.CO;2-9](https://doi.org/10.1002/(SICI)1097-0088(19980630)18:8<873::AID-JOC255>3.0.CO;2-9)
- Frei, A, R Brown, JA Miller, and DA Robinson. 2005. “Snow Mass over North America: Observations and Results from the Second Phase of the Atmospheric Model Intercomparison Project.” *Journal of Hydrometeorology* 6(5): 681–695, <https://doi.org/10.1175/JHM443.1>
- Gevaert, AI, DG Miralles, RAM Jeu, J Schellekens, and AJ Dolman. 2018. “Soil moisture temperature coupling in a set of land surface models.” *Journal of Geophysical Research Atmospheres* 123(3): 1481–1498, <https://doi.org/10.1002/2017JD027346>
- Gochis, DJ, L Brito-Castillo, and WJ Shuttleworth. 2006. “Hydroclimatology of the North American Monsoon Region in northwest Mexico.” *Journal of Hydrology* 316(1-4): 53–70, <https://doi.org/10.1016/j.jhydrol.2005.04.021>
- Gochis, D, J Busto, K Howard, J Deems, N Coombs, I Maycumber, K Bormann, A Dugger, L Karsten, N Langley, J Mickey, T Painter, M Richardson, SM Skiles, and L Tang. 2016. Final Report: Upper Rio Grande Basin Snowfall Measurement and Streamflow (RIO-SNO-FLOW) Forecasting Improvement Project. Colorado Water Conservation Board and Conejos Water Conservancy District. <https://www.sciencebase.gov/catalog/item/56e97e2be4b0f59b85d8194b>
- Grantz, K, B Rajagopalan, M Clark, and E Zagona. 2007. “Seasonal Shifts in the North American Monsoon.” *Journal of Climate* 20(9): 1923–1935, <https://doi.org/10.1175/JCLI4091.1>
- Groot Zwaafink, CD, R Mott, and M Lehning. 2013. “Seasonal simulation of drifting snow sublimation in Alpine terrain.” *Water Resources Research* 49(3): 1581–1590, <https://doi.org/10.1002/wrcr.20137>
- Gutzler, DS. 2000. “Covariability of spring snowpack and summer rainfall across the Southwest United States.” *Journal of Climate* 13(22): 4018–4027, [https://doi.org/10.1175/1520-0442\(2000\)013<4018:COSSAS>2.0.CO;2](https://doi.org/10.1175/1520-0442(2000)013<4018:COSSAS>2.0.CO;2)
- Hamlet, AF, PW Mote, MP Clark, and DP Lettenmaier. 2007. “Twentieth-century trends in runoff, evapotranspiration, and soil moisture in the western United States.” *Journal of Climate* 20(8): 1468–1486, <https://doi.org/10.1175/JCLI4051.1>
- Hallar, AG, G Chirokova, I McCubbin, TH Painter, C Wiedinmyer, and C Dodson. 2011. “Atmospheric bioaerosols transported via dust storms in the western United States.” *Geophysical Research Letters* 38(17): L17801, <https://doi.org/10.1029/2011GL048166>
- Hansen, J, and L Nazarenko. 2004. “Soot climate forcing via snow and ice albedos.” *Proceedings of the National Academy of Sciences of the United States of America* 101(2): 423–428, <https://doi.org/10.1073/pnas.2237157100>
- Harrington, JY, K Sulia, and H Morrison. 2013. “A method for Adaptive Habit Prediction in Bulk Microphysical Models. Part I: Theoretical Development.” *Journal of the Atmospheric Sciences* 70(2): 349–364, <https://doi.org/10.1175/JAS-D-12-040.1>

- Helgason, W, and J Pomeroy. 2012. “Problems Closing the Energy Balance over a Homogeneous Snow Cover during Midwinter.” *Journal of Hydrometeorology* 13(2): 557–572, <https://doi.org/10.1175/JHM-D-11-0135.1>
- Henn, B, MP Clark; D Kavetski; AJ Newman; M Hughes; B McGurk; and JD Lundquist. 2016. “Spatiotemporal patterns of precipitation inferred from streamflow observations across the Sierra Nevada mountain range.” *Journal of Hydrology* 556: 993–1012, <https://doi.org/10.1016/j.jhydrol.2016.08.009>
- Henn, B, AJ Newman, B Livneh, C Daly, and JD Lundquist. 2018. “An assessment of differences in gridded precipitation datasets in complex terrain.” *Journal of Hydrology* 556: 1205–1219, <https://doi.org/10.1016/j.jhydrol.2017.03.008>
- Higgins, W, and D Gochis. 2007. “Synthesis of Results from the North American Monsoon Experiment (NAME) Process Study.” *Journal of Climate* 20(9): 1601–1607, <https://doi.org/10.1175/JCLI4081.1>
- Hock, R. 2005. “Glacier melt: a review of processes and their modelling.” *Progress in Physical Geography: Earth and Environment* 29(3): 362–391, <https://doi.org/10.1191/0309133305pp453ra>
- Huffman, JA, AJ Prenni, PJ DeMott, C Pöhlker, RH Mason, NH Robinson, J Fröhlich-Nowoisky, Y Tobo, VR Després, E Garcia, DJ Gochis, E Harris, I Müller-Germann, C Ruzene, B Schmer, B Sinha, DA Day, MO Andreae, JL Jimenez, M Gallagher, SM Kreidenweis, AK Bertram, and U Pöschl. 2013. “High concentrations of biological aerosol particles and ice nuclei during and after rain.” *Atmospheric Chemistry and Physics* 13(13): 6151–6164, <https://doi.org/10.5194/acp-13-6151-2013>
- Huss, M, B Bookhagen, C Huggel, D Jacobsen, R Bradley, J Clague, M Vuille, W Buytaert, D Cayan, G Greenwood, B Mark, A Milner, R Weingartner, and M Winder. 2017. “Toward mountains without permanent snow and ice.” *Earth's Future* 5(5): 418–435, <https://doi.org/10.1002/2016EF000514>
- Hubbard, SS, C Varadharajan, Y Wu, H Wainwright, and D Dwivedi. 2020. “Emerging technologies and radical collaboration to advance predictive understanding of watershed hydrobiogeochemistry.” *Hydrological Processes* 34(15): 3175–3182, <https://doi.org/10.1002/hyp.13807>
- Jackson, R, S Collis, T Lang, and C Potvin. 2019. PyDDA: A New Pythonic Wind Retrieval Package. NASA Technical Report Services, MSFC-E-DAA-TN68855.
- Jambon-Puillet, E, N Shahidzadeh, and D Bonn. 2018. “Singular sublimation of ice and snow crystals.” *Nature Communications* 9: 4191, <https://doi.org/10.1038/s41467-018-06689-x>
- James, T, et al. 2014. The economic importance of the Colorado River to the basin region. Final Report, L. William Seidman Research Institute, Arizona State University 54, <http://azsmart-dev.wpcarey.asu.edu/wp-content/uploads/2015/01/PTF-Final-121814.pdf>
- Jennings, K, TS Winchell, B Livneh, and NP Molotch. 2018. “Spatial variation of the rain-snow temperature threshold across the Northern Hemisphere.” *Nature Communications* 9(1): 1148, <https://doi.org/10.1038/s41467-018-03629-7>

- Jones, A, DR Feldman, DJ Paynter, V Ramaswamy, WD Collins, and R Pincus. 2017. “A New Paradigm for Diagnosing Contributions to Model Aerosol Forcing Error.” *Geophysical Research Letters* 44(23): 12004–12012, <https://doi.org/10.1002/2017GL075933>
- Kaspari, SD, M Schwikowski, M Gysel, MG Flanner, S Kang, S Hou, and PA Mayewski. 2011. “Recent increase in black carbon concentrations from a Mt. Everest ice core spanning 1860–2000 AD.” *Geophysical Research Letters* 38(4): L04703, <https://doi.org/10.1029/2010GL046096>
- Kassianov, E, M Pekour, C Flynn, LK Berg, J Beranek, A Zelenyuk, C Zhao, LR Leung, PL Ma, L Riihimaki, JD Fast, J Barnard, AG Hallar, IB McCubbin, EW Eloranta, A McComiskey, and PJ Rasch. 2017. “Large Contribution of Coarse Mode to Aerosol Microphysical and Optical Properties: Evidence from Ground-Based Observations of a Transpacific Dust Outbreak at a High-Elevation North American Site.” *Journal of the Atmospheric Sciences* 74(5): 1431–1443, <https://doi.org/10.1175/JAS-D-16-0256.1>
- Kinar, NJ, and JW Pomeroy. 2015. “Measurement of the physical properties of the snowpack.” *Review of Geophysics* 53(2): 481–544, <https://doi.org/10.1002/2015RG000481>
- Kerminen, V, X Chen, V Vakkari, T Peja, M Kulmala, and F Bianchi. 2018. “Atmospheric new particle formation and growth: review of field observations.” *Environmental Research Letters* 13(10): 103003, <https://doi.org/10.1088/1748-9326/aadf3c>
- Kumjian, MR, SA Rutledge, RM Rasmussen, P Kennedy, and M Dixon. 2014. “High-resolution polarimetric radar observations of snow generating cells.” *Journal of Applied Meteorology and Climatology* 53(6): 1636–1658, <https://doi.org/10.1175/JAMC-D-13-0312.1>
- Kumjian, MR, and KA Lombardo. 2017. “Insights into the evolving microphysical and kinematic structure of northeastern U.S. winter storms from dual-polarization Doppler radar.” *Monthly Weather Review* 145(3): 1033–1061, <https://doi.org/10.1175/MWR-D-15-0451.1>
- Laskin, A, J Laskin, and SA Nizkorodov. 2015. “Chemistry of Atmospheric Brown Carbon.” *Chemical Reviews* 115(10): 4335–4382, <https://doi.org/10.1021/cr5006167>
- Lee, W-L, Y Gu, KN Liou, LR Leung, and HH Hsu. 2015. “A global model simulation for 3-D radiative transfer impact on surface hydrology over the Sierra Nevada and Rocky Mountains.” *Atmospheric Chemistry and Physics* 15: 5405–5413, <https://doi.org/10.5194/acp-15-5405-2015>
- Li, D, ML Wrzesien, M Durand, J Adam, and DP Lettenmaier. 2017. “How much runoff originates as snow in the western United States, and how will that change in the future?” *Geophysical Research Letters* 44(1): 6163–6172, <https://doi.org/10.1002/2017GL073551>
- Liang, X, J Zhu, KE Kunkel, M Ting, and JX Wang. 2008. “Do CGCMs Simulate the North American Monsoon Precipitation Seasonal–Interannual Variability?” *Journal of Climate* 21(17): 4424–4448, <https://doi.org/10.1175/2008JCLI2174.1>
- Liston, G. 1995. “Local advection of momentum, heat, and moisture during the melt of patchy snow covers.” *Journal of Applied Meteorology* 34(7): 1705–1715, <https://doi.org/10.1175/1520-0450-34.7.1705>

- Liston, GE, and M Sturm. 2002. “Winter precipitation patterns in arctic Alaska determined from a blowing-snow model and snow-depth observations.” *Journal of Hydrometeorology* 3(6): 646–659, [https://doi.org/10.1175/1525-7541\(2002\)003<0646:WPPIAA>2.0.CO;2](https://doi.org/10.1175/1525-7541(2002)003<0646:WPPIAA>2.0.CO;2)
- Lo, F, and MP Clark. 2002. “Relationships between spring snow mass and summer precipitation in the southwestern United States associated with the North American monsoon system.” *Journal of Climate* 15(11): 1378–1385, [https://doi.org/10.1175/1520-0442\(2002\)015<1378:RBSSMA>2.0.CO;2](https://doi.org/10.1175/1520-0442(2002)015<1378:RBSSMA>2.0.CO;2)
- López-Moreno, JI, S Gascoïn, J Herrero, EA Sproles, M Pons, E Alonso-González, L Hanich, A Boudhar, KN Musselman, NP Molotch, J Sickman, and J Pomeroy. 2017. “Different sensitivities of snowpacks to warming in Mediterranean climate mountain areas.” *Environmental Research Letters* 12(7): 074006, <https://doi.org/10.1088/1748-9326/aa70cb>
- Lundquist, JD, DR Cayan, and MD Dettinger. 2003. “Meteorology and Hydrology in Yosemite National Park: A Sensor Network Application.” In Zhao, F, and L Guibas (eds.) *Information Processing in Sensor Networks*. Lecture Notes in Computer Science, vol. 2634. Springer, Berlin, Heidelberg. https://doi.org/10.1007/3-540-36978-3_35
- Lundquist, JD, PJ Neiman, B Martner, AB White, DJ Gottas, and FM Ralph. 2008. “Rain versus Snow in the Sierra Nevada, California: Comparing Doppler Profiling Radar and Surface Observations of Melting Level.” *Journal of Hydrometeorology* 9(2): 194–211, <https://doi.org/10.1175/2007JHM853.1>
- Lundquist, JD, M Hughes, B Henn, ED Gutmann, B Livneh, J Dozier, and P Neiman. 2015. “High-Elevation Precipitation Patterns: Using Snow Measurements to Assess Daily Gridded Datasets across the Sierra Nevada, California.” *Journal of Hydrometeorology* 16(4): 1773–1792, <https://doi.org/10.1175/JHM-D-15-0019.1>
- Lundquist, J, M Hughes, E Gutmann, and S Kapnick. 2019. “Our Skill in Modeling Mountain Rain and Snow is Bypassing the Skill of Our Observational Networks.” *Bulletin of the American Meteorological Society* 100(12): 2473–2490, <https://doi.org/10.1175/BAMS-D-19-0001.1>
- Lynn, B, A Khain, D Rosenfeld, and WL Woodley. 2007. “Effects of aerosols on precipitation from orographic clouds.” *Journal of Geophysical Research Atmospheres* 112(D10): D10225, <https://doi.org/10.1029/2006JD007537>
- Maddox, RA, J Zhang, JJ Gourley, and KW Howard. 2002. “Weather Radar Coverage over the Contiguous United States.” *Weather Forecasting* 17(4): 927–934, [https://doi.org/10.1175/1520-0434\(2002\)017<0927:WRCOTC>2.0.CO;2](https://doi.org/10.1175/1520-0434(2002)017<0927:WRCOTC>2.0.CO;2)
- Malm, WC, JF Sisler, D Huffman, RA Eldred, and TA Cahill. 1994. “Spatial and seasonal trends in particle concentration and optical extinction in the United States.” *Journal of Geophysical Research Atmospheres* 99(D1): 1347–1370, <https://doi.org/10.1029/93JD02916>
- Marchand, R, GG Mace, AG Hallar, IB McCubbin, SY Matrosov, and MD Shupe. 2013. “Enhanced Radar Backscattering due to Oriented Ice Particles at 95 GHz during StormVEx.” *Journal of Atmospheric and Oceanic Technology* 30(10): 2336–2351, <https://doi.org/10.1175/JTECH-D-13-00005.1>

- McCabe, GJ, DM Wolock, GT Pederson, CA Woodhouse, and S McAfee. 2017. “Evidence that Recent Warming is Reducing Upper Colorado River Flows.” *Earth Interactions* 21(10): 1–14, <https://doi.org/10.1175/EI-D-17-0007.1>
- McCluskey, CS, PJ DeMott, AJ Prenni, EJT Levin, GR McMeeking, AP Sullivan, TCJ Hill, S Nakao, CM Carrico, and SM Kreidenweis. 2014. “Characteristics of atmospheric ice nucleating particles associated with biomass burning in the US: Prescribed burns and wildfires.” *Journal of Geophysical Research Atmospheres* 119(17): 10,458–10,470, <https://doi.org/10.1002/2014JD021980>
- McFarlane, SA, T Shippert, and J Mather. 2011. Radiatively Important Parameters Best Estimate (RIPBE): An ARM Value-Added Product. U.S. Department of Energy. [DOE/SC-ARM/TR-097](https://doi.org/10.1002/2014JD021980).
- Meng, XH, JP Evans, and MF McCabe. 2014. “The Impact of Observed Vegetation Changes on Land–Atmosphere Feedbacks during Drought.” *Journal of Hydrometeorology* 15(2): 759–776, <https://doi.org/10.1175/JHM-D-13-0130.1>
- Milly, PCD, and KA Dunne. 2020. “Colorado River flow dwindles as warming-driven loss of reflective snow energizes evaporation.” *Science* 367(6483): 1252–1255, <https://doi.org/10.1126/science.aay9187>
- Mlawer, EJ, JS Delamere, SA Clough, MH Zhang, MA Miller, KL Johnson, RA Ferrare, TR Shippert, CN Long, RT Cederwall, and RG Ellingson. 2002. “The broadband heating rate profile (BBHRP) VAP.” *Proceedings of the 12th Atmospheric Radiation Measurement (ARM) Science Team Meeting*. St. Petersburg, Florida. U.S. Department of Energy, https://arm.gov/publications/proceedings/conf12/extended_abs/mlawer-ej.pdf
- Mlawer, EJ, JS Delamere, SA Clough, RA Ferrare, MA Miller, KL Johnson, RT Cederwall, SC Xie, TR Shippert, CN Long, JA Ogren, RG Ellingson, JJ Michalsky, and MH Zhang. 2003. “Recent developments on the broadband heating rate profile value-added product.” *Proceedings of the 13th Atmospheric Radiation Measurement (ARM) Science Team Meeting*. Broomfield, Colorado. U.S. Department of Energy, https://arm.gov/publications/proceedings/conf13/extended_abs/mlawer-ej.pdf
- Moisseev, D, S Lautaportti, J Tyynela, and S Lim. 2015. “Dual-polarization radar signatures in snowstorms: Role of snowflake aggregation.” *Journal of Geophysical Research Atmospheres* 120(24): 12644–12655, <https://doi.org/10.1002/2015JD023884>
- Mote, PW, S Li, DP Lettenmaier, M Xiao, and R Engel. 2018. “Dramatic declines in snowpack in the western US.” *NPJ Climate and Atmospheric Science* 1: 2, <https://doi.org/10.1038/s41612-018-0012-1>
- Mott, R, D Scipión, M Schneebeli, N Dawes, A Berne, and M Lehning. 2014. “Orographic effects on snow deposition patterns in mountainous terrain.” *Journal of Geophysical Research Atmospheres* 119(3): 1363–1385, <https://doi.org/10.1002/2013JD019880>
- Mott, R, V Vionnet, and T Grunewald. 2018. “The Seasonal Snow Cover Dynamics: Review on Wind-Driven Coupling Processes.” *Frontiers in Earth Science*, <https://doi.org/10.3389/feart.2018.00197>
- Moulin, L, E Gaume, and C Obled. 2009. “Uncertainties on mean areal precipitation: assessment and impact on streamflow simulations.” *Hydrology and Earth System Sciences* 13(2): 99–114, <https://doi.org/10.5194/hess-13-99-2009>

- MRI Mountain Research Initiative. 2015. “Elevation-dependent warming in mountain regions of the world.” *Nature Climate Change* 5(5): 424–430, <https://doi.org/10.1038/nclimate2563>
- Mühlbauer, A, and U Lohmann. 2006. Aerosol-cloud interactions and the effects on orographic precipitation. In 12th AMS Conference on Cloud Physics, Madison, Wisconsin.
- Mühlbauer, A, and U Lohmann. 2008. “Sensitivity studies of the role of aerosols in warm-phase orographic precipitation in different dynamical flow regimes.” *Journal of the Atmospheric Sciences* 65(8): 2522–2542, <https://doi.org/10.1175/2007JAS2492.1>
- Musselman, KN, F Lehner, K Ikeda, MP Clark, AF Prein, C Liu, M Barlage, and R Rasmussen. 2018. “Projected increases and shifts in rain-on-snow flood risk over western North America.” *Nature Climate Change* 8: 808–812, <https://doi.org/10.1038/s41558-018-0236-4>
- National Research Council, Board on Atmospheric Sciences and Climate. 2002. *Weather radar technology beyond NEXRAD*. National Academies Press, Washington, D.C.
- Neelin, JD. 2007. “Moist dynamics of tropical convection zones in monsoons, teleconnections, and global warming.” In T Schneider and AH Sobel (eds.), *The Global Circulation of the Atmosphere* 267–301. Princeton University Press, Princeton, New Jersey.
- Nguyen, TB, A Laskin, J Laskin, and SA Nizkorodov. 2013. “Brown carbon formation from ketoaldehydes of biogenic monoterpenes.” *Faraday Discussions* 165: 473, <https://doi.org/10.1039/C3FD00036B>
- Nishita, C, K Osada, M Kido, K Matsunaga, and Y Iwasaka. 2008. “Nucleation mode particles in upslope valley winds at Mount Norikura, Japan: Implications for the vertical extent of new particle formation events in the lower troposphere.” *Journal of Geophysical Research Atmospheres* 113(D6): D06202, <https://doi.org/10.1029/2007JD009302>
- Oaida, CM, JT Reager, KM Andreadis, CH David, SR Levee, TH Painter, KJ Bormann, AR Trangstrom, M Giroto, and JS Famiglietti. 2019. “A High-Resolution Data Assimilation Framework for Snow Water Equivalent Estimation across the Western United States and Validation with the Airborne Snow Observatory.” *Journal of Hydrometeorology* 20(3): 357–358, <https://doi.org/10.1175/JHM-D-18-0009.1>
- Oleson, KW, DM Lawrence, GB Bonan, B Drewniak, M Huang, CD Koven, S Levis, F Li, WJ Riley, ZM Subin, SC Swenson, PE Thornton, A Bozbiyik, R Fisher, E Kluzek, J-F Lamarque, PJ Lawrence, LR Leung, W Lipscomb, S Muszala, DM Ricciuto, W Sacks, Y Sun, J Tang, and Z-L Yang. 2013. Technical Description of version 4.5 of the Community Land Model (CLM). National Center for Atmospheric Research, Boulder, Colorado, <https://opensky.ucar.edu/islandora/object/technotes:515>
- Palazzi, E, L Filippi, and J von Hardenberg. 2017. “Insights into elevation-dependent warming in the Tibetan Plateau-Himalayas from CMIP5 model simulations.” *Climate Dynamics* 48: 3991–4008, <https://doi.org/10.1007/s00382-016-3316-z>
- Palazzi, E, L Mortarini, S Terzago, and J von Hardenberg. 2019. “Elevation-dependent warming in global climate model simulations at high spatial resolution.” *Climate Dynamics* 52: 2685–2702, <https://doi.org/10.1007/s00382-018-4287-z>

- Pan, M, J Sheffield, EF Wood, KE Mitchell, PR Houser, JC Schaake, A Robock, D Lohmann, B Cosgrove, Q Duan, L Luo, RW Higgins, RT Pinker, and JD Tarpley. 2003. "Snow process modeling in the North American Land Data Assimilation System (NLDAS): 2. Evaluation of model simulated snow water equivalent." *Journal of Geophysical Research Atmospheres* 108(D22): 8850, <https://doi.org/10.1029/2003JD003994>
- Plüss, C, and A Ohmura. 1997. "Longwave Radiation on Snow-Covered Mountainous Surfaces." *Journal of Applied Meteorology and Climatology* 36(6): 818–824, <https://doi.org/10.1175/1520-0450-36.6.818>
- Prat, OP, and AP Barros. 2010. "Assessing satellite-based precipitation estimates in the Southern Appalachian mountains using rain gauges and TRMM PR." *Advances in Geosciences* 25: 143–153, <https://doi.org/10.5194/adgeo-25-143-2010>
- Prein, AF, W Langhans, G Fosser, A Ferrone, N Ban, K Goergen, M Keller, M Tölle, O Gutjahr, F Feser, E Brisson, S Kollet, J Schmidli, NPM van Lipzig, and LR Leung. 2015. "A review on regional convection permitting climate modeling: Demonstrations, prospects, and challenges." *Review of Geophysics* 53(2): 323–361, <https://doi.org/10.1002/2014RG000475>
- Prenni, AJ, Y Tobo, E Garcia, PJ DeMott, C McCluskey, SM Kreidenweis, J Prenni, A Huffman, U Pöschl, and C Pöhlker. 2013. "The impact of rain on ice nuclei populations." *Geophysical Research Letters* 40(1): 227–231, <https://doi.org/10.1029/2012GL053953>
- Qian, Y, MG Flanner, LR Leung, and W Wang. 2011. "Sensitivity studies on the impacts of Tibetan Plateau snowpack pollution on the Asian hydrological cycle and monsoon climate." *Atmospheric Chemistry and Physics* 11(5): 1929–1948, <https://doi.org/10.5194/acp-11-1929-2011>
- Ramanathan, V, and G Carmichael. 2008. "Global and regional climate changes due to black carbon." *Nature Geoscience* 1: 221–227, <https://doi.org/10.1038/ngeo156>
- Rangwala, I, and JR Miller. 2012. "Climate change in mountains: a review of elevation-dependent warming and its possible causes." *Climatic Change* 114: 527–547, <https://doi.org/10.1007/s10584-012-0419-3>
- Rasmussen, R, B Baker, J Kochendorfer, T Meyers, S Landolt, AP Fischer, J Black, JM Theriault, P Kucera, D Gochis, C Smith, R Nitu, M Hall, K Ikeda, and E Gutmann. 2012. "How well are we measuring snow: The NOAA/FAA/NCAR winter precipitation test bed." *Bulletin of the American Meteorological Society* 93(6): 811–829, <https://doi.org/10.1175/BAMS-D-11-00052.1>
- Rhoades, AM, X Huang, PA Ullrich, and CM Zarzycki. 2016. "Characterizing Sierra Nevada Snowpack Using Variable-Resolution CESM." *Journal of Applied Meteorology and Climatology* 55(1): 173–196, <https://doi.org/10.1175/JAMC-D-15-0156.1>
- Rhoades, AM, PA Ullrich, and CM Zarzycki. 2018a. "Projecting 21st century snowpack trends in western USA mountains using variable-resolution CESM." *Climate Dynamics* 50: 261–268, <https://doi.org/10.1007/s00382-017-3606-0>

- Rhoades, AM, PA Ullrich, CM Zarzycki, H Johansen, SA Margulis, H Morrison, Z Xu, and WD Collins. 2018b. “Sensitivity of mountain hydroclimate simulations in variable-resolution CESM to microphysics and horizontal resolution.” *Journal of Advances in Modeling Earth Systems* 10(6): 1357–1380, <https://doi.org/10.1029/2018MS001326>
- Rhoades, AM, AD Jones, and PA Ullrich. 2018c. “Assessing mountains as natural reservoirs with a multimetric framework.” *Earth's Future* 6(9): 1221–1241, <https://doi.org/10.1002/2017EF000789>
- Rodriguez, S, Y Gonzales, E Cuevas, R Ramos, R Romero, PM Romero, J Abreu-Afonso, and A Redondas. 2009. “Atmospheric nanoparticle observations in the low free troposphere during upward orographic flows at Izana Mountain Observatory.” *Atmospheric Chemistry and Physics* 9(17): 6319–35, <https://doi.org/10.5194/acp-9-6319-2009>
- Rutter, N, R Essery, J Pomeroy, N Altimir, K Andreadis, I Baker, A Barr, P Bartlett, A Boone, H Deng, H Douville, E Dutra, K Elder, C Ellis, X Feng, A Gelfan, A Goodbody, Y Gusev, D Gustafsson, R Hellstrom, Y Hirabayashi, T Hirota, T Jonas, V Koren, A Kuragina, D Lettenmaier, W-P Li, C Luce, E Martin, O Nasonova, J Pumpanen, RD Pyles, P Samuelsson, M Sandells, G Schadler, A Shmakin, TG Smirnova, M Stahli, R Stockli, U Strasser, H Su K Suzuki, K Takata, K Tanaka, E Thompson, T Vesala, P Viterbo, A Wiltshire, K Xia, Y Xue, and T Yamazaki. 2009. “Evaluation of forest snow processes models (SnowMIP2).” *Journal of Geophysical Research Atmospheres* 114(D6): D06111, <https://doi.org/10.1029/2008JD011063>
- Saleeby, SM, WR Cotton, D Lowenthal RD Borys, and MA Wetzel. 2009. “Influence of cloud condensation nuclei on orographic snowfall.” *Journal of Applied Meteorology and Climatology*, 48(5): 903–922, <https://doi.org/10.1175/2010JAMC2594.1>
- Saleeby, SM, WR Cotton, and JD Fuller. 2011. “The cumulative impact of cloud droplet nucleating aerosols on orographic snowfall in Colorado.” *Journal of Applied Meteorology and Climatology* 50(3): 604–625, <https://doi.org/10.1175/2010JAMC2594.1>
- Schlögl, S, M Lehning, K Nishimura, H Huwald, NJ Cullen, and R Mott. 2017. “How do Stability Corrections Perform in the Stable Boundary Layer over Snow?” *Boundary-Layer Meteorology* 165: 161–180, <https://doi.org/10.1007/s10546-017-0262-1>
- Schrom, RS, and MR Kumjian. 2016. “Connecting microphysical processes in Colorado winter storms with vertical profiles of radar observations.” *Journal of Applied Meteorology and Climatology* 55(8): 1771–1787, <https://doi.org/10.1175/JAMC-D-15-0338.1>
- Schrom, RS, MR Kumjian, and Y Lu. 2015. “Polarimetric radar signatures of dendritic growth zones within Colorado winter storms.” *Journal of Applied Meteorology and Climatology* 54(12): 2365–2388, <https://doi.org/10.1175/JAMC-D-15-0004.1>
- Serreze, MC, MP Clark, and A Frei. 2001. “Characteristics of large snowfall events in the montane western United States as examined using snowpack telemetry (SNOTEL) data.” *Water Resources Research* 37(3): 675–688, <https://doi.org/10.1029/2000WR900307>
- Sevruk, B. 1997. “Regional Dependency of Precipitation-Altitude Relationship in the Swiss Alps.” *Climatic Change* 36: 355–369, <https://doi.org/10.1023/A:1005302626066>

Shaw, GE. 2007. “Aerosols at a mountaintop observatory in Arizona.” *Journal of Geophysical Research – Atmospheres* 112(D7): D07206, <https://doi.org/10.1029/2005JD006893>

Sheffield, J, AP Barrett, B Colle, D Nelun Fernando, R Fu, KL Geil, Q Hu, J Kinter, S Kumar, B Langenbrunner, K Lombardo, LN Long, E Maloney, A Mariotti, JE Meyerson, KC Mo, J David Neelin, S Nigam, Z Pan, T Ren, A Ruiz-Barradas, YL Serra, A Seth, JM Thibeault, JC Stroeve, Z Yang, and L Yin. 2013. “North American Climate in CMIP5 Experiments. Part I: Evaluation of Historical Simulations of Continental and Regional Climatology.” *Journal of Climate* 26(23): 9209–9245, <https://doi.org/10.1175/JCLI-D-12-00592.1>

Shen, X, J Sun, X Zhang, N Kivekas, Y Zhang, T Wang, X Zhang, Y Yang, D Wang, Y Zhao, and D Qin. 2016. “Particle climatology in central East China retrieved from measurements in planetary boundary layer and in free troposphere at a 1500-m high mountain top site.” *Aerosol and Air Quality Research* 16(3): 689–701, <https://doi.org/10.4209/aaqr.2015.02.0070>

Skiles, SM, TH Painter, J Belnap, L Holland, RL Reynolds, HL Goldstein, and J Lin. 2015. “Regional variability in dust on snow processes and impacts in the Upper Colorado River Basin.” *Hydrological Processes* 29(26): 5397–5413, <https://doi.org/10.1002/hyp.10569>

Skiles, SM, and TH Painter. 2016. A 9-yr record of dust-on-snow in the Colorado River Basin, Proceedings of the 12th Biennial Conference of Science and Management on the Colorado Plateau. U.S. Geological Survey Scientific Investigations Report 2015–5180, 3-11, <https://doi.org/10.3133/sir20155180>

Skiles, SM, and TH Painter. 2017. “Daily evolution in dust and black carbon content, snow grain size, and snow albedo during snowmelt, Rocky Mountains, Colorado.” *Journal of Glaciology* 63(237): 118–132, <https://doi.org/10.1017/jog.2016.125>

Slater, AG, CA Schlosser, CE Desborough, AJ Pitman, A Henderson-Sellers, A Robock, K Ya Vinnikov, J Entin, K Mitchell, F Chen, A Boone, P Etchevers, F Habets, J Noilhan, H Braden, PM Cox, P de Rosnay, RE Dickenson, Z-L Yang, Y-J Dai, Q Zeng, Q Duan, V Koren, S Schaake, N Gedney, YM Gusev, ON Nasonova, J Kim, EA Kowalczyk, AB Shmakin, TG Smirnova, D Verseghy, P Wetzel, and Y Xue. 2001. “The Representation of Snow in Land Surface Schemes: Results from PILPS 2(d).” *Journal of Hydrometeorology* 2(1): 7–25, [https://doi.org/10.1175/1525-7541\(2001\)002<0007:TROSIL>2.0.CO;2](https://doi.org/10.1175/1525-7541(2001)002<0007:TROSIL>2.0.CO;2)

Stigter, EE, M Litt, JF Steiner, PNJ Bonekamp, JM Shea, MFP Bierkens, and WW Immerzeel. 2018. “The Importance of Snow Sublimation on a Himalayan Glacier.” *Frontiers in Earth Science* 6: 108, <https://doi.org/10.3389/feart.2018.00108>

Stoelinga, MT, RE Stewart, G Thompson, and JM Theriault. 2013. “Microphysical processes within winter orographic cloud and precipitation systems.” in *Mountain Weather Research and Forecasting*, Chow, FK, SFJ De Wekker, and BJ Snyder, eds., pp. 345–408, Springer Atmospheric Sciences, Amsterdam, doi:10.1007/978-94-007-4098-3_7

Strasser, U, M Bernhardt, M Weber, GE Liston, and W Mauser. 2008. “Is snow sublimation important in the alpine water balance?” *Cryosphere* 2(1): 53–66, <https://doi.org/10.5194/tc-2-53-2008>

- Sturm, M, MA Goldstein, and C Parr. 2017. “Water and life from snow: A trillion-dollar science question.” *Water Resources Research* 53(5): 3534–3544, <https://doi.org/10.1002/2017WR020840>
- Sullivan, RC, DR Cook, VP Ghate, VR Kotamarthi, and Y Feng. 2019a. “Improved spatiotemporal representativeness and bias reduction of satellite-based evapotranspiration retrievals via use of in situ meteorology and constrained canopy surface resistance.” *Journal of Geophysical Research Biogeosciences* 124(2): 342–352, <https://doi.org/10.1029/2018JG004744>
- Sullivan, RC, VR Kotamarthi, and Y Feng. 2019b. “Recovering evapotranspiration trends from biased CMIP5 simulations and sensitivity to changing climate over North America.” *Journal of Hydrometeorology* 20(8): 1619–1633, <https://doi.org/10.1175/JHM-D-18-0259.1>
- Svoma, BH. 2016. “Difficulties in Determining Snowpack Sublimation in Complex Terrain at the Macroscale.” *Advances in Meteorology* 18: 1–10, <https://doi.org/10.1155/2016/9695757>
- Tang, S, M Zhang, and S Xie. 2016. “An ensemble constrained variational analysis of atmospheric forcing data and its application to evaluate clouds in CAM5.” *Journal of Geophysical Research Atmospheres* 121(1): 33–48, <https://doi.org/10.1002/2015JD024167>
- Taylor, P. 1998. “The Thermodynamic Effects of Sublimating, Blowing Snow in the Atmospheric Boundary Layer.” *Boundary-Layer Meteorology* 89: 251–283, <https://doi.org/10.1023/A:1001712111718>
- U.S. Department of Energy. 2019. Atmospheric Radiation Measurement (ARM) User Facility ARM Mobile Facility Workshop Report. DOE/SC-0197. Office of Biological and Environmental Research, Office of Science, Germantown, Maryland. https://science.osti.gov/-/media/ber/pdf/community-resources/2019/ARM_Mobile_Facility_Workshop_Report.pdf
- Venzac, H, K Sellegri, and P Laj. 2007. “Nucleation events detected at the high altitude site of the Puy de Dôme Research Station, France.” *Boreal Environment Research* 12(3): 345–359.
- Vionnet, V, E Martin, V Masson, G Guyomarc'h, FN Bouvet, A Prokop, Y Durand, and C Lac. 2014. “Simulation of wind-induced snow transport and sublimation in alpine terrain using a fully coupled snowpack/atmosphere model.” *The Cryosphere* 8(2): 395–415, <https://doi.org/10.5194/tc-8-395-2014>
- Viviroli, D, DR Archer, W Buytaert, HJ Fowler, GB Greenwood, AF Hamlet, Y Huang, G Koboltschnig, MI Litaor, JI López-Moreno, S Lorentz, B Schadler, H Schreier, K Schwaiger, M Vuille, and R Woods. 2011. “Climate change and mountain water resources: overview and recommendations for research, management and policy.” *Hydrology and Earth System Sciences* 15(2): 471–504, <https://doi.org/10.5194/hess-15-471-2011>
- Vivoni, ER, K Tai, and DJ Gochis. 2009. “Effects of initial soil moisture on rainfall generation and subsequent hydrologic response during the North American monsoon.” *Journal of Hydrometeorology* 10(3): 644–664, <https://doi.org/10.1175/2008JHM1069.1>
- von Lerber, A, D Moisseev, LF Bliven, W Petersen, A Harri, and V Chandrasekar. 2017. “Microphysical Properties of Snow and Their Link to Z_e -S Relations during BAEC 2014.” *Journal of Applied Meteorology and Climatology* 56(6): 1561–1582, <https://doi.org/10.1175/JAMC-D-16-0379.1>

Walter, B, H Huwald, J Gehring, Y Bühler, and M Lehning. 2020. “Radar measurements of blowing snow off a mountain ridge.” *The Cryosphere* 14(6): 1779–1794, <https://doi.org/10.5194/tc-14-1779-2020>

Weber, RJ, PH McMurry, FL Eisele, and DJ Tanner. 1995. “Measurement of expected nucleation precursor species and 3–500 nm diameter particles at Mauna Loa Observatory, Hawaii.” *Journal of the Atmospheric Sciences* 52(12): 2242–2257, [https://doi.org/10.1175/1520-0469\(1995\)052<2242:MOENPS>2.0.CO;2](https://doi.org/10.1175/1520-0469(1995)052<2242:MOENPS>2.0.CO;2)

Willis, IC, NS Arnold, and BW Brock. 2002. “Effect of snowpack removal on energy balance, melt and runoff in a small supraglacial catchment.” *Hydrological Processes* 16(14): 2721–2749, <https://doi.org/10.1002/hyp.1067>

Wrzesien, ML, MT Durand, TM Pavelsky, SB Kapnick, Y Zhang, J Guo, and CK Shum. 2018. “A new estimate of North American mountain snow accumulation from regional climate model simulations.” *Geophysical Research Letters* 45(3): 1423–1432, <https://doi.org/10.1002/2017GL076664>

Wu, C M, M-H Lo, W-T Chen, and C-T Lu. 2015. “The impacts of heterogeneous land surface fluxes on the diurnal cycle precipitation: A framework for improving the GCM representation of land atmosphere interactions.” *Journal of Geophysical Research Atmospheres* 120(9): 3714–3727, <https://doi.org/10.1002/2014JD023030>

Wu, G-M, Z-Y Cong, S-C Kang, K Kawamura, P-Q Fu, Y-L Zhang, X Wan, S-P Gao, and B Liu. 2016. “Brown carbon in the cryosphere: Current knowledge and perspective.” *Advances in Climate Change Research* 7(1-2): 82–89, <https://doi.org/10.1016/j.accr.2016.06.002>

Wu, C, X Liu, Z Lin, AM Rhoades, PA Ullrich, CM Zarzycki, Z Lu, and SR Rahimi-Esfarjani. 2017. “Exploring a variable-resolution approach for simulating regional climate in the Rocky Mountain region using the VR-CESM.” *Journal of Geophysical Research Atmospheres* 122(20): 10,939–10,965, <https://doi.org/10.1002/2017JD027008>

Yang, Y, J Fan, RL Leung, C Zhao, Z Li, and D Rosenfeld. 2016. “Mechanisms Contributing to Suppressed Precipitation in Mt. Hua of Central China, Part I -Mountain Valley Circulation.” *Journal of the Atmospheric Sciences* 73(3):1351–1366, <https://doi.org/10.1175/JAS-D-15-0233.1>

Zhang, Z, S Glaser, R Bales, M Conklin, R Rice, and D Marks. 2017. “Insights into mountain precipitation and snowpack from a basin-scale wireless-sensor network.” *Water Resources Research* 53(8): 6626–6641, <https://doi.org/10.1002/2016WR018825>

Zhu, C, DP Lettenmaier, and T Cavazos. 2005. “Role of antecedent land surface conditions of north American monsoon rainfall variability.” *Journal of Climate* 18(16): 3104–3121, <https://doi.org/10.1175/JCLI3387.1>



www.arm.gov

U.S. DEPARTMENT OF
ENERGY

Office of Science